Role of oxidative stress in the balding dermal papilla

A thesis submitted in accordance with regulations for the degree of PhD

September 2012

Jamie Upton

Centre for Cutaneous Research

Bart's and The London School of Medicine and Dentistry

Queen Mary's University of London

Abstract

The dermal papillae of the hair follicle control its growth, differentiation and apoptosis via a range of growth factors. These secreted growth factors are known to differ between those of non-balding scalp and those of balding scalp and can even differ in response to a common stimuli – androgen. In balding scalp androgen stimulates the secretion of negative growth factors, while in non-balding scalp androgen is found to exert little or no effect. Dermal papilla cells (DPCs) can be cultured *in vitro*, however those from balding scalp have been found to undergo premature senescence compared to those from non-balding scalp. A major cause of premature senescence is oxidative stress – the gradual accumulation of reactive oxygen species within the cell causing deleterious loss of function. Reactive oxygen species are known to be mediated in response to androgens and growth factors and in turn may affect growth factor signalling within the cell. Using low oxygen cell culture as a means of reducing oxidative stress, balding and non-balding DPCs were grown and characterised. It was confirmed that low oxygen culture could increase proliferation, delay senescence and reduce reactive oxygen species with both DPC types and that balding DPCs showed a higher sensitivity to oxidative stress. It was also found that secretions of growth factors by the balding DPCs in response to different oxygen conditions differed greatly to that of the occipital DPCs. Androgen, but not TGF-β was found to modulate DPC production of catalase, an antioxidant, under low oxygen conditions and this caused a reduction in reactive oxygen species in the balding DPCs. Balding DPCs also demonstrated an upregulation of the antioxidant total glutathione, however had a reduced fraction of the active reduced form of the molecule. In addition, it was shown for the first time

that under cell culture conditions balding DPCs express TGF-β receptors and it was shown that proliferation and migration of the balding DPCs could be affected by addition of exogenous TGF-β, highlighting a potential role for TGF-β as an autocrine growth factor in the balding dermal papilla.

Table of contents

Index of tables

Index of figures

Abbreviations

% v/v	percentage volume to volume ratio
% w/v	percentage weight to volume ratio
(NH4)2SO4	Ammonium sulphate
°C	Centigrade
5αR	5α-reductase
A.U.	Arbitrary units
Ab	Antibody
AGA	androgenic alopecia
ANOVA	Analysis of variance
AR	Androgen receptor
ARE	Androgen response element
ATM	Ataxia telangiectasia mutated protein
BMI-1	B lymphoma Mo-MLV insertion region 1 homolog
BSA	Bovine serum albumin
CDK	Cyclin dependent kinase
cDNA	Complimentary deoxyribonucleic acid
CHAPS	3-[(3-cholamidopropyl)dimethylammonio]-1-propanesulfonate
CO2	Carbon dioxide
CTS	Connective tissue sheath
DAPI	4', 6-diamidion-2-phenylindole dihydrochloride
DEPC	Diethyl-pyrocarbonate
DHEA	Dehydroepiandrosterone
DHEA-S	Dehydroepiandrosterone sulphate

DHT	Dihydrotestosterone
DKK-1	Dikkopf-1
DMEM	Dulbecco's modified essential medium
DMSO	Dimethyl sulfoxide
DP	Dermal papilla
DPBS	Dulbecco's phosphate buffered saline
DPC	Dermal papilla cell
DTNB	5,5'-dithiobis-(2-nitrobenzoic acid)
DTT	Dithiothreitol
ECL	Electrochemiluminescence
ECM	Extracellular matrix
EDTA	Ethylene diamine tetra-acetic acid (Versene)
ELISA	Enzyme linked immunosorbent assay
ERK	Extracellular signal-regulated protein kinase
ETC	Electron transport chain
FBS	Foetal bovine serum
G	Gravitational constant
GAPDH	Glyceraldehyde-3-phosphate dehydrogenase
GCL	Glutamate cysteine ligase
GSH	Glutathione [Gluta-sulfhydryl] (reduced glutathione)
GSSG	Glutathione disulfide (oxidised glutathione)
h	Hour
H2DCFDA	5-(and-6)-carboxy-2´,7´-dichlorodihydrofluorescein diacetate
HAOX	Alpha hydroxy acid oxidase
HCl	Hydrogen chloride

HRP	Horse radish peroxidase
HSD	hydroxysteroid dehydrogenase
HSP27	Heat shock protein 27
IGF-1	Insulin-like growth factor 1
IgG	Immunoglogulin G
IRS	Inner root sheath
LTBP	Latent TGF-β binding protein (1, 2, 3 or 4)
M	Molar
MAPKs	Mitogen-activated protein kinase
MES	2-(N-morpholino)ethanesulfonic acid
MgCl2	Magnesium chloride
min	Minute
mM	Millimolar
MPA	Metaphosphoric acid
mRNA	Messenger ribosenucelic acid
MT1-MMP	Membrane type 1 metalloprotease
MU-Gal	4-Methylumbelliferyl β-D-galactopyranosidase
N2	Nitrogen
NaCl	Sodium chloride
NADH	Nicotinamide adenine dinucleotide (reduced form)
NADPH	Nicotinamide adenine dinucleotide phosphate (reduced form)
NaOH	Sodium chloride
nm	Nanometres
nM	Nanomolar
NS	Non-significant

O2	Oxygen
ORS	Outer root sheath
PAGE	Polyacrilamide gel electrophoresis
PAI-1	Plasminogen activator inhibitor-1
pH	log hydrogen ion concentration
PI	Propidium Iodide
pM	Picomolar
pmol	picomole
PMSF	phenazine methosulfate
pRB	Phosphorylated Retinoblastoma-associated protein
R.F.U.	Relative fluorescence units
R-1881	Metribolone
RIPA	Radioimmunoprecipitation assay (buffer)
ROS	Reactive oxygen species
RT	Reverse transcriptase
RT°C	Room temperature
RT-PCR	Reverse transcription polymerase chain reaction
S.E.M.	Standard error of mean
SA-β-Gal	Senescence associated β-galactosidase
SDS	Sodium dodecyl sulphate
sec	Second
SOD	Superoxide dismutase (1 or 2)
SP-1	Specificity protein-1 (transcription factor)
TAD	Transactivation domain
TBE	Tris borate EDTA buffer

TBS	Tris buffered saline
TBS-T	Tris buffered saline (with Tween)
TEAM	Triethanolamine
TF	Transcription factor
TGF-β	Tranforming growth factor β (1 or 2)
TGF-βR	Tranforming growth factor β receptor (I or II)
U.V.	Ultra violet
X-Gal	5-Bromo-4-chloro-3-indolyl β-D-galactopyranoside
μM	Micromolar

Acknowledgements

My PhD was funded under a BBSRC (CASE) studentship with industrial funding from Unilever.

First and foremost I would like to thank Professor Mike Philpott who has both guided the course of this investigation while simultaneously encouraging me to "follow the science" helping me to develop my skills as a scientist.

Secondly, I wish to thank the whole of the Centre for Cutaneous Research, with particular thanks going to Dr. Adiam Bahta – whose work formed the fundamental basis for this investigation; Dr. Ros Hannen – whose is has been my greatest role model, both as a scientist and as a friend; Dr. Dan Tattersall, Luke Gammon, Dr. Ann Wheeler, Mohammed Rahman, Dr. Sahira Khan, Dr. Kristin Braun and Dr. Louise Russell – whose technical support have proven invaluable.

Funding and support from Unilever came about as the result of the collaboration with Dr. Ranjit Bhogal, and many thanks are due for her support and encouragement.

None of this research would have been possible without the generous donation of scalp tissue from the Farjo Medical Centre in Manchester. Doctors Bessam and Nilofer Farjo's ongoing support and interest in our research is a huge boon to our ongoing studies.

A special note must be given to my own frontal scalp follicles, who have undergone a statistically significant ($P < 0.001$) terminal-to-vellus switch over a 4-year timecourse experiment ($n = 1$).

Finally, I wish to thank my friends and family whose love and support throughout my 4 years study have helped to get me through. Particular thanks are owed to Jennifer Glyn for encouraging me to apply for the PhD in the first place and Ruby Smith for her kindness and patience when it counted most.

Chapter 1

Introduction

1.1 The hair follicle

During evolution, mammals have developed hair, which serves a number of functions. Fur coats aid thermoregulation; coat thickness in many mammals increases during colder months of the year to provide increased thermal insulation which can then be shed when the warmer season begins. Hair acts as a protective barrier against the harmful effects of solar radiation. Hair coverage and its colour can also aid camouflage in many mammals, which may have conferred an evolutionary advantage (Stenn and Paus, 2001). Hairs have also evolved for specialised functions. For example, whisker (vibrissae) hairs aid rodents' ability to sense their environment.

Compared to our primate relatives, the bodies of modern humans have limited thick 'terminal' hair coverage; however, the only external regions of human skin devoid of hair follicles are the palms of the hands and soles of the feet. Many regions, such as the forehead, only have very fine unpigmented 'vellus' hairs. The total number of hair follicles in the skin of an adult human is estimated at 5 million, with 1 million on the head of which 100,000 alone cover the scalp. The hair fibre is also one of the fastest growing structures in the human body, with a growth rate of human scalp hairs of approximately 0.35 mm per day (Myers and Hamilton, 1951).

Hair patterning is of great importance to social and sexual communication. This is as true of humans as it is of other animals. Hair, especially that of the scalp, allows people to form judgements on other individuals' virility, health, age and social standing. One of the most common hair follicle disorders is male pattern baldness, also known as androgenic alopecia (AGA). This involves the progressive replacement of the larger and pigmented terminal hairs with thinner and shorter

vellus ones, in a predictable pattern on the scalp (Hamilton, 1951, Randall *et al.*, 2001). This affects over 50% of males by the time they reach their fifties (Hamilton, 1951). For this reason male androgenic alopecia has become a major focus of the cosmetics industry. The most widely sold treatment is minoxidil – a topically applied drug which is thought to improve blood flow to the balding scalp to allow regrowth of the hair. Another treatment is finasteride – a drug taken orally which inhibits the body's metabolism of testosterone into dihydrotestosterone to reduce androgen driven hair loss (for explanation of androgenic control of the hair follicle see **Section 1.8**).

1.2 Histomorphology of the hair follicle

The mammalian hair follicle is a complex, highly compartmentalised structure composed of both epithelial and dermal components: the germinative epithelium, matrix, inner root sheath (IRS) and outer root sheath (ORS); and dermal papilla (DP) and connective tissue sheath (CTS). As discussed in **Section 1.3**, the hair follicle undergoes cyclical remodelling which can be divided into three distinct stages: anagen, catagen and telogen (Dry, 1926). Approximately 90% of human hair follicles are in an active growth stage, anagen, during which the hair fibre is produced in the follicle (Paus, 1998). **Figure 1.1** demonstrates the basic structure of a late anagen hair follicle (Norlen *et al.*, 1999).

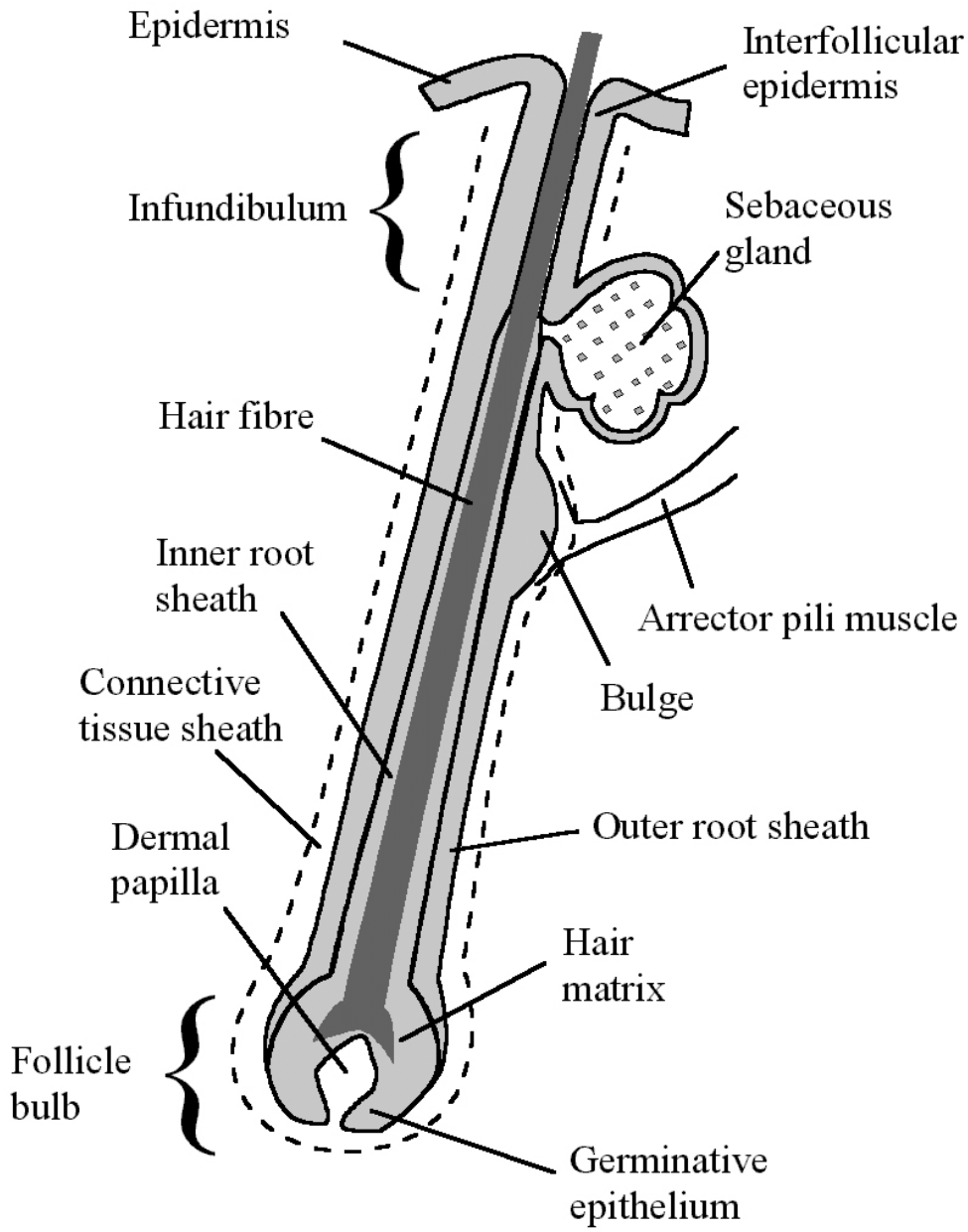

Figure 1.1: Basic structure of a late anagen hair follicle. Schematic diagram showing the organisation of the key compartments of the hair follicle and associated sebaceous gland. (Taken from Bull, 2002).

1.2.1 The follicle bulb

Figure 1.1 demonstrates the location of the follicle bulb at the proximal tip of the follicle. It is composed of germinative and hair matrix epithelium, melanocytes, dermal papilla (DP) and connective tissue sheath (CTS) fibroblasts and endothelial cells which vascularise this highly metabolically active region (Norlen *et al.*, 1999).

1.2.2 Dermal papilla

The DP is pear-shaped structure almost fully enclosed by the follicle bulb epithelium. The DP consists of specialised mesenchymal fibroblasts. As well as mesoderm-derived fibroblasts, neuronal and endothelial cells form nerve fibres and blood vessels respectively that penetrate the base of the hair capsule and invade into the DP area. There is a close correlation between the size of the DP and the size of the hair follicle (Elliott *et al.*, 1999). The larger the DP, the larger the hair follicle and the thicker the hair fibre produced (Elliott *et al.*, 1999, Van Scott and Ekel, 1958).

Signalling between the DP and follicle epithelium is vital for hair follicle functioning (reviewed in (Jahoda and Reynolds, 1996). As well as orchestrating hair follicle development, the DP possesses an instructive ability which governs the activities of the hair follicle. The importance of the DP was demonstrated by the work of Roy Oliver. He discovered that a) DP was essential for hair growth (Oliver, 1966), b) if the lower third of the hair follicle is removed the proximal CTS cells are capable of forming a new DP and inducing regeneration of a new follicle bulb (Oliver, 1966) and c) the DP is vital for inducing hair growth (Oliver, 1967, Oliver, 1971).

DP cells retain their embryonic hair follicle development inducing abilities, even after culturing *in vitro* (Jahoda *et al.*, 1984). Implantation of DP cells below the epidermis of adult rat ear and footpad skin can recruit and transdifferentiate epidermal cells into forming a *de novo* hair follicle (Jahoda *et al.*, 1984, Reynolds and Jahoda, 1992). Similarly, hair follicle neogenesis has been achieved by the implantation of CTS cells underneath adult human epidermis (Reynolds *et al.*, 1999). In another key study, implantation of murine embryonic mesoderm-derived cells under rabbit corneal epithelium resulted in transdifferentiation of the epithelial cells, with ectopic hair follicle development and epidermal-type keratin expression. This is important as it demonstrates that a) the underlying mesenchyme controls epithelial cell fate, including skin appendage formation and b) the signalling pathways are conserved between species.

1.2.3 Connective tissue sheath

Surrounding the epithelial components of the hair follicle is the connective tissue sheath (CTS), also known as the dermal sheath. The CTS consists of mesenchymal cells, namely fibroblasts and endothelial cells (which form the perifollicular blood vessels), in a collagen rich extracellular matrix. The CTS provides structural reinforcement to the rest of the follicle. Epithelial-mesenchyme interactions between the ORS and CTS are thought to play an important role in hair follicle function. In the follicle bulb, the CTS is continuous with the DP and migration between the two compartments may occur (Tobin *et al.*, 2003). When the proximal hair follicle is amputated, CTS cells can form a new DP, enabling the follicle bulb to regenerate (Oliver, 1966). Cultured human CTS cells allogenically grafted onto a into human skin activate hair follicle neogenesis wherein the new follicle maintains the donor's

genetic profile (Reynolds *et al.*, 1999). Notably, this paper also demonstrated that this process did not trigger graft versus host disease highlighting the hair follicle's "immune privilege".

1.2.4 Hair follicle epithelial cells

The hair fibre and IRS are produced by the follicle bulb epithelium, which almost completely enclose the DP. The germinative epithelium are highly proliferative cells (Weinstein, 1980), which give rise to a constant stream of hair matrix cells in concentric layers that move up away from the DP. The mitogenic stimuli for the proliferation of the germinative epithelium are growth factors secreted by the dermal papilla (see **Section 1.4**). The diffusion of growth factors from the dermal papilla also dictates the differentiation of the epithelial cells of the hair matrix into the concentric layers of the cortex, IRS and ORS keratinocytes.

The cortex cells become gradually more keratinised as they move away from the proximal tip to make up the hair fibre. The IRS acts as rigid scaffold to the cortex, moulding and directing its growth. The IRS ends around the infundibulum area of the follicle (the section above the sebaceous gland) to allow the hair fibre greater flexibility. The ORS is continuous with the epithelium of the skin and encloses the IRS. Around the area below the sebaceous gland duct is a specialised region of ORS called the 'bulge' region. This bulge although not anatomical visible in the human follicle is thought to harbour the major stem cell reservoir for the hair follicle and surrounding skin (Cotsarelis *et al.*, 1990).

1.3 The hair follicle growth cycle

Hair fibre growth is not a continuous event. The hair follicle undergoes cycles of hair fibre growth, followed by regression and a phase of relative quiescence before regenerating and beginning hair fibre production again. The length of the hair fibre produced is therefore determined by the duration of the growth phase (anagen). By having a hair growth cycle the length of the hair fibre can be controlled – providing a 'biological haircut' for the mammal (Stenn and Paus, 2001).

Stages of the human hair growth cycle were characterised by Albert Kligman (1959). For a comprehensive review on the hair cycle, see Stenn and Paus, 2001.

There are three distinct stages of the hair growth cycle: the active growth stage (anagen) during which the hair fibre is produced; a regressive stage (catagen) in which the follicle partially degenerates, followed by a relatively quiescent stage (telogen), in which the hair follicle waits for new signals to re-enter anagen (Dry, 1926). More recently, a extra fourth stage has been proposed entitled exogen in which the hair fibre is shed (Milner *et al.*, 2002).

The hair follicle can be divided into two portions with respect to the hair growth cycle. The distal (upper) portion of the follicle, down to just below the bulge region, is said to be the 'permanent' region of the follicle, as it maintained throughout the hair growth cycle. The region proximal (lower) to this is described as the 'cycling' portion of the follicle, as it undergoes marked remodelling during the hair cycle. For an overview of the hair follicle growth cycle stages see **Figure 1.2**.

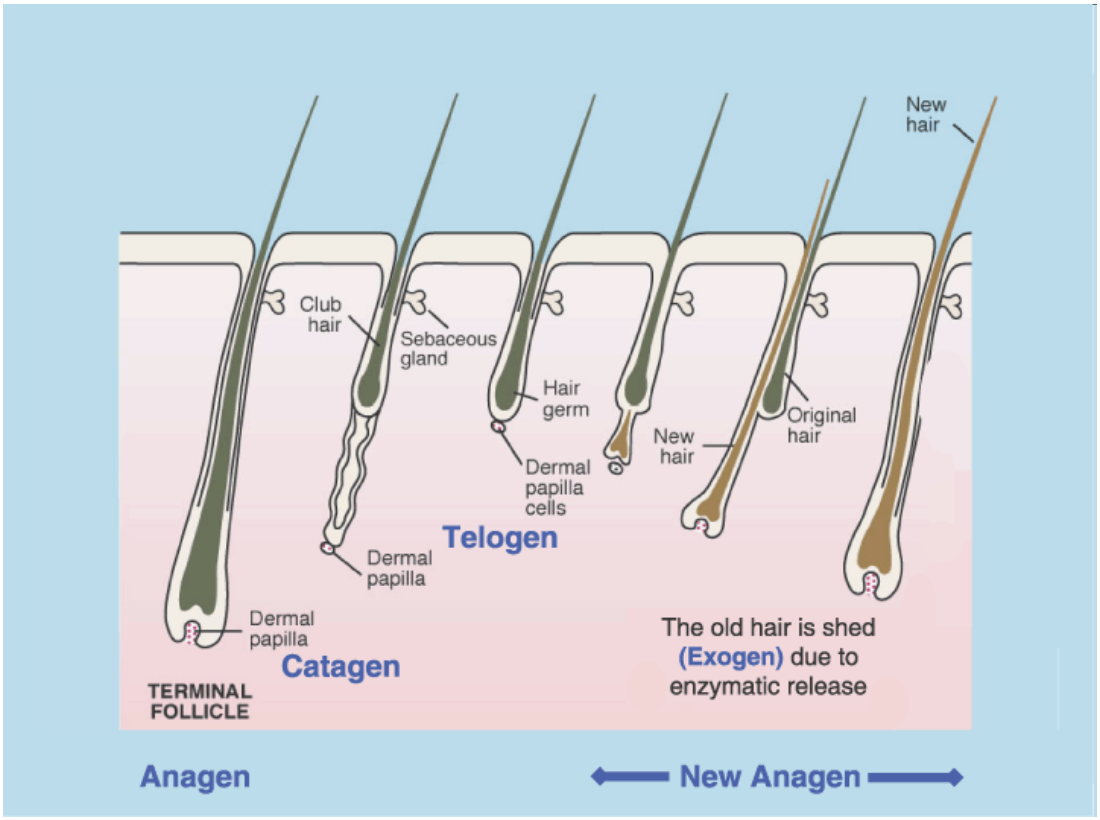

Figure 1.2: The hair follicle growth cycle. Hair follicles go through well-established repeated cycles of development and growth (anagen), regression (catagen), and rest (telogen) to enable the replacement of hairs, often by another of differing colour or size. An additional phase, exogen, has been reported where the resting club hair is released. (Diagram taken from Randall, 2008)

1.3.1 Anagen

At the start of anagen, previously quiescent epithelial cells in the proximal follicle adjacent to the DP (the 'secondary hair germ') and in the bulge are activated, by as yet uncharacterised signals, to proliferate. This results in enlargement and down-growth of the hair germ. The DP enlarges and becomes partially enclosed by the proximal hair follicle epithelium, which reforms the bulb as follicle elongates. This regeneration phase of anagen is sometimes described as pro-anagen. As with hair follicle development, once a destined down-growth length has been reached, proximal epithelial cells neighbouring the DP reverse their growth direction and progress distally back towards the epidermis. It is these cells that then undergo lineage restricted terminal differentiation, forming the hair fibre and IRS. Once the cycling portion of follicle has fully reformed, the follicle is in late anagen, during which the time the hair fibre grows is continuous. The structure of the late anagen hair follicle is described in **Section 1.2**. Late anagen is a prolonged phase in large (terminal) human hair follicles, which can last for 1-6 years and account for over 80-90% of all scalp follicles (Paus, 1998).

1.3.2 Catagen

Late anagen ceases and the follicle enters what is known as catagen. Cessation of germinative epithelium cell proliferation occurs and consequently hair fibre production stops. This coincides with many epithelial cells in the cycling portion of the follicle, particularly in the proximal follicle epithelium, undergoing programmed cell death, known as apoptosis (for a review on apoptosis, see (Hengartner, 2000). Selective loss of cells results in shrinkage of the follicle bulb, causing the proximal epithelium to disclose the DP and retreat up towards the bulge region as an epithelial

strand. This shrinkage causes the no-longer-growing hair fibre, known as the club hair, to be drawn upwards at the same time. Meanwhile, the DP becomes rounded and condenses, before trailing behind the regressing epithelial strand. Another clear histological sign of catagen is the marked thickening of the vitreous or glassy membrane of the CTS (Kligman, 1959). The DP, trailed by the CTS then retreats upward towards the bulge region. These changes in follicle morphology have long been characterised in detail by light microscopy (Kligman, 1959) and by electron microscopy (Parakkal, 1970).

Catagen lasts two to three weeks in human hair follicles (Kligman, 1959). Catagen provides a mechanism whereby the hair follicle stops production of its hair fibre and moves it towards the skin surface for subsequent shedding. It is unclear how the apoptosis is orchestrated so that some epithelial cells of the follicle are selectively lost without causing a disintegration of the proximal follicle. Several factors are thought to control catagen, including the transforming growth factor beta (TGF-β) isoforms (Foitzik *et al.*, 2000, Foitzik *et al.*, 1999) and dickkopf-1 (DKK-1) (Kwack *et al.*, 2012), although the factor or factors controlling the switch from anagen to catagen have yet to be determined, there is thought to be an important role for CLOCK genes which regulate circadian rhythms (Geyfman and Andersen, 2010).

1.3.3 Telogen

Following catagen, the shrunken hair follicle goes into a more quiescent phase. The non-growing hair fibre (known as a club hair) left from anagen resides in the follicle, but is eventually shed. Around 10-20% of scalp follicles are in telogen at any given time. In human scalp hairs, telogen lasts for approximately 2 months before the follicle receives signals that induce a return to anagen and the cycle repeats itself

(Paus, 1998). As with the anagen to catagen switch, CLOCK genes regulating circadian rhythm are thought to regulate the duration for which the follicles remain in this quiescent state (Geyfman and Andersen, 2010).

1.3.4 Exogen

The club hair's excision from the hair follicle is not, as was originally thought, a passive process, rather it is an active stage in of itself known as exogen (Van Neste *et al.*, 2007). During this stage the club hair loses all anchorage from the surrounding CTS through the loss of the ORS layer. The loose club hair is then forced upwards by the newly formed secondary germ as it forms the next anagen follicle (Higgins *et al.*, 2009).

1.4 Growth factor signalling in the hair follicle

Growth factors are secreted from the dermal papilla into the surrounding germinative epithelium and hair matrix keratinocytes and are responsible for a range of cell activities. Growth factors provide the mitogenic stimuli for the rapidly proliferating germinative epithelium during anagen. Growth factor diffusion is also responsible for stimulating differentiation of the hair matrix into their varying concentric layers. One such growth factor is IGF-1, which acts as both a mitogenic and a differentiation signal (see **Section 1.7**)(Philpott *et al.*, 1994). Growth factors also stimulate the onset of apoptosis in the ORS which triggers the involution of the follicle during the regressive catagen stage of the growth cycle. Growth factors known to induce this response are the TGF-βs and DKK-1 (**see Sections** 1.5 and 1.6)(Foitzik *et al.*, 1999; Foitzik *et al.*, 2000; Kwack *et al.*, 2012).

Many other signalling pathways have been shown to play important roles in hair follicle development. These include epithelial growth factors, bone morphogenic proteins, epidermal growth factor, fibroblast growth factors and insulin-like growth factors (Danilenko *et al.*, 1996, Philpott, 1998, Yamanishi, 1998, McElwee and Hoffmann, 2000).

1.5 TGF-β

TGF-β exists as three distinct isoforms TGF-β1 -β2 and -β3, which confer different roles depending on cell and tissue type. In fibroblasts, the TGFβs typically stimulate tissue remodelling during processes such as wound healing, wherein an altered combination and organisation of ECM components such as collagen and fibronectin (Keski-Oja *et al.*, 1988, Raghow *et al.*, 1987, Vayalil *et al.*, 2005). They have also been found to modulate cellular functions such as proliferation in lung fibroblasts (Moses *et al.*, 1987) or motility as well as being indicated in modulating cell migration in myofibroblasts (Brenmoehl *et al.*, 2009) or lung fibroblasts (Postlethwaite *et al.*, 1987).

TGF-β1 has a growth inhibitory effect on human hair follicles (Philpott *et al.*, 1990). Both TGF-β1 and TGF-β2 have been shown to be expressed in the human hair follicle, and are known to mediate the hair follicle's initiation into catagen (Foitzik *et al.*, 2000, Foitzik *et al.*, 1999). TGF-β3, a mediator of embryonic wound healing (Cowin *et al.*, 2001) is not known to be expressed in the adult cycling hair follicle.

1.5.1 TGFβ receptor

The active TGF-β receptor is formed from two proteins – TGF-βRI and TGF-βRII (**Figure 1.3**). Together these form a heteromeric, membrane bound structure which binds all TGFβ isoforms as well as a number of other Activin-family molecules (including bone morphogenic protein - BMP). Although a third TGF-β receptor exists (TGF-βRIII) it is not known to be expressed in the human hair follicle. TGF-βRII is required for the initial binding of the TGF-β1, -β2 or -β3 ligands. TGF-β1 and -β3 bind to the receptor with a higher affinity than TGF-β2. TGF-βRI is unable to bind TGF-β isoforms, instead it is phosphorylatively activated by TGF-βRII, causing TGF-βRI to undergo a conformational change (Wrana *et al.*, 1994) activating its ability to carry out threonine/serine phosphorylation of its intracellular mediators (see **Section 1.5.2**).

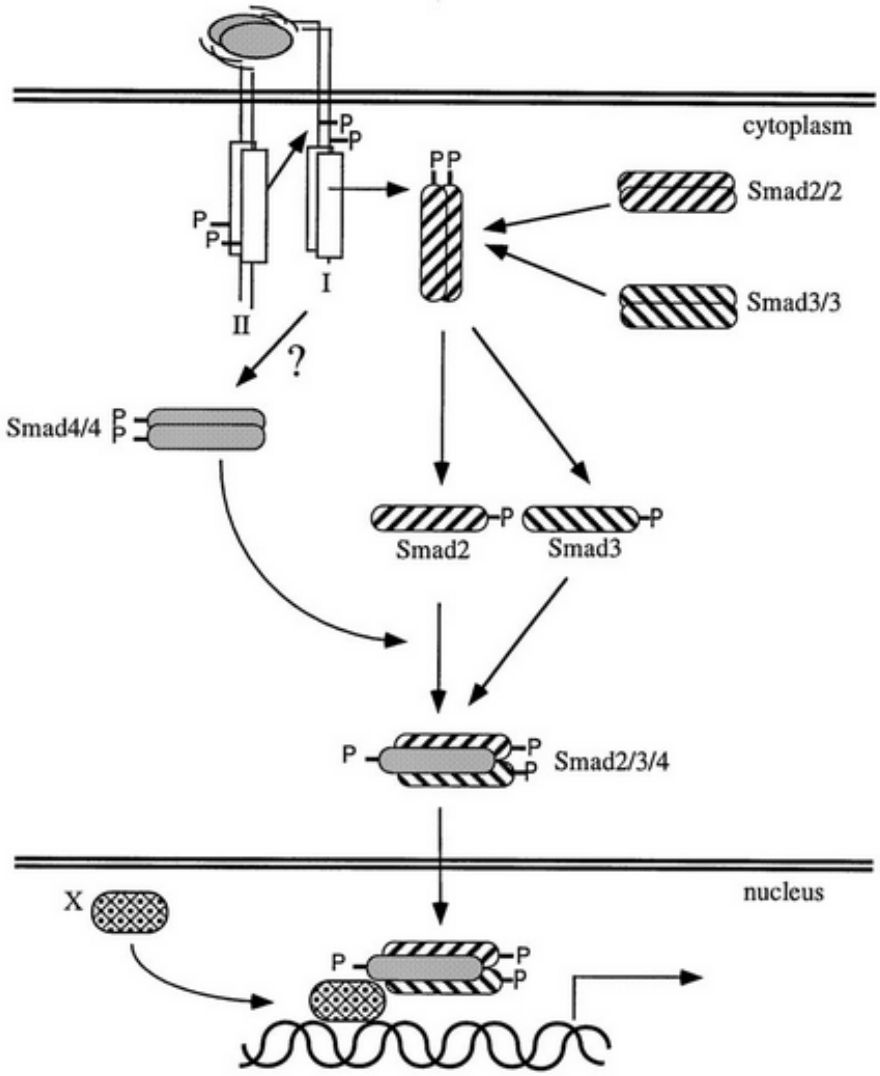

Figure 1.3: TGFβ cell surface receptors and intracellular Smad signalling pathway. TGFβ ligands bind to TGFβRII (II) which undergoes conformational change to reveal phosphorylative activation sites (P) which have serine/threonine kinase activation of TGFβRI (I). TGFβRI in turn phosphorylates Smads 2 and/or 3 which subsequently form a heteromeric complex with Smad 4. Smad 2/3/4 heteromer subsequently translocates to the nucleus wherein to interact with specific DNA binding proteins (X) such as AP-1 and SP-1 instigating the transcription of target genes.(Nakao ***et al.***, 1997)

1.5.2 TGF-β intracellular mediators

The canonical intracellular transduction pathway of TGF-β signalling occurs through the Smad proteins (Lutz and Knaus, 2002). TGF-βRI phosphorylates the C-terminus of the Smad2 or Smad3 protein which forms a heteromer with the Smad4 protein (**Figure 1.3**). This complex then translocates to the nucleus wherein it activates transcription of genes controlling a wide array of processes.

TGF-β signal transduction has also been found to be mediated via the intracellular signalling occurs via the mitogen activated protein kinases (MAPKs) family of proteins (Yamashita *et al.*, 2008, Shim *et al.*, 2005).

Two of the major promoter targets of Smad are the AP1 and SP1 transcription factors, which promote the transcription of genes controlling a wide range of cellular functions, including proliferation, apoptosis, migration, cellular redox as well as autoregulating components of the TGF-β signalling pathways itself (Vayalil *et al.*, 2007).

1.5.3 TGF-β binding proteins (LTBPs)

The rate-limiting step controlling the level of secretion of TGF-β isoforms is controlled via carrier proteins known as the latent TGF-β binding proteins (LTBPs) 1-4. For TGF-β to be secreted into the extracellular space, it must be bound and chaperoned out of the cells by LTBP-1, -3 or -4 (Saharinen *et al.*, 1999).

The LTBPs are able to bind to ECM components such as fibronectin or fibrillin, thus they are able to target TGFβs to tissues with specific ECM (Hyytiainen and Keski-Oja, 2003, Hyytiainen *et al.*, 2004). LTBP-2 which does not contain a binding domain for TGF-β, is able to act as a competitive antagonist for these ECM binding sites, effectively blocking the targeting of TGF-β to tissues (Hirani *et al.*, 2007).

TGFβ is released from the binding protein through enzymatic cleavage by plasmin, thrombin and MT1-MMP (Taipale *et al.*, 1992, Tatti *et al.*, 2008). A number of other factors, including the presence of reactive oxygen species, can increase the rate at which this cleavage occurs (Koli *et al.*, 2001).

1.6 DKK-1

DKK-1 functions by disrupting Wnt signalling. Wnt signal is transduced via the transmembrane protein family the Frizzleds, which co-localise in the membrane with LRP5 or LRP6 (Niehrs and Shen, 2010). DKK-1 is able to bind to LRP5/6 when associated with the co-factor Kremen (Daoussis and Andonopoulos, 2011). This process does not trigger a signalling event directly, instead it cause the internalisation of the Kremen-LRP5/6 complex, thus reducing the total available LRP5/6 exposed to the extracellular domain for Wnt ligands (Daoussis and Andonopoulos, 2011).

Wnt10b has been shown to stimulate epithelial differentiation and hair follicle growth (Ouji *et al.*, 2007) therefore DKK-1 action in the hair follicle may be to disrupt this positive growth signal. It has been shown that mice over-expressing DKK-1 display an early onset of catagen or can fail to develop follicles altogether (Andl *et al.*, 2002). In humans, DKK-1 has also been shown to be secreted by the DP which then induces the onset of catagen (Kwack *et al.*, 2012).

1.7 IGF-1

Insulin-like growth factor (IGF) is a well established positive growth regulator of hair follicle growth *in vitro* with the IGF-1 isoform being approximately 10 times more potent than the IGF-1 isoform (Philpott *et al.*, 1994). IGF-1 has been shown to

be secreted by the DP (Messenger, 1989) and stimulates mitogenic growth of the follicle keratinocytes as well as inducing differentiation of the varying keratinocyte root sheaths (Rudman *et al.*, 1997).

IGF-1 signalling is transduced via the IGF-1 receptor which is expressed in the epidermal keratinocytes of the hair follicle (Hodak *et al.*, 1996). IGF is able trigger a number of signalling cascades within the cell that induce survival or differentiation pathways, including the PI3K-AKT pathway and the ERK pathway (Lewis *et al.*, 2009).

1.8 Androgens and hair growth

Human hair growth is influenced by a number of hormones, including thyroid hormones and female sex hormones which are implicated largely during pregnancy. During this time, hair follicles remain in anagen, however postpartum when the maternal physiology returns to normal, these follicles move into catagen and telogen and are shed (Lynfield, 1960).

The most obvious regulators of human hair follicles are the androgens. This was first established by the work of Hamilton (1942) in which he observed that male eunuchs failed to go bald. Further to this, it was observed that men who had begun to show signs of balding before castration did not demonstrate any further hair loss, although hair did not grow back either. In addition to this, 4 out of 12 eunuchs treated with testosterone injections began showing signs of baldness and all 4 of these subjects came from families with a prevalence of AGA.

Androgens are mediators of terminal hair growth throughout the body (**Figure 1.4**). With sexual maturity, androgens cause enlargement of vellus hairs to form terminal

follicles in the axilla and pubis of both sexes, and on the face, trunk and extremities in men (Marshall, 1970). Paradoxically, in those who are genetically predisposed, androgen can trigger the development of male pattern baldness (also known as androgenic alopecia (AGA)) manifested as miniaturisation of scalp hair follicles in the frontal and crown regions of the scalp. Polymorphisms in the androgen receptor (AR) gene represent a major prerequisite in the mediation of early-onset AGA (Hillmer *et al.*, 2005). The location of this gene on the X-chromosome emphasises the importance of the maternal line in the inheritance of this condition.

The paradoxical effects of androgens on scalp and body hair are as yet not fully understood. However, androgen effects on hair growth at particular body areas are believed to be due, at least in part, to factors such as increased number of androgen receptors, increased local production of high-potency androgens, and/or reduced degradation of androgens (Randall *et al.*, 2000).

Hamilton (1951) first established the importance of androgens in human hair growth, when he found that castration of males before puberty prevented beard and auxiliary hair growth and after puberty reduced both (Hamilton, 1951, Hamilton *et al.*, 1958). However, the strongest evidence that androgens are involved in regulating human hair growth is provided by the changes seen at puberty when the appearance of pubic and axillary hair occurs in parallel with the rise in plasma androgens (Wilson, 1975). In addition, one of the primary methods of treatment for androgenic alopecia is the androgen antagonist, finasteride (Trueb, 2006)

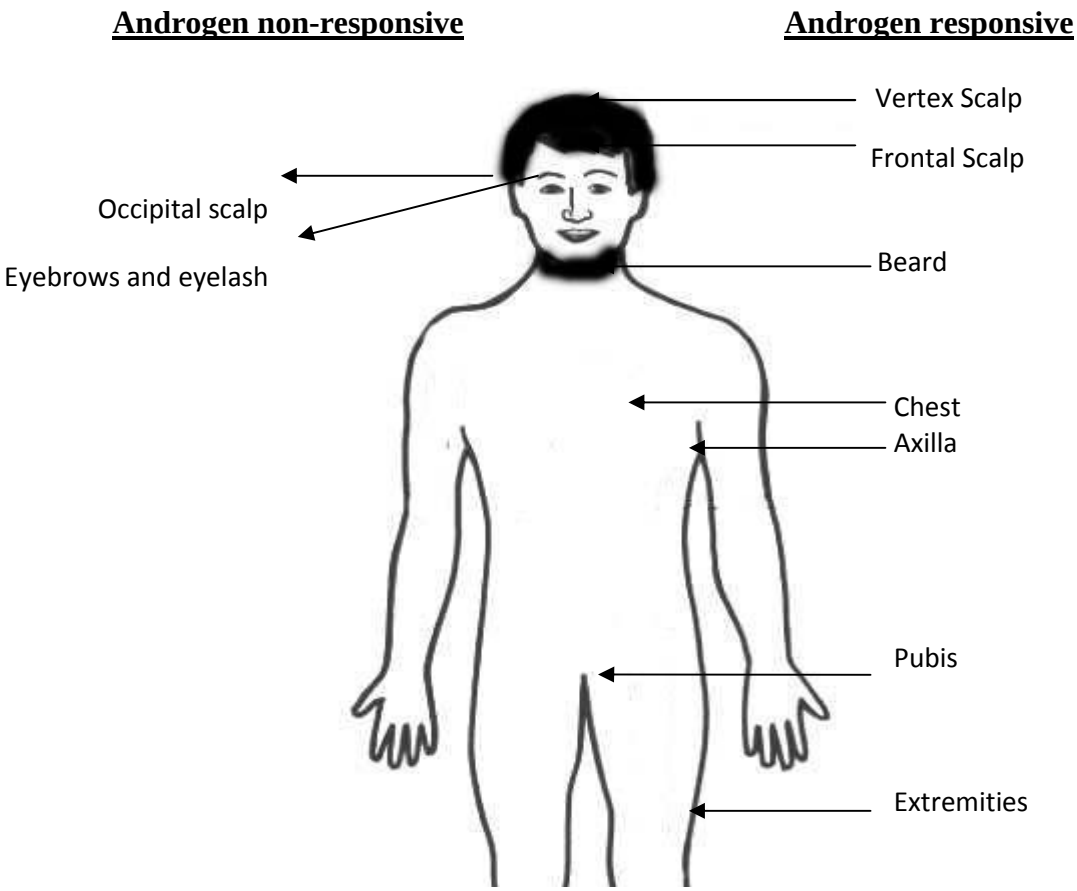

Figure 1.4: Schematic showing the differential effects of androgens on hair growth. Androgens have different effects on hair growth, depending on body location: On the beard, chest, pubis, axillae and extremities, where, beginning at puberty, hair follicles are stimulated to become terminal follicles; on the scalp, where follicles are inhibited in a patterned distribution in men with a hereditary predisposition to baldness.

1.8.1 Androgen metabolism

The major circulating plasma androgens are testosterone in men and androstenedione in women; however the effects of androstenedione may be dependent on the enzymatic conversion to testosterone in peripheral tissues by the enzyme 17B-hydroxysteroid dehydrogenase. Androgens exist in circulation; 70% bound to sex-hormone binding globulin, 19% bound to albumin and the rest circulates as free androgen. Androgen production can be both glandular and extraglandular. Androgen synthesis begins with cholesterol which is converted to pregnenolone (Hoffmann, 2002). Following α-hydroxylation at the C17-position, the action of the enzyme C17-20 lysase cleaves distal carbon moieties, leaving a C-19 carbon steroid with a C-17 ketone in the distal ring. These '17-ketosteroids' make up a group of relatively weak androgens, such as dehydroepiandrosterone (DHEA), defined by their relatively low affinity for the androgen receptor. Approximately 75% of DHEA and 95% of dehydroepiandrosterone sulphate (DHEA-S) is derived from the adrenal gland (Hinson and Khan, 2004). These weak androgens can be enzymatically converted to more potent androgens such as testosterone, which is the major circulating androgen (**Figure 1.5**). In the hair follicle the principal pathways involved in the conversion of weak to more potent androgens are through activity of the enzymes 3β-hydroxysteroid dehydrogenase/isomerase (3β-HSD) and 17β-hydroxysteroid dehydrogenase (17β-HSD).

In most target organs, testosterone can be further metabolised to DHT via the action of 5**α**-reductase (5αR). The affinity of DHT to the androgen receptor is approximately five fold higher than that of testosterone. There are two distinct forms of 5αR, referred to as types 1 and 2, which differ in their tissue distribution (Silver *et*

al., 1994). Type 1 5αR is prominent in sebaceous glands, while type 2 5αR is prominent in the genitourinary tract and within hair follicles, in the outer root sheath and proximal part of the inner root sheath (Bayne *et al.*, 1999). Other studies have suggested that type 2 5αR may also be the predominant form of this enzyme in dermal papillae (Eicheler *et al.*, 1998).

The pathway of steroid hormone metabolism studied most thoroughly in relation to hair growth is testosterone and conversion of testosterone to DHT (Siiteri and Wilson, 1970). Hair follicles of the balding scalp have been shown to express higher levels of 5αR2 compared to relatively low amounts in the occipital scalp, making the total levels of the more potent DHT much higher in the balding follicle (Hamada *et al.*, 1996).

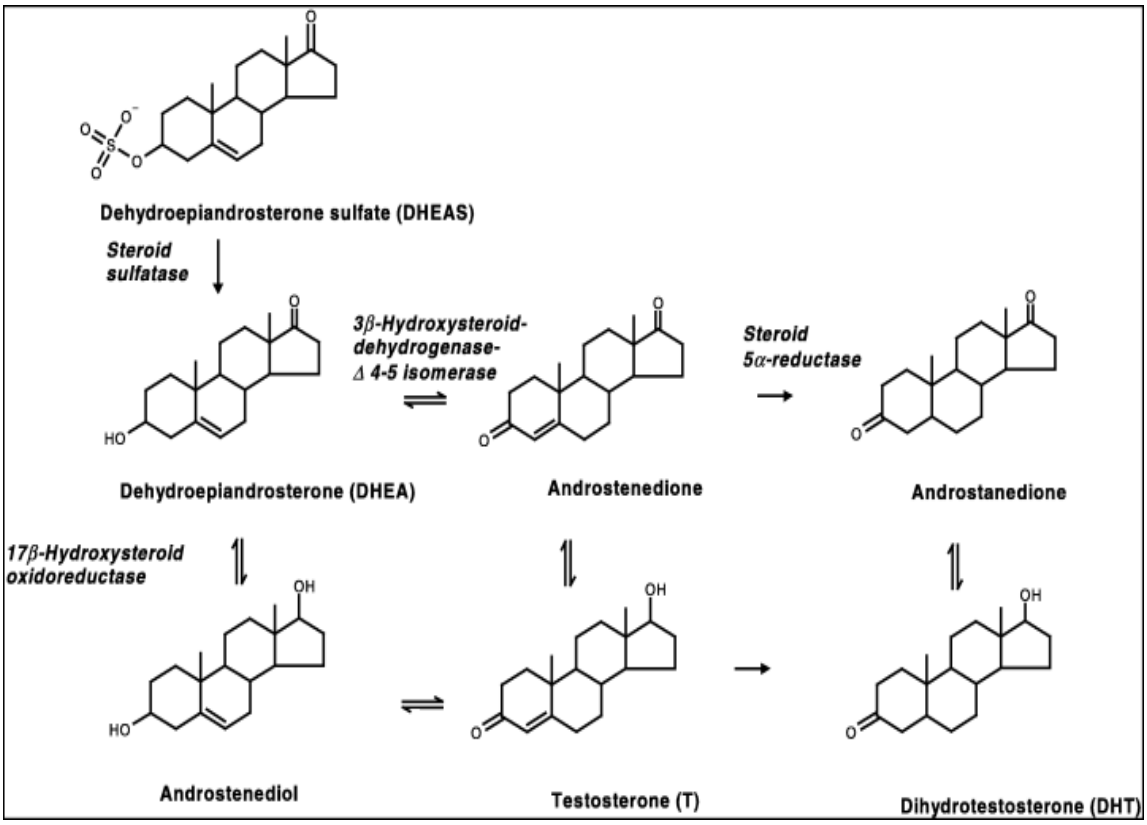

Figure 1.5: Androgen metabolic pathways. Schematic diagram showing interconversion of DHEAS to more potent androgens (figure is taken from (Hoffmann, 2002)

.

1.8.2 Androgen receptor

The AR is an intracellular transcription factor that belongs to the steroid/nuclear receptor superfamily (Quigley *et al.*, 1995). When the AR is ligand-activated by androgens, it translocates to the nucleus, and binds in dimerised form to specific genomic DNA sequences, which are called androgen response elements in the regulatory regions of androgen-dependent genes (see **Figure 1.6**). Binding of the androgen-AR complex activates or represses the expression of androgen-regulated proteins (Choong and Wilson, 1998). Thus, AR controls the transcription of androgen-dependent proteins from embryogenesis to adulthood. The AR gene is localised on the X chromosome at Xq11-12 (Brown *et al.*, 1989), is encoded in eight exons (Lubahn *et al.*, 1988) and has, like other members of the steroid receptor superfamily, three main functional domains: the transactivation domain (TAD), the DNA-binding domain and the ligand-binding domain (Mangelsdorf *et al.*, 1995)

All steroid hormones act by diffusing through the plasma membrane and binding to specific intracellular receptors; these hormone-receptor complexes undergo conformational changes, exposing DNA binding sites. The activated complexes then bind to specific hormone response elements in the DNA, promoting the expression of specific hormone-regulated genes. Variations in the levels of androgen receptor expression and testosterone

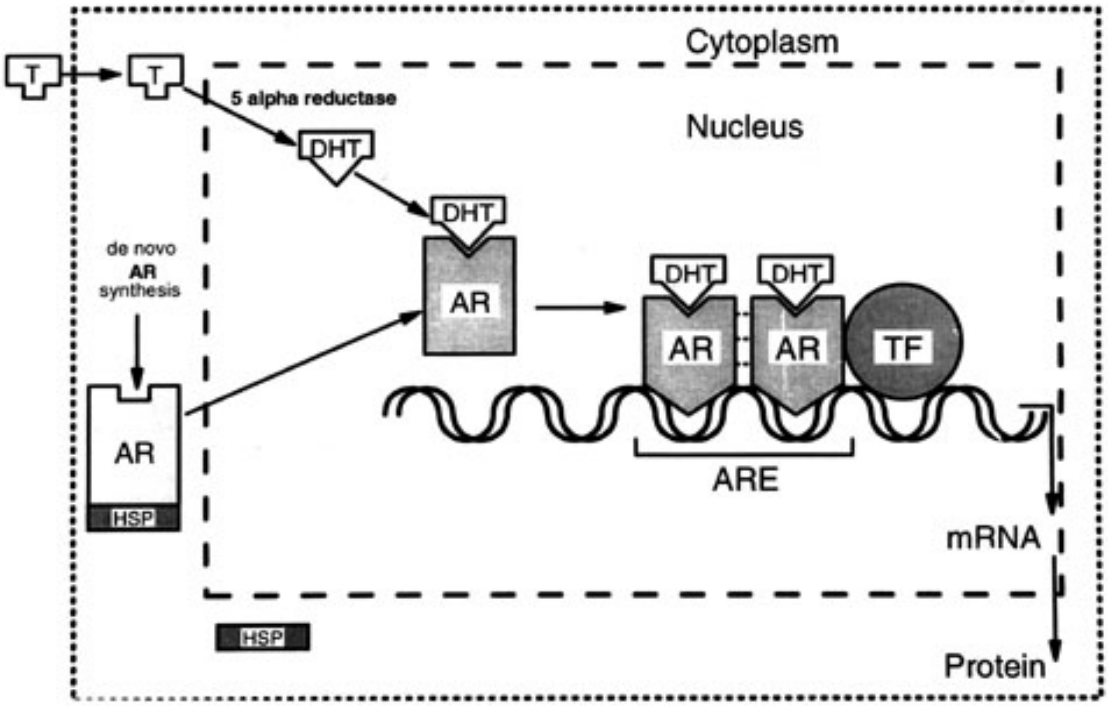

Figure 1.6: Mechanism of androgen action. Testosterone (T) enters the cell and is converted by 5α-reductase to 5α-dihydrotestosterone (DHT). DHT binds to the androgen receptor (AR) leading to a conformational change in the protein and the dissociation of several accessory proteins, including heat shock proteins (HSP). Binding of the AR to the androgen response element (ARE), along with other transcription factors (TF) regulates the transcription of mRNAs. (Itami, 1992).

metabolism are thought to explain the variability which exists in androgen responsiveness at different body sites and between individuals in terms of androgen mediated hair growth. Scalp hair follicle growth is thought not to be androgen dependent as a full head of terminal hair is achieved during childhood in the absence of high levels of circulating androgens.

The mesenchyme derived dermal papilla plays an important regulatory role in the follicle, altering many parameters and determining the type of hair produced. As steroids act via mesenchyme in many developing steroid-dependent tissues including breast and prostate, androgens act on the other components of the follicle via the dermal papilla (Itami and Inui, 2005). As shown in **Figure 1.7**, circulating androgen enters the dermal papilla via its blood capillaries where they bind to androgen receptor within the DP cells of androgen-dependent hair follicles. Whether or not androgens are first metabolised intracellularly to DHT would depend on the site of the follicle. There is evidence to suggest that some follicles require the reduction to DHT while others metabolise testosterone without this step. In male pseudohermaphrodites with 5α-reductase deficiency; normal scalp, pubic and auxiliary hair growth occurs but no beard growth or temporal recession is found. This occurs even though plasma testosterone concentrations are high (Imperato-McGinley *et al.*, 1986). This suggests that although pubic and auxiliary hair follicles are also dependent on androgens, the intracellular mechanism of androgen action differs from that of beard follicles. The 5α-reduction of testosterone appears to be necessary for the growth of beard hair but not for pubic and auxiliary hair growth. Itami *et al.* (1991) have shown using an assay for 5α-reductase activity that beard DP cells show increased levels of 5α-reductase activity compared to DP cells from the occipital scalp which would support this hypothesis, while

Hamada and co-workers (1996) have now shown using thin layer chromatography, that pubic and auxiliary PD cells utilise testosterone as the primary androgen, while very little DHT was utilised in these cells (Hamada *et al.*, 1996).

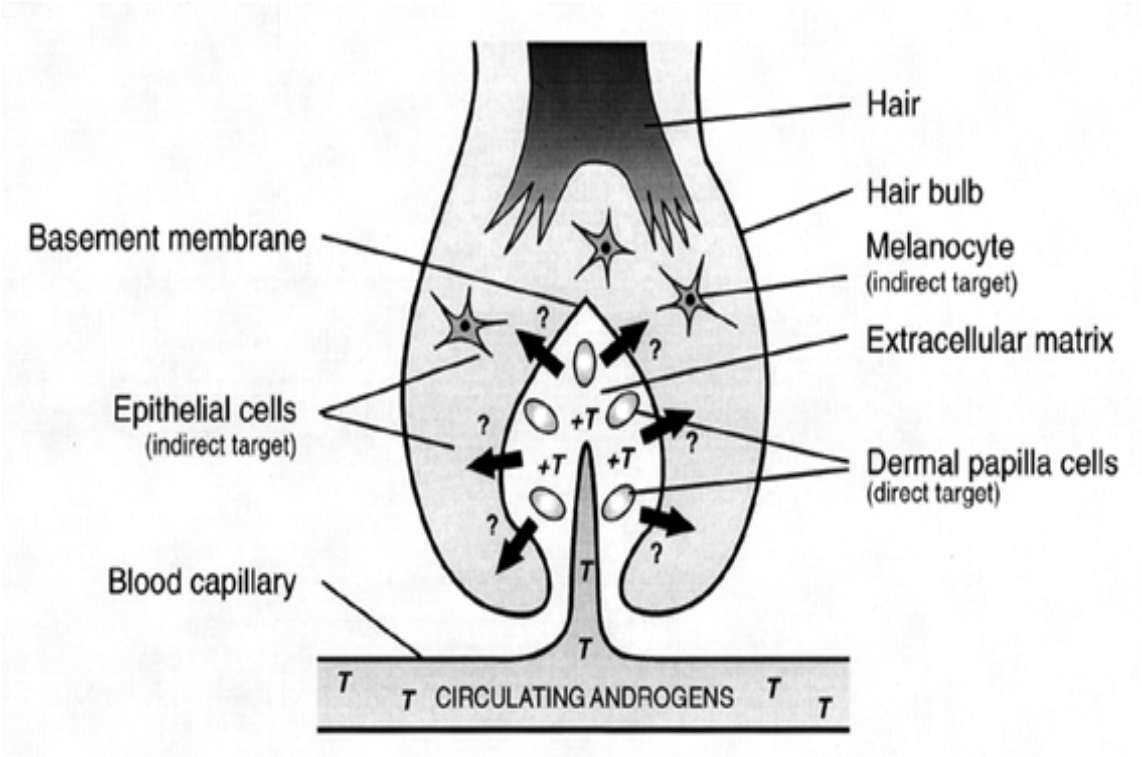

Figure 1.7: Model for the mode of androgen action in the hair follicle. Testosterone (T) is transported to the dermal papilla via the capillary network and diffuses into the DPCs. Once inside the DPCs testosterone is converted to analogues with higher affinity for the androgen receptor (T+). These androgens then cause the transcription and secretion of a range of unknown paracrine factors (?) which diffuse into the extracellular matrix to induce a range of cell functions including proliferation, differentiation and apoptosis. Diagram taken from from Randall, (2000).

1.8.3 Androgenetic alopecia (AGA) and androgens

AGA that affects both men and women, is one of the main clinical conditions of hair growth involving androgens and occurs in genetically predisposed individuals (Hamilton, 1960, Birch and Messenger, 2001). Although AGA is not a life-threatening condition it causes great psychological distress, affecting the individual's quality of life (Moerman, 1988, Wilson *et al.*, 1991). AGA affects at least 50% of Caucasian men by the age of 50 years, and up to 70% of all males in later life (Norwood, 1975). There are marked racial variations in incidence, for example Caucasians are four times more likely to develop AGA than are males of African origin (Setty, 1970). The genetic basis of AGA is polygenic, with the patterning, age of onset and rate of progression being determined through the culmination of a large number of genes, reflecting the complex array of proteins involved in hair growth and patterning (Hoffmann, 2002).

One of the major driving factors of AGA is expression of the X-linked AR gene (Hillmer *et al.*, 2005). This fact leads to AGA occasionally being incorrectly referred to as an autosomal dominant condition (Bergfeld, 1995).

The critical event of AGA is the shortening of the anagen (growth) phase leading to miniaturisation of the hair follicle (**see Figure 1.8**), eventually leading to the transformation of hair from long pigmented terminal to short fine vellus type hair (Paus and Cotsarelis, 1999). This slow transformation occurs in a precise, well defined pattern on the scalp in men where the frontal recession is initiated and is followed by balding on the crown and vertex (Hamilton, 1951, Norwood, 1975). The anagen phase in a normal adult scalp lasts from two to as long as seven years. However, in men with AGA, this decreases from several years to months, or even

weeks, while the telogen phase remains the same or lengthens (Jackson, 2000) as the affected hairs cycle more quickly. This leads to a marked reduction in the anagen-to-telogen ratio from a normal 6 to 8:1 ratio to an abnormal 0.1 to 3:1 ratio (Whiting, 1993). Moreover, the lag period between the telogen and anagen phase becomes progressively longer, leading to a reduction in the number of hairs present on the scalp at any one time (Courtois *et al.*, 1994). The miniaturised hair follicle ascends from the reticular dermis to the papillary dermis (Kligman, 1988). On histological examination of scalp biopsies, the miniaturisation of terminal hairs is often associated with perifollicular lymphocytic infiltration, and eventually fibrosis (Jaworsky *et al.*, 1992).

Androgen receptor expression in the hair follicle is seen only in those mesenchymal portions of the follicle, namely the dermal papilla and the connective tissue sheath; no expression was seen in the matrix cells of the follicle bulb or in the outer root sheath (Choudhry *et al.*, 1992). The keratinocytes of the follicle do not express ARs, highlighting that it is only the mesenchymal cells of the follicle which act as an androgen target (Inui *et al.*, 2000)

Differences in androgen receptor expression have been observed by Randall *et al.*, (Randall *et al.*, 1992), who showed by measuring synthetic androgen bound to endogenous androgen receptors on cultured dermal papillae from androgen-dependent human hair follicles i.e. beard, pubis and scrotum and from relatively non-androgen dependent non-balding scalp follicles, that dermal papilla cultures from androgen dependent follicles express more androgen receptors than those from non-balding areas of the scalp (Hibberts *et al.*, 1998).

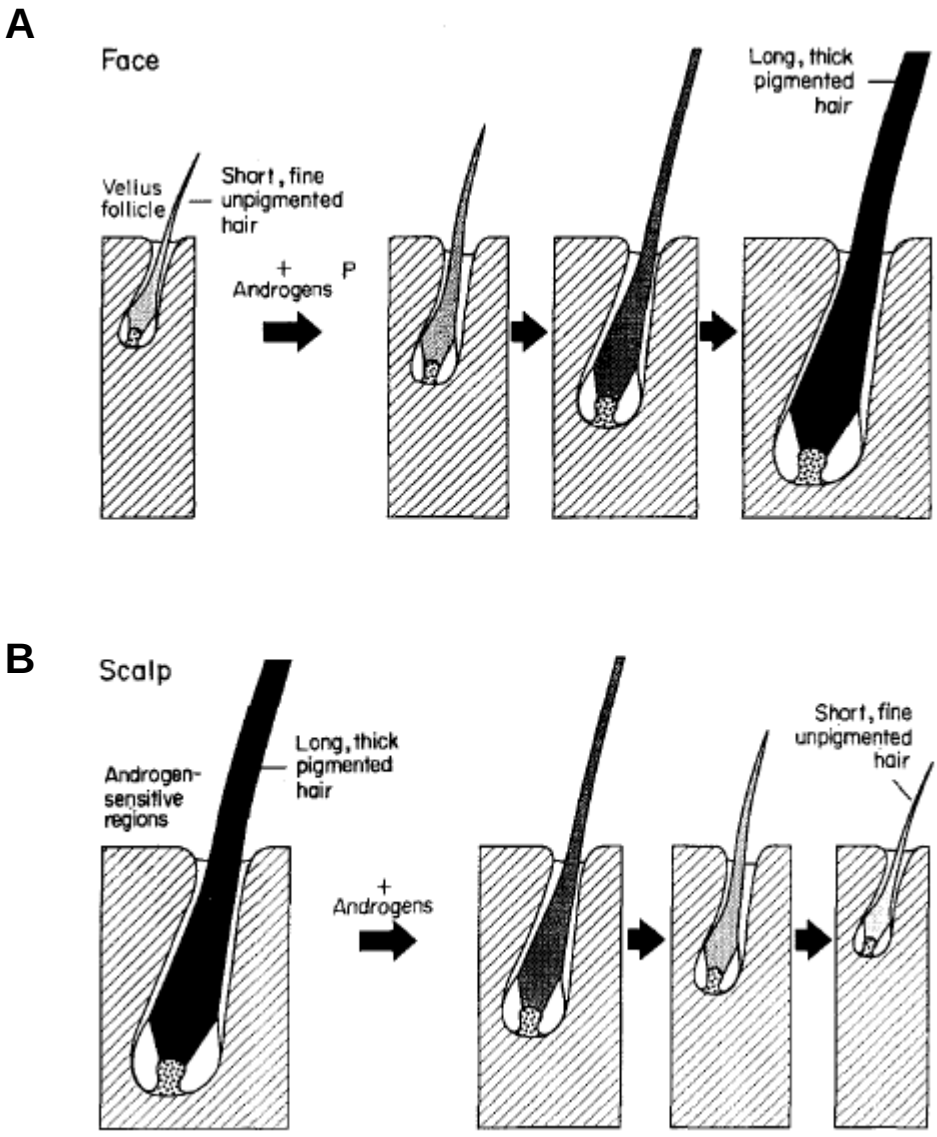

Figure 1.8. Diagrammatic representation of the hair follicles in response to androgens. showing gradual changes which occur in A, in areas stimulated by androgens, e.g. beard and B, on the scalp of genetically disposed individuals.

As steroids act via the mesenchyme in many steroid-dependent tissues, androgens have been proposed to act on epithelial component of the hair follicle indirectly via the dermal papilla (**Figure 1.7**) (Randall *et al.*, 1991, Randall *et al.*, 1994). The DP has been shown to contain androgen receptors (Randall *et al.*, 1991) and it has been proposed that circulating androgens; e.g. testosterone, enter the DP via its blood capillaries and bind to androgen receptors within the DP and cells of androgen-dependent hair follicle.

Follicles from the frontal scalp region of the receding hairline which are neither full terminal nor completely miniaturised vellus follicles are described as intermediate follicles. These follicles when compared to terminal follicles from the occipital region are smaller, less bulbous towards the proximal tip, have a reduced pigmentation of the hair fibre and have a smaller, more rounded dermal papilla (Miranda *et al.*, 2010).

These follicles serve as an effective model for examining the pathogenesis of androgenic alopecia as cells cultured from them exhibit markedly different behaviour when cultured *in vitro*, most notably that they are show a higher sensitivity to altered growth factor secretion when stimulated with androgens (Bahta *et al.*, 2008, Kwack *et al.*, 2008, Inui *et al.*, 2002). Once bound by the androgen receptors present within dermal papilla cells of androgen-sensitive follicles, androgens cause alterations in the production of paracrine regulatory factors. These paracrine factors then influence the activity of other follicular cells. In some follicles, depending on the site of the follicle, testosterone is metabolised to 5alpha-dihydrotestosterone (DHT) prior to binding the androgen receptor (Randall and Ebling 1982). In balding follicles it has been shown that androgens stimulate the production and secretion of inhibitory

growth factors such as TGF-β1 and DKK-1 (Kwack *et al.*, 2012, Inui *et al.*, 2002). However, in the androgen-sensitivehair follicles of regions such as the beard, axilla and pubis androgens have been shown to stimulate the production and secretion of the positive growth factor IGF-1 (Itami *et al.*, 1995).

1.9 Cellular senescence and ageing

Normal diploid cells, enter a state of senescence after a limited number of population doublings, characterised by irreversible growth arrest, enlarged and flattened morphology, and a significantly different gene expression profile. Cellular senescence was first observed by Hayflick and Moorhead (Hayflick and Moorhead, 1961) who characterised the process in normal human fibroblasts which entered a state of irreversible growth arrest after serial cultivation *in vitro*.

In 2007, Itahana *et al.* found that senescent cells show activity of an abnormal β-galactosidase enzyme which is termed senescence-associated β-galactosidase (SA β-gal) activity (Itahana *et al.*, 2007). β-galactosidase is a lysosomal hydrolase and is normally active at pH 4. But the SA β-gal correlated with senescent cells is active at pH 6. Both *in vitro* and *in vivo*, the percentage of cells positive for SA β-gal increases with respectively cumulative population doubling and age (Dimri *et al.* 1995). In addition, it is possible to find association between the increase in SA β-gal and the appearance of the senescent morphotypes (Toussaint *et al.*, 2000). Lysosomes are reported to increase in number and size in senescent cells (Robbins *et al.*, 1970, Brunk *et al.*, 1973). SA β-gal appears to be the result of increased lysosomal activity at a suboptimal pH, which becomes detectable in senescent cells due to an increase in lysosomal contents (Kurz *et al.*, 2000). The results of similar studies suggest that during *in vitro* ageing increased digestion of the cell's organelles

may be associated with an increase of lysosomal mass and SA β-gal (Gerland *et al.*, 2003).

Senescence may contribute to ageing by two mechanisms, namely the net accumulation of senescent cells in tissues, and by limiting the regenerative potential of stem cell pools (Gutteridge 1992). Ageing is a genetic physiological process associated with morphological and functional changes in cellular and extracellular components, forced by throughout- life injury and resulting in a progressive imbalance of the control regulatory systems of the organism, which includes the hormonal, autocrine and neuroendocrine, and immune homeostatic mechanisms (Yu and Yang 1996). Ageing has been characterised as a time-dependent functional decline, leading to the cell's inability to resist external and internal challenges. According to this description, ageing is, therefore, the result of two independent biological processes: the loss of functionality, and the loss of resistance to stress. The causal factors that underlie the time-dependent, deleterious processes of ageing have not yet been well defined, and no single adequate molecular explanation for ageing is currently available. The theory of biological ageing is observed as an organism's failure to maintain homeostasis (Gutteridge 1992). The ageing process's contribution to functional changes are small early in life but rapidly increases with age due to the exponential nature of the process (Harman, 1991, Harman, 1992, Timiras, 1994). The free radical theory of ageing was proposed by Harman in 1954 which suggests that ageing results from imperfect protection against tissue damage caused by free radicals.

1.9.1 $P16^{INK4a}$ and pRB signalling

There are various different stimuli that can induce a senescence response. However, they converge on one or two pathways that establish and maintain senescence growth arrest. These pathways are directed by the tumour suppressor proteins p53, $P16^{INK4a}$ and pRB (Bringold and Serrano, 2000, Campisi, 2001). These proteins are transcriptional regulators. Senescence that occurs after a predetermined number of cell divisions is commonly referred to as replicative senescence which occurs as the result of shortening and/or uncapping of telomeres and is mediated by p53 tumour suppressor protein and its downstream effector, $p21^{Cip1}$(Serrano and Blasco, 2001, Ben-Porath and Weinberg, 2005). Alternatively, cells may senesce rapidly in a telomere-independent manner in response to inadequate culture conditions. This stress-induced premature activation of the senescence program is thought to be mediated by another CDK inhibitor, the $P16^{INK4a}$ protein (Jacobs and de Lange, 2004).

Senescent cells up-regulate $P16^{INK4a}$; which also controls pRB activity (Hara *et al.*, 1996, Alcorta *et al.*, 1996). pRB and $P16^{INK4a}$ function in a common pathway that is important in the growth arrest of cells after a finite number of population doubling. P16INK4a is a positive regulator of pRB and tumour suppressor in its own right (Sherr and McCormick, 2002). $P16^{INK4a}$, acting through the pRB pathway, is thought to be important for the senescence response (Serrano, 1997, Stein *et al.*, 1999, Ohtani *et al.*, 2001, Jacobs and de Lange, 2004). $P16^{INK4a}$ is induced by certain oncogenes (Zhu *et al.*, 1998) and other damage or stress signals (Robles and Adami, 1998, Chen, 2000, Ramirez *et al.*, 2001), and is required for the telomere independent senescence of some cells (Kiyono *et al.*, 1998, Rheinwald *et al.*, 2002). Cell

proliferation may be limited by $P16^{INK4a}$ by a mechanism distinct from that utilised by p53, since some human epithelial cells senesce with relatively long telomeres and high $P16^{INK4a}$ expression (Kiyono *et al.* 1998; Ramirez *et al.* 2001). Moreover, ectopic expression of telomerase does not protect such cells from replicative senescence, suggesting that $P16^{INK4a}$ expression and function are independent of telomere status (Kiyono *et al.* 1998; Ramirez *et al.* 2001). Phosphorylation regulates pRB function by inducing E2F release and following the expression of E2F-dependent proteins, such as cdc2 and cyclin A. These genes are not expressed in senescent fibroblasts dependable with a block in pRB phosphorylation at senescence (Cristofalo *et al.*, 1992). Additionally, pRB is found in a hypophosphorylated state in senescent fibroblasts (Stein *et al.* 1999). Overcoming this senescence block is possible by fusion with cells containing the viral oncogene E7, which binds unphosphorylated pRB (Stein *et al.*, 1999). $P16^{INK4a}$ blocks pRB phosphorylation by binding Cyclin dependent kinases 4 and 6 (cdk4, cdk6) and inhibiting their association with cyclin D (Serrano *et al.*, 1993). This results in a inhibtion of pRB phosphorylation and E2F release and concludes in G1 cell cycle arrest. It has been shown in several studies that $P16^{INK4a}$ levels increase in human and rodent fibroblasts as cells are passed to terminal senescence (Hara *et al.*, 1996, Alcorta *et al.*, 1996). The cell cycle arrest induced by the introduction of $P16^{INK4a}$ occurs only in cells that retain functional pRB (Lukas *et al.*, 1995)

(Lukas *et al.*, 1995). The importance of $P16^{INK4a}$ as a tumour suppressor is highlighted by its regular inactivation in different types of human malignancies (Ruas and Peters, 1998).

The $P16^{INK4a}$ and presumably the pRB pathway activate a barrier to cell proliferation, which cannot be overcome by loss of p53 function. Once the pRB

pathway is engaged, particularly by $P16^{INK4a}$, the senescence growth arrest cannot be reversed by subsequent inactivation of p53, silencing of $P16^{INK4a}$, or inactivation of pRB (Beausejour *et al.*, 2003). Thus, once pRB establishes repressive chromatin at E2F target genes and possibly other loci, maintenance of the heterochromatic domains no longer requires $P16^{INK4a}$ or pRB activity, which explains the remarkable stability of the senescence growth arrest. Thus, the $P16^{INK4a}$ /pRB pathway appears to be particularly important for ensuring that the senescence growth arrest is essentially irreversible and refractory to subsequent inactivation of p53, pRB, or both (Itahana *et al.*, 2001). The p53, $P16^{INK4a}$ and pRB pathways are significant for establishing the replicative senescence of human cells that lead to a growth arrest that cannot be reversed by known physiological signals. However, in the absence of $P16^{INK4a}$ expression, the senescence arrest can be reversed by inactivation of p53.The replicative senescence of human cells, therefore, is not necessarily irreversible once established and $P16^{INK4a}$ plays a critical role in preventing its reversal by p53 inactivation.

$P16^{INK4a}$ and $p19^{ARF}$ ($p14^{ARF}$ in humans) tumour suppressor proteins are encoded in the INK4a locus and the INK4a locus is a critical target of BMI-1. BMI-1 is a transcriptional repressor belonging to the polycomb group gene family (van der Lugt *et al.*, 1994). Polycomb group proteins, and the counteracting trithorax group proteins, are important for maintaining proper gene expression patterns during development (Pirrotta, 1998). BMI-1 was identified as a c-myc-cooperating oncogene in murine B- and T-cell lymphomagenesis (van Lohuizen *et al.*, 1991, Haupt *et al.*, 1991). BMI-1 has a RING finger at the amino-terminus and a central helix-turn-helix domain. It is reported that in WI-38 human foetal lung fibroblasts, BMI-1 is downregulated when the cells undergo replicative senescence. In the

absence of BMI-1, both the $P16^{INK4a}$ and the $p19^{Arf}$ genes from the Ink4a locus are expressed (Quelle *et al.*, 1995). BMI-1 extends replicative lifespan but does not induce immortalisation when overexpressed (Itahana *et al.*, 2003). Lifespan extension by BMI-1 is mediated in part by suppression of the $p16^{Ink4a}$ dependent senescence pathway and requires an intact pRB pathway, but not the p53 tumour-suppressor protein. Furthermore, deletion of RING finger mutant acted as a dominant negative, inducing $p16^{Ink4a}$ and premature senescence (Itahana *et al.* 2003).

1.9.2 The "oxygen paradox"

Most cells are well insulated from environmental oxygen exposure. Within the dermal layers of the skin the concentration of oxygen is 1-5% (Wang, 2005). By taking cells outside our body and exposing them to air, the cells experience the much higher oxygen tension of around 21%. Normally, cell culture conditions include 21% oxygen, which was initially used by Hayflick and Moorhead and most subsequent studies thereafter. Oxygen molecules can be converted into free radicals through chemical and biological reactions. By reducing oxygen tension, we can reduce the level of free radicals. When human dermal fibroblasts are cultured closer to physiological conditions at 3% O_2, they attain a further 20 population doublings (Chen *et al.*, 1995). In contrast, different types of human cells cultured above 21% oxygen exhibit a reduced growth rate and undergo fewer population doublings (von Zglinicki *et al.*, 1995). Similarly, some human cells fail to immortalise even after expressing telomerase, unless grown in low-oxygen environments (Forsyth *et al.*, 2003), demonstrating that the growth arrest of these cells in atmospheric oxygen was not due to telomere-based replicative senescence, but rather stress induced senescence.

Therefore, despite the fact that higher eukaryotic aerobic organisms cannot exist without oxygen, oxygen itself is deleterious to their development an unregulated high concentrations, causing the formation of ROS (see **Section 1.9.3**) which can be deleterious to the cell at high levels. This phenomena is known as the "oxygen paradox" (Davies, 1995).

1.9.3 Reactive oxygen species

Oxygen metabolism produces reactive oxygen species (ROS) that are highly toxic to the cell. ROS are primarily produced in the mitochondria as a by-product of the electron transport chain (ETC). Complex I and complex III of the ETC generate oxygen. Other sources of ROS comprises: the endoplasmic reticulum (through cytochrome P450); the plasma membrane (through the activity of NADPH oxidases); the cytosol (CuZn-SOD); and the Krebs' cycle (aketoglutarate dehydrogenase) (Starkov *et al.*, 2004, Tretter and Adam-Vizi, 2004).

For organisms living in an aerobic environment, exposure to ROS is continuous and unavoidable. These ROS include both free radicals (containing highly reactive unpaired electrons) such as the superoxide anion (O_2^-) hydroxyl radicals (OH^-), nitric oxide (NO^-), and non-radical molecules such as hydrogen peroxide (H_2O_2) and peroxynitrite ($ONOO^-$) (Thannickal and Fanburg 2000). ROS are also from exogenous sources, either being taken up directly by cells from the extracellular surroundings, or produced as a result of the cell's exposure to some environmental stress. Transient variations in ROS serve important regulatory functions, but when present at high and/or sustained levels ROS can cause severe damage to DNA, protein, and lipids. Such deleterious events can then trigger the upregulation of stress-induced senescence cascades such as the $P16^{INK4a}$/pRB pathway.

In addition to this ROS are able to act as cellular signalling molecules in their own right (Thannickal and Fanburg, 2000). Many intracellular signalling molecules contain redox sensitive peptide regions which allow ROS to trigger conformational alterations to their protein structure, conferring the proteins altered binding or transportation properties.

It has been proposed that the pathogenesis of balding may be a ROS-induced process, fitting with the "free-radical theory of ageing" (Trueb, 2009). Greying of the hair follicle has been shown to be at least in part down to a loss of catalase activity (Kauser *et al.*, 2010) (for further reading on catalase see **Section 1.9.4**). Previous work by our group has shown that balding DPCs had a heightened sensitivity to oxidative stress as seen via an upregulation of a number of cellular stress response elements and antioxidants (Bahta *et al.*, 2008).

There are a number of defence systems developed to fight the accumulation of ROS. These include various non-enzymatic molecules (e.g., glutathione, vitamins A, C, and E, and flavenoids) as well as enzymatic scavengers of ROS (e.g. superoxide dismutases (SOD), catalase, and glutathione peroxide). However, these defence mechanisms are not always adequate to counteract the production of ROS, resulting in what is termed a state of oxidative stress (Alaluf *et al.*, 2000, Bai and Cederbaum, 2001, Gutteridge and Quinlan, 1992, Yu and Yang, 1996).

ROS production is also believed to be induced by TGF-β1 and in epithelial cells such as foetal rat hepatocytes or lung fibroblasts of human origin; TGF-β1 induces the production of ROS and a decrease of the antioxidant enzymes early in the apoptotic process (Thannickal and Fanburg, 1995, Herrera *et al.*, 2001). TGF-β1 induces ROS production through NADPH oxidases in foetal rat hepatocytes and

partially via complex I of the mitochondrial respiratory chain. Moreover, it was observed that after exposure to TGF-β1, there was a reduction in the expression of antioxidant enzymes, primarily catalase and Mn-SOD, and treatment with an analogue of Mn-SOD protects against TGF-β1 induced apoptosis. Thus, the early TGF-β1-induced production of ROS has two different mechanisms to mediate, the first of which is the involvement of extra mitochondrial NADPH oxidase-like production of ROS and the second is the rapid down-regulation of antioxidant genes (Herrera *et al.,* 2004a).

1.9.4 Catalase

Catalase is the heme containing tetrameric enzyme found in living organisms, usually located in a cellular organelle called the peroxisome (Chance and Oshino, 1971). Peroxisomes are essential for proper functioning of human cells and they efficiently compartmentalise enzymes responsible for a number of metabolic processes, including the essential β-oxidation of specific fatty acid chains (Chance and Oshino, 1971. These and other oxidative reactions produce hydrogen peroxide, which, in most cases is immediately processed to water and oxygen and the responsible peroxidase: catalase. But, in some circumstances, the tightly regulated balance of hydrogen peroxide producing and degrading activities in peroxisomes is disturbed, leading to the net production and accumulation of hydrogen peroxide (H_2O_2) and downstream reactive oxygen species (ROS). H_2O_2 is a harmful by-product of many normal metabolic processes and must be quickly converted into other, less dangerous substances so as to prevent damage. Catalase is frequently used by cells to rapidly catalyse the decomposition of H_2O_2 into less reactive gaseous oxygen and water molecules (Gaetani *et al.,* 1996). Catalase is disorganised in

ageing, missing or present at reduced levels in certain disease states, and inactivated in response to exposure to specific xenobiotics. H_2O_2 and ROS initiate a negative twist of molecular events resulting in oxidative damage to cellular constituency.. It has been shown that non-toxic concentrations of H_2O_2 drove early passage cells to a senescent-like state which can be demonstrated as a direct connection between accumulation of ROS and ageing (Chen and Ames, 1994). Cell morphology, growth, and function were all affected. Intracellular localisation of catalase and another peroxisomal marker enzyme, alpha-hydroxy acid oxidase (HAOX), in the livers of guinea pig was studied using immunoelectron microscopy and catalase were found in not only in peroxisomes but also in the cytoplasm and the nuclear matrix (Yamamoto *et al.*, 1988).

1.9.5 Glutathione

GSH consists of three amino acids: L-glutamic acid, L-cysteine, and glycine and is formed in a two-step process. Firstly, L-glutamic acid and L-cysteine are covalently bonded via the enzyme glutamate-cysteine ligase (which consists of an essential catalytic subunit - GCL-C - and a rate-limiting modifier subunit – GCL-M); Secondly, the glycine residue is added via glutathione synthetase - GSS.

The L-cysteine residue contains a thiol group. This group may also be termed as a sulfhydryl or -SH group, hence the shorthand GSH.

GSH in its reduced form is able to form a disulphide bond with another molecule of GSH to be oxidised into glutathione disulphide (GSSG). The disulphide bond can be broken by accepting the spare electron from a ROS molecule, thereby neutralising the ROS's reactive potential. Two molecules of reduced GSH can then be reclaimed from the oxidised GSSG via the enzyme glutathione reductase - GSR. Therefore, the

higher the concentration of GSH within the cell, the greater the cells ability to reduce ROS levels (Maher, 2005).

GSH, but not GSSG, is also able to modulate cellular signalling, via intervention in transcription factor signalling (Vayalil *et al.*, 2007). GSH disrupts the binding of both AP-1 and SP-1 to their promoter binding sequences in the DNA thus altering gene transcription as a result. This represents another indirect pathway by which ROS may alter intracellular activity.

1.10 Working Hypothesis

Androgen activity is associated with hair loss (Randall, 2008). Androgens have been found to stimulate a number of growth factors including TGF-β in the DPCs of balding follicles (Inui *et al.*, 2002). TGF-β and androgens have both been linked to oxidative stress (Herrera *et al.*, 2004b, Thannickal and Fanburg, 1995, Pathak *et al.*, 2008). Previous work by our group has shown that balding DPCs senesce prematurely under cell culture conditions and this effect is associated with increased expression of oxidative stress response proteins (Bahta *et al.*, 2008). There is therefore the possibility that either androgen or TGF-β may be indicated in producing this stress response in the balding dermal papilla.

Alternatively, oxidative stress may induce functional changes within cells to cause TGF-β secretion, directly via ROS acting as a signalling molecule (Thannickal and Fanburg, 2000), through crosstalk between antioxidants and TGF-β upstream regulators (Vayalil *et al.*, 2007) or indirectly through downstream senescence mediators which themselves can alter cellular function (Frippiat *et al.*, 2001). Characterisation of the cause-effect relationship between oxidative stress and the androgen-growth factor signalling is a primary aim for this investigation.

In addition it has been found that balding DPCs secrete negative autocrine growth factors whose identity is unknown (Hamada and Randall, 2006). TGF-β is known to be involved in autocrine regulation in other tissues (Geiser *et al.*, 1993). Therefore a secondary aim for this investigation is to assess TGF-β potential role as an autocrine regulator of the DPCs.

Chapter 2

Materials and methods

2.1 Primary cell culture

All experiments described in this study were carried out on primary cells taken from balding male patients. In all cases patient matched samples were taken from the frontal balding region or occipital non-balding region to allow direct comparison of the pathology of balding versus normal hair follicle cell physiology.

All cell culture was performed in a laminar flow hood under aseptic conditions in accordance with standard tissue culture technique. All sterile disposable tissue culture flasks, plates and dishes were purchased from Nunc (Roskilde, Denmark). For tissue culture all centrifuge steps were using an IEC Centra-3C Centrifuge (International Equipment company, Dunstable, U.K.), for sample analysis a SciQuip 1 – 15 K (Sigma-Aldrich, Poole, U.K.) centrifuge was used unless otherwise stated.

2.1.1 Hair follicle acquisition

Hair follicles were donated with patients' consent prior to the patient undertaking elective cosmetic surgery. Hair follicles of the occipital region were acquired as excess redundant tissue from the surgical process. Hair follicles from the frontal balding region were acquired as a 2mm punch biopsy. Follicles were then transferred to transportation media: Williams Media E (Sigma, Poole, U.K.); 100 units/ml Penicillin (PAA, Consett, U.K.); 100mg/ml Streptomycin (PAA, Consett, U.K.); 2 mM L-Glutamine (PAA, Consett, U.K.); 10µg/ml Insulin (Sigma, Poole, U.K.); 100 ng/ml Hydrocortisone (PAA, Consett, U.K.).

2.1.2 Dermal papilla isolation and explant culture

Hair follicle samples were individually transferred to a 30 mm Petri dish containing RPMI cell culture media (PAA Laboratories, Consett, U.K.) mixed (1:1) with

Dulbecco's phosphate buffered saline (DPBS) (PAA Laboratories). All steps were carried out under a stereo dissecting microscope (Nikon, Richmond, U.K.). Using a scalpel (Fisher-Scientific, Leicestershire, U.K.) and watchmakers forceps (Fisher-Scientific, Leicestershire, U.K.) the fibrous dermal tissue and subcutaneous fat were removed. Next, the proximal end of the follicle was transversely dissected just above the distal tip of the DP.

Using 2x microlance-3 needles 25g x 5/8" (Becton Dickinson, Cowley, U.K.) the DP was manipulated from the surrounding connective tissue sheath to expose the connecting stalk between the DP and CTS. The stalk was then dissected from the DP side using needle in a shearing motion.

Three to five DP were dissected in this way and transferred to a T25 cm^2 flask. One ml of DPC media (Williams Media E (Sigma, Poole, UK); 15% (v/v) FBS (Biosera, Ringmer, UK); 100 units/ml Penicillin (PAA, Consett, UK); 100 mg/ml Streptomycin (PAA, Consett, UK); 2 mM L-Glutamine (PAA, Consett, UK); 10 µg/ml Insulin (Sigma, Poole, UK); 100 ng/ml Hydrocortisone (PAA, Consett, UK)) was pipetted into the flask and DPs were left overnight in a Sci-tive stem cell incubator (Ruskinn Technologies, Bridgend, U.K.) to allow DPs to adhere to the flask surface. After ~16 h a further 9 mL of DPC media was added and DPs were left for 2-3 weeks to allow them to explant.

The Sci-tive stem cell incubator (Ruskinn Technologies, Bridgend, U.K.) is an airlocked cell culture chamber, which allows for cells to be cultured, passaged and assayed under controlled oxygen conditions. For the purposes of this investigation DPCs were cultured at 2% oxygen and 5% carbon dioxide, i.e.:- within their normal 1-6 % physiological oxygen levels. After 2 passages cells were then split. Half were

maintained at 2% oxygen while the other half were transferred to a normal cell culture incubator (21% (atmospheric) oxygen and 5% carbon dioxide). For certain experiments DPCs were switched from one oxygen condition to another after a later passage (P4).

Dermal papilla cells (DPCs) were then coded thus: alphabetically according to which patient they had been acquired from and designated as either O (Occipital) or B (Balding), A (grown at atmospheric oxygen levels*) or L (grown at low oxygen levels*) and a number indicating what passage the cells were currently at. (e.g.:- “KoL4”, would indicate the flask contained cells from patient K, from the occipital region, grown under low (2%) oxygen at passage 4.)

2.1.3 Passaging DPCs

DPCs were passaged when they were 70% confluent by washing once in 5 ml DPBS, once in 5 ml Trypsin/EDTA and incubating for approximately 5 min until all the cells had detached. The trypsinisation process was monitored under a Leica DMIRB light microscope and stopped by adding 5 ml culture medium containing 10% (v/v) FBS. The cells were centrifuged at 1,000 G, for 5 min at room temperature. The supernatant was aspirated, the cell pellet resuspended in 10 ml culture medium and the cells counted using a haemocytometer (see **Section 2.2.1**). Cells were then seeded for experiments, propagated at 10-20% of their original density or cryopreserved.

2.1.4 Cryopreservation

Trypsinised cells were centrifuged at 1,000 G at room temperature and resuspended in freezing medium (10% (v/v) diethyl sulphoxide (DMSO) (Fisher-Scientific,

Leicestershire, U.K.), 90% (v/v) complete culture medium containing serum) to a concentration of 2 x 10^6 cells per ml. DMSO was included in the freezing medium to prevent the formation of crystals during the freezing process that would otherwise lyse the cells.

The cell suspension (1 ml) was transferred into each cryovial and frozen to –80°C. After 1 – 3 days, the cell vials were transferred and stored in liquid nitrogen until required.

When cryopresereved cells were required, the vial was removed from liquid nitrogen storage and thawed rapidly at 37°C in a waterbath. As soon as the cell aliquot had thawed, the cells were transferred to a 50 ml centrifuge tube containing 10 ml complete culture medium (relevant to the cell type) and centrifuged at 1,000 G for 5 min. The supernatant DMSO was aspirated and the cell pellet was resuspended in complete culture medium and DPCs were seeded in T75 cm2 flasks at 2 million cells per flask.

2.1.5 Immortalised cell lines

In addition to primary cell cultures, Swiss 3T3 fibroblast cells were purchased from ATCC (Manassas, VA, U.S.A.). This cell line was established from Swiss 3T3 cells that were originally isolated from disaggregated embryos of Swiss mouse and deposited by G. Todaro and H. Green in 1962. The cells were cultured in T75 or T175 cm^2 polystyrene culture flasks with Dulbecco's Modified Eagle's medium (DMEM) (PAA laboratories GmbH, Pasching, Austria) with 10% (v/v) FBS (ATCC, Manassas, VA, U.S.A.), 2 mM L-glutamine (PAA Laboratories GmbH, Pasching, Austria) and 1x penicillin/streptomycin (PAA Laboratories GmbH, Pasching, Austria) at 37°C in an humidified chamber at 5% CO2/95% atmospheric air. The

culture medium was changed every two to three days and the cells were passaged (**Section 2.1.3**) before reaching 70% confluency to prevent transformation.

2.2 Cell counting

Two methods were used for cell counting, depending on the level of accuracy required.

2.2.1 Trypan Blue method

After trypsinisation, cells (10µl of cell suspension) were counted using a haemocytometer (Weber Scientific International Ltd, Middlesex, U.K.). To count live cells, a 10 µl aliquot of cells was diluted 1:2 with trypan blue (Sigma-Aldrich, Poole, U.K.) and 10 µl of this solution was deposited on the haemocytometer. The haemocytometer grid arrangement had four primary squares, each containing sixteen squares. The cells in one of the major squares were counted, those that lay inside the square or touched the top or left boundary were included; those that lay outside the square, or touched the lower or right boundary were excluded. Cells in another major grid were counted and an average of the two counts was taken. The average count was then multiplied by $1x10^4$ to give the value of cells per ml. An average count was multiplied by two to allow for the 1:1 trypan blue to cell dilution factor.

2.2.2 Nucleocassette® method

Where multiple cell cultures required fast quantification and reseeding, Nucleocassettes® (Chemometec, Allerød, Denmark) were used. The Nucleocassettes® contain propidium iodide (PI) which intercalates with the DNA of the cells allowing them to be quickly and accurately be quantified by placing the cassette into the Chemometec 200® - a spectrophotometer.

To prepare samples a 100 µl of trypsinised cells was aliquotted prior to centrifugation and mixed with 100 µl lysis reagent (Chemometec, Allerød, Denmark), briefly vortexed, mixed with 100 µl of neutralisation reagent (Chemometec, Allerød, Denmark) and briefly vortexed again. Lysed samples were then aspirated into the cassette and placed in the spectrophotometer. Readings were given as cells per ml and were multiplied by a factor of 3 (1:2 sample to reagent dilution). Population doublings were calculated as the $\log_2$(cell count at end of passage ÷ cell count at seeding).

2.3 Immunofluorescence cytochemistry

Immunofluorescence cytochemistry is a technique using a fluorescent secondary antibody to detect a primary antibody bound to an antigen (i.e. protein of interest) within a tissue or cell sample. This identifies the expression pattern of a specific protein within the sample.

All primary and secondary antibodies were diluted in 1% (w/v) BSA TBS-T (50 mM Tris base, 140 mM NaCl, 0.1% (v/v) Tween-20, pH 7.6) and all incubations were carried out in a humidified chamber at room temperature. For primary antibodies used see **Table 2.1**. DPCs were seeded (1×10^4) onto sterile 15 mm diameter circular coverslips (VWR, Leicestershire, U.K.) in a 12 well plate and allowed to adhere overnight. DPCs were then washed twice in DPBS and fixed and permeabilised in ice-cold methanol:acetone (1:1 (v/v); (Sigma-Aldrich, Abingdon, U.K) for 2 min. Cells were washed three times in TBS-T for 5 min per wash before incubating in blocking solution, 1% (w/v) BSA (Sigma-Aldrich, Poole, U.K.) TBS-T for 30 min. Coverslips were then removed and inverted on top of 20 µl of blacking solution containing primary antibody (see **Table 2.1**) and were incubated at RT°C for 1 h.

Cells were washed three times for 5 min per wash in TBS-T in a 12 well plate and then inverted onto 20 µl Alexa Fluor® Secondary IgG (H+L) antibodies (2 µg/ml) (Molecular Probes, Invitrogen, Paisley, U.K.) raised against the corresponding species (see **Table 2.1**). Coverslips were incubated in the dark, to prevent photo-bleaching, for 1 h.

Where double staining was required, primary and secondary antibody steps were carried out in parallel, with antibodies combined in the blocking solution/TBS-T.

Protein	Ab raised in	Supplier (Product Code)	Dilution
P16^{INK4a}	Mouse	Santa Cruz Sc-468	1:100
pRB	Mouse	Millipore ABC 132	1:100
BMI-1	Mouse	Millipore 05-637	1:100

Table 2.1: Antibodies and conditions for immunofluorescence. All antibodies were suspended in Serum from animal which secondary Ab had been raised in (4%) TBS-T (v/v).

Cells were washed once in TBS-T and then once in TBS for 5 min per wash. Samples were then washed in TBS containing 2 µg/ml 4',6-diamidion-2-phenylindole dihydrochloride (DAPI) (Sigma-Aldrich, Poole, U.K.).

The coverslips were inverted and mounted with a drop of fluorescent mounting medium (DakoCytomation, Glostrup, Denmark) onto Superfrost® Plus microscope slides (Knittel Glaser, Germany) and allowed to set overnight in the dark at 4°C. The fluorescent signal was observed using a Carl Zeiss Laser Scanning Microscope LSM 510 META (Carl Zeiss Ltd., Hertfordshire, U.K.) and analysed using Zeiss LSM Image Browser software (Carl Zeiss Ltd., Hertfordshire, U.K.).

2.4 Protein analysis

Protein was isolated from DPCs to be used for western blot analysis. Two methods, one using a RIPA buffer and the other a urea buffer, were used to isolate protein as outlined below. Samples were then analysed using the western blot method.

2.4.1 Total protein isolation

DPCs seeded in 6 well plates were washed twice in ice-cold 1 ml DPBS (PAA laboratories GmbH, Pasching, Austria) and then incubated in ice-cold 300 µl RIPA buffer (Tris 50 mM, pH 7.3, NaCl 150 mM, SDS 0.1% (w/v), NP-40 0.1% (v/v) (all from Sigma-Aldrich, Poole, U.K.) and 1X Complete Protease Cocktail Inhibitor (Roche Diagnostics GmbH, Mannheim, Germany) for 20 min. The protein was harvested in 1.5 ml microfuge tubes and pulse sonicated twice for 3 sec (Vibra Cell, Sonic and Material Incs, Danbury, CT, USA). The samples were then centrifuged for 5 min, 4°C, 10,000 x g to remove cell debris. The protein concentration of the

supernatant was determined using a Bradford assay (**Section 2.4.2**) and samples were stored at –80°C.

As an alternative, protein isolation method 8 M urea buffer was used. Cells were seeded in 6 well plates were washed twice in ice-cold 1 ml DPBS and then incubated in 300 µl of 8 M urea buffer (8 M urea, 1 M thiourea, 0.5% (w/v) 3-[(3-cholamidopropyl)dimethylammonio]-1-propanesulfonate (CHAPS), 50 mM dithiothreitol (DTT), 24 mM spermine) for 5 min at room temperature. This is a strong buffer which rapidly lyses the cells and denatures all protein. The sample suspension was harvested in 1.5 ml microfuge tubes and centrifuged at 10,000 x g for 5 min at 4°C. The supernatant (containing protein isolate) was transferred to fresh microfuge tubes and protein concentration was determined by Bradford assay (**Section 2.4.2**) and, if not assayed immediately, samples were stored at -80°C.

2.4.2 Total protein quantification – Bradford assay

The concentration of isolated protein was estimated using the DC Bio-Rad protein assay kit (Bio-Rad Laboratories, Hertfordshire, U.K.) based on the Bradford assay (Bradford, 1976). A protein standard curve was generated using 0.2 to 1.5 mg/ml BSA that had been reconstituted in the same buffer (RIPA or 8M urea) as the samples to be analysed. Protein standard or sample (5 µl) was pipetted in triplicate into well of a clear, flat bottomed 96-well plate (Fisher-Scientific, Leicestershire, U.K.). To this, 25 µl of reagent A^1 was added (a 50:1 mix of reagent A and reagent S) into each well. Following this, 200 µl of reagent B was added to each well and mixed thoroughly. The intensity of the solution colour in each well, which was proportional to the amount of protein, was measured using a spectrophotometer plate reader measuring absorbance at 600 nm (Victor 1420 Multi-Label Counter, Wallac,

PerkinElmer, MA, USA). A standard curve was plotted (intersecting the y-axis at 0 since the value of the blank was subtracted from all readings) and the protein concentration of each sample was calculated according the equation of the straight line from the standard graph. From these readings protein concentrations in the samples were normalised and re-analysed to ensure equal total protein counts in each sample.

2.4.3 Protein analysis

Western blotting can be used to estimate the expression of a specific protein in cell lysates. Protein isolated from the cell is first denatured and then separated according to size by sodium dodecyl sulphate (SDS) gel electrophoresis. SDS applies a negative charge to any positive ion on the protein, thus allowing the protein to be transferred to a nitrocellulose membrane by electrophoresis. A specific protein is then detected on the membrane using a primary antibody, which a secondary antibody that is coupled to horseradish peroxidase (HRP) binds to. The bound secondary antibody can be detected by luminescence due to a chemical reaction with HRP upon the addition of ECL plus (GE Healthcare, Buckinghamshire, U.K.). The resulting light emission is detected using an autoradiography film.

2.4.4 Sodium dodecyl sulphate - polyacrylamide gel electrophoresis (SDS-PAGE)

Protein samples were adjusted to 1 mg/ml protein according to the outcome of the Bradford assay. Protein was reduced and denatured by adding 1:4 Laemmli buffer (Invitrogen Ltd, Paisley, U.K.), 2% (v/v) β-mercaptoethanol (VWR, Leicestershire, U.K.) and heating for 5 min at 95°C. A NuPAGE 10% (w/v) Bis-Tris gel (Invitrogen, Paisley, U.K.) was assembled into a Novex Mini-cell gel electrophoresis

tank (Invitrogen, Paisley, U.K.) according to manufacturers instructions and the tank was filled with 1X MOPS Running buffer (Invitrogen, Paisley, U.K.). Equal protein concentration and volume of each sample was loaded into the wells of the gel. In addition,10 µl of SeeBlue Plus Two protein standard molecular weight marker (Inivtrogen, Paisley, U.K.) was loaded into one well of the gel. The proteins were separated at 200 V for 50 min until the dye front reached the base of the gel.

2.4.5 Western blotting

Proteins were transferred from the polyacrylamide gel to a 45 micron Hybond C Extra nitrocellulose membrane (GE Healthcare, Buckinghamshire, U.K.) in 1X NuPAGE transfer buffer (Invitrogen, Paisley, U.K.) including 10% (v/v) methanol (Fisher-Scientific, Leicestershire, U.K.) at 150 V, 250 mA for 90 min at 4°C. The membrane was removed and immediately immersed in blocking solution and incubated according to **Table 2.2**. The success of the transfer was estimated by checking the protein marker was present on the membrane. The membrane was then incubated in 10 ml of primary antibody (see **Table 2.2** for the conditions of each antibody) on a rocking platform.

The membrane was washed three times for 5 min in TBS-T and then transferred into 10 ml 0.05 mM swine anti-rabbit HRP secondary antibody (DakoCytomation, Glostrup, Denmark) (**Table 2.2**). All secondary antibodies were diluted 1:1000 in the same buffer as the primary antibody and incubated on a rocking platform for 1 h at room temperature. After 1 h the membrane was washed three times for 5 min in TBS-T.

The protein of interest was detected by covering the membrane in 1 ml ECL-Plus chemiluminesence solution (GE Healthcare, Buckinghamshire, U.K.). The blot was

wrapped in cling-film. The resulting luminescence was observed by exposing the blot to light-sensitive Hyperfilm (GE Healthcare, Buckinghamshire, U.K.) for 1 – 30 min, depending on signal intensity, in a dark room and the film was developed using a Hyperprocessor automatic Autoradiography Film Processor (GE Healthcare, Buckinghamshire, U.K.).

2.4.7 Semi-quantitative densitometry analysis

Western blots were semi-quantitatively analysed via densitometry analysis using Image-J software (Public domain, NIH). Measurements were taken as arbitrary units (A.U.) from 3 individual western blots and averaged. Units were normalised against measurements taken from protein loading controls (β-actin or β-tubulin).

2.4.8 Western blot membrane stripping and reprobing

In order to re-use blot membranes, a stripping step was carried out before probing with different antibodies. Thus a housekeeping gene, such as β-actin, can be detected to check equal loading between samples. Membranes were stripped by incubation with stripping buffer (62.5 mM Tris pH 6.8, 2% (w/v) SDS, 100 mM β-mercaptoethanol, all from Sigma-Aldrich, Poole, U.K.) for 30 min at 60°C in an oven on a rocking platform. The blot was then washed three times in TBS-T for 5 min at room temperature and then blocked and re-probed with primary and secondary antibody according to **Section 2.4.5** and **Table 2.2**.

Protein	Ab raised in	Supplier (Product Code)	Dilution	Expected Band (kDa)
TGF-βRI	Rat	R&D MAB5871	1:1000	53
TGF-βRII	Mouse	Abcam ab61213	1:1000	63
$P16^{INK4a}$	Mouse	Santa Cruz sc-468	1:500	16
pRB	Mouse	Millipore ABC132	1:500	110
Catalase	Rabbit	Abcam ab1877	1:1000	65
pSmad3	Rabbit	Cell Signaling #9513	1:500	52
β-actin	Goat	Abcam Ab8229	1:500	42
B-tubulin	Mouse	Millipore 05-611	1:5000	50

Table 2.2: Antibodies and conditions for western blotting. All antibodies were suspended in milk protein (3%) TBS-T (v/v).

Table 2Table 2.2: Antibodies and conditions for western blotting.

2.5 Reverse transcriptase - polymerase chain reaction

Reverse transcriptase-polymerase chain reaction (RT-PCR) is a method to detect genes that are transcribed into RNA in cells or tissue. Extracted RNA is transcribed into cDNA by reverse transcriptase. The presence of a specific DNA sequence is then targeted and amplified by PCR with the aid of oligonucleotide primers that are complementary to the flanking DNA regions of interest. The PCR product is separated by size by running the sample on an ethidium bromide-agarose gel that can be visualised with ultra violet (U.V.) light. If the size of the PCR product correlates with the expected size, the product can be extracted and authenticated with DNA sequencing.

2.5.1 Total RNA extraction from cultured cells

Cells were trypsinised as described in **Section 2.1.3** and centrifuged for 5 min at 1,000 G at room temperature. The cells were then washed twice in ice-cold DPBS and centrifuged for 5 min at 1,000 G. The work surface and pipettes were prepared with RNase Zap (Ambion, Cambridgeshire, U.K.) to remove enzymes that digest RNA. RNA extraction was carried out using an RNeasy Mini Kit (Qiagen, West Sussex, U.K.). All centrifugation steps were at 13,000 G for 15 sec at room temperature unless stated otherwise. All flow-throughs were also discarded unless stated otherwise. The supernatant was aspirated and the cell pellet was resuspended in 600 µl RLT buffer. The RLT buffer acts to lyse the cells and contains guanidine isothiocyanate, which deactivates RNase enzymes. The cell lysate was transferred and passed through a QIAshredder Mini Spin column by centrifugation at 13,000 G for 2 min. The flow through solution was retained and mixed with 600 µl of 70% (v/v) ethanol. The sample was then transferred into an RNeasy Mini Spin column

and RNA (and DNA) within the sample was adhered to the column by centrifugation. RW1 wash buffer (350 µl) was added and the column was centrifuged. Genomic DNA was digested by adding 80 µl 1:5 (v/v) DNase: RDD buffer (RNase Free DNase Set, Qiagen, Crawley, West Sussex, U.K.) to the column and incubating for 15 min at room temperature. The digested DNA was washed from the column with 350 µl RW1 following centrifugation. The column was then washed with 700 µl RPE buffer (part of RNeasy Mini kit) and centrifuged. The column was washed again with 500 µl RPE buffer and centrifuged for 2 min at 13,000 G. Finally, the column was transferred to a fresh RNase-free microfuge tube and the RNA was eluted by addition of 30 µl RNase free water to the column followed by centrifugation at 10,000 G for 1 min. The RNA was stored at -80°C until required.

2.5.2 RNA quantification

Isolated RNA was quantified using a NanoDrop ND-1000 Spectrophotometer (Labtech International Ltd, East Sussex, U.K.). The instrument was blanked against 1.5 µl diethyl-pyrocarbonate (DEPC)-treated water (Sigma-Aldrich, Dorset, U.K.). The sample RNA content and quality was estimated from a 1.5 µl aliquot on the spectrophotometer measured at 260 to 280 nm.

2.5.3 Reverse transcriptase complementary cDNA synthesis

Reverse transcriptase is an enzyme that transcribes single-stranded RNA into doublestranded complimentary DNA (cDNA). Complimentary DNA synthesis from the RNA sample was achieved using SuperScript III First-Strand Synthesis SuperMix (Invitrogen, Paisley, U.K.). Firstly, the following reagents (10 µl 2x RT Reaction Mix, 2 µl RT Enzyme Mix, DEPC-treated water (all from Invitrogen, Paisley, U.K.) and 1 µg of sample RNA (final volume 20 µl) were mixed together

and incubated for 10 min at 25°C. The tube was then incubated for 30 min at 50°C. The cDNA synthesis reaction was terminated by heating the sample to 85°C for 5 min, followed by chilling on ice. Finally, 1 µl (2 units) of *E. coli* RNase H was added to the mix and incubated for 20 min at 37°C to remove the RNA template. The cDNA sample was stored at –20°C until required. To generate two negative controls for PCR, the reverse transcriptase reaction was carried out as described above but with the omission of (a) sample RNA or (b) RT Enzyme Mix.

2.5.4 Primer selection and sequences

Sense and anti-sense oligonucleotide primer sequences for PCR analysis were designed using. Primer 3 using gene sequences from the ensembl database (http://www.ensembl.org/index.html). All primers were checked for non-specific binding using NCBI genebank BLAST analysis (http://blast.ncbi.nlm.nih.gov/Blast.cgi). Primer pairs shown in **Table 2.3**.

2.5.5 Polymerase chain reaction

Polymerase chain reaction (PCR) was conducted by combining 2 µl of cDNA with 0.5 µl of sense primer, 0.5 µl of anti-sense primer, 44 µl 1.1X ReddyMix PCR Master Mix (ABgene, Epsom, Surrey, U.K.) and 3 µl DEPC-treated water in a PCR tube and subjecting the sample to thermal cycling conditions as described in **Table 2.4**. The 1.1x ReddyMix PCR Master Mix contained 1.25 units of Taq DNA polymerase, mM Tris HCl (pH 8.8 at 25°C), 20 mM ammonium sulphate ($(NH_4)2SO_4$), 1.5 mM magnesium chloride ($MgCl_2$). 0.01% Tween 20, 0.2 mM deoxyadenosine 5'-triphosphate (dATP), 0.2 mM deoxycytosine 5'-triphosphate (dCTP), 0.2 mM deoxyguanine 5'-triphosphate (dGTP), 0.2 mM deoxythymine 5'-triphosphate (dTTP), an inert red dye and gel loading precipitant. The 1.1x

ReddyMix was a simple one-step master mix for PCR and also allowed the PCR product to be loaded directly onto an agarose gel without further addition of a loading dye.

Two negative controls (RNA-free and reverse transcriptase enzyme-free) generated from the reverse transcriptase reaction (see **Section 2.5.3**) were concurrently subjected to the PCR. cDNA from mouse 3T3s, an immortalised mouse fibroblast cell line, was used as a positive control for TGF-βRI, TGF-βRII, LTBP1 and LTBP2. Equal loading was confirmed by β-actin.

Target	Forward primer	Reverse Primer	Amplicon (b.p.)
TGF-βRI	AGACGAAGCACACTGGTCCAGC	CGTTACAGTGTTTCTGCCACCT	301
TGF-βRII	AATATCCTCGTGAAGAACGA	CAGTCAACGTCTCACACACC	400
LTBP1	ACCTGCGATTGCTTTGATGG	TCAAGGCGGTATTCAACGGA	207
LTBP2	CCCATCCTTGAGTCTCCTTTGC	GAGGCCATTTCCAGGTAGTAGTTGC	399
B-actin	ATATCGCTGCGCTGGTCGTC	AGGATGGCGTGAGGGAGAGC	516

Table 2.3 PCR Primer pairs. Forward and reverse primers used for RT-PCR analysis with expected amplicon base pair (b.p.) sizes.

Step	Function	Temp (°C)	Duration (sec)	No. Of Cycles
1	Denaturation	95	60	1
2	Denaturation	95	15	30
	Annealing	58-62	30	
	Extension	72	30	
3	Extension	72	300	1
4	Hold	4	∞	∞

Table 2.4: Conditions used during thermal cycling for PCR. PCR cycles conducted according to standard procedure. Cycle number and annealing temperature were optimised according to each primer pair.

2.5.6 Agarose gel electrophoresis

PCR products (10 µl) were loaded on to a 1% (w/v) agarose-tris-acetate ethylediaminetetra-borate acid (TBE) gel containing 1 mg/ml ethidium bromide (Sigma-Aldrich, Poole, U.K.) in a gel tank with TAE running buffer. Ethidium bromide intercalates with DNA, the intercalation causes the ethidium bromide molecule to strongly fluoresce when exposed to U.V. light. This allows for the location of DNA to be visualised on the gel under U.V. light. The samples were run against 10 µl Trackit 1 kB DNA ladder (Invitrogen, Paisley, U.K.), to estimate the product size, and separated by electrophoresis for 30 min at 120 V. Finally the PCR products were visualised by U.V. light and the gel was photographed using a Multi Image Light Cabinet (Alpha Innotech Corporation, San Leandro, CA, U.S.A.).

2.6 Cell senescence

A key difference previously observed in balding DPCs was their greater tendency to senesce at an earlier passage than occipital DPCs (Bahta *et al.*, 2008). While this effect can be easily observed from the flattened morphology and the reduced proliferation rate, two methods (described in **Sections 2.6.1** and **2.6.2**) were used to quantify and compare the level of senescence between the two cell types.

2.6.1 Senescence: X-Gal method

Senescence of cells can be indicated using the pH specific colorimetric dye 5-Bromo-4-chloro-3-indolyl β-D-galactopyranoside (X-Gal) used at pH 6 (Dimri *et al.*, 1995). At this pH only senescent and quiescent cells have active β-galactosidase.

Cells were fixed in 2% (v/v) gluteraldehyde (Sigma-Aldrich, Poole, U.K.) in DPBS (PAA Laboratories) and then incubated in X-Gal staining solution (10mg/mL X-gal,

40 mM citrate, 40 mM sodium phosphate, 2 mM $MgCl_2$, 5 mM potassium ferrocyanide, 5 mM potassium ferricyanide) for 16-24 h.

Photo images of the cells were then taken at x10000 magnification using a brightfield microscope (Leica). Positive cells could be identified as those exhibiting blue staining.

2.6.2 Senescence: 4-MU-Gal method

Senescence was quantified according to the 4-MU-Gal assay first described by Gary and Kindell (2005). DPCs were either grown at 2% or 21% oxygen for the entire duration of their cell culture (7 passages), or switched from one condition to the other at passage 4. DPCs were grown to 80-90% confluence in 12-well plates, for each condition in triplicate. Cells were then lysed in 450 µL of buffer (40 mM citrate, 40 mM sodium phosphate, 5 mM 3-[(3-cholamidopropyl)dimethylammonio]-1-propanesulfonate (CHAPS) and protease inhibitor cocktail (Roche, Lewes, U.K.); buffer adjusted to pH 6.0) and removed from flask into a 1.5 mL polypropylene tubes using a cell scraper.

Lysates were centrifuged for 5min at 12,000 G, the pellet was discarded and the supernatant was mixed with an equal measurement of 2x reaction buffer (40 mM citrate, 40 mM sodium phosphate, 300 mM NaCl, 4 mM $MgCl_2$, 10 mM β-mercaptoethanol and 1.7 mM of 4-MU-Gal (dissolved at 20x concentration in DMSO); buffer adjusted to pH 6.0).

Reaction mix was then incubated at 37°C in a water bath for 1h, after which time 50 µL aliquots were taken and mixed with 400 mM sodium bicarbonate solution to raise the pH from 6.0 to 11.0, thus halting the senescent specific β-galactosidase activity.

Three aliqots (150 µL) of the halted reaction mix were then pipetted into each well of a 96 well plate and measured at excitation/emission wavelengths of 360/465nm.

2.7 ROS quantification

ROS levels were quantified using 5-(and-6)-carboxy-2´,7´-dichlorodihydrofluorescein diacetate (H_2DCFDA) a fluorophore which fluoresces after having its two acetate groups cleaved by intracellular esterases and is subsequently oxidised by ROS (Royall, 1993).

Cells were seeded at 2 x 10^3 into each well of a 96 well plate in DPC media, made up with Red-Phenol-Free William's Media E. Cells were treated with TGF-β1 or BSA control for 1-3h before analysis. After treatment, media was replaced with 100 µL DPC media containing 10 µM of H_2DCFDA, and then incubated wrapped in foil, to prevent photo-bleaching, for 30 min under regular DPC culture conditions.

After incubation H_2DCFDA-containing DPC media was removed, cells were washed 3 times with DPBS and 100 µL of fresh red phenol-free media was added. Cells were measured for fluorescence immediately using a 96 well plate reader set at a temperature of 37°C and an excitation/emission wavelengths of 485/527nm. A kinetic measurement of fluorescence was conducted wherein readings were taken every 5 min for 30 min to give a linear plot of relative fluorescence.

2.8 Total/reduced glutathione assay

Total and reduced glutathione were measured simultaneously using a multiwell kit (Cayman Scientific, Michigan, U.S.A.). Reagents were made up according to the protocol provided.

DPCs were cultured to 70-80% confluence in 6 well plates. Media was removed and cells were washed three times with ice cold DPBS (10 mL). After the third wash DPBS was left on cultures. Using a cell scraper cells were removed from the flask and transferred to a 15 mL centrifuge tube.

The tubes were spun down for at 1,000 G for 5 min at 4°C. DPBS was removed and the pellet was resuspended in 1 mL of ice cold DPBS. Cells were then centrifuged at 10,000 G for 5 min at 4°C. The supernatant was removed and 500 µL of MES buffer was added. Pellets were lysed using a sonicator. Lysed samples were then centrifuged at 18,000 G for 15 min at 4°C. Supernatants were transferred to fresh polypropylene tubes and the pellets were discarded.

An aliquot (50 µL) was taken from the supernatant for protein quantification. The remainder of the supernatant was deproteinated by adding an equal volume of 1 M metaphosphoric acid (MPA)(Sigma-Aldrich, Poole, U.K.) and left to stand for 5 min at RT°C.

Deproteinated samples were centrifuged at 2,000 G for 5 min, 800 µL of supernatant was mixed with 40 µL 4M triethanolamine (TEAM)(Sigma-Aldrich, Poole, U.K.) in a clean polypropylene tube.

To measure only the reduced form of GSH samples divided and half were derivitised using 2-vinylpyridine (Sigma-Aldrich, Poole, U.K.). 1 µL of 1M 2-vinylpyridine was added to 100 µL of each sample. Samples were vortexed and left to stand at RT°C for 1 h.

The cocktail was added to each well using a multiwell pipette set to 150 µL, the plate was then covered, wrapped in foil and placed on an orbital shaker for 5min.

Plate was then put in a Synergy HT fluorescent microplate reader (Biotek, Vermont, U.S.A.) set to measure absorbance at 405nm at 5min intervals for 30min.

2.9 Catalase assay

Samples were prepared for the catalase assay by first growing cells to 70-80% confluence in a 6 well plate under atmospheric or low oxygen conditions. Plates were then washed in ice cold DPBS before having the DPCs removed using a cell scraper (Fisher-Scientific, Leicestershire, U.K.) in 0.5 ml ice-cold DPBS. DPCs were then pelleted at for 5min @ 12,000 G in a refrigerated centrifuge (4°C) and the pellet was sonicated for 3 x 3 seconds (Vibra Cell, Sonic and Material Inc., Danbury, CT, U.S.A.). Sonicated samples were then re-pelleted and the supernatant was removed for protein quantification and subsequent catalase functional analysis.

The catalase assay was carried out using the Molecular Probes: Amplex Red® catalase assay kit (Invitrogen, Paisley, U.K.) according to the protocol provided. Sample, standard or negative controls (25 µL) were pipetted into each well of a 96 well-plate, a further 25 µL of µM H_2O_2 solution was then added to all wells. Plates were then incubated at room temperature for 30 minutes. Following incubation, 50 µL of Amplex Red® reagent containing 1.6 Units/L HRP, 2.6 µg/mL Amplex Red® in DMSO was added to each well and plates were incubated for a further 30 minutes at 37°C while protected from light to prevent photobleaching of the fluorescent reagents. After the incubation period had elapsed, plates were read using a Synergy HT fluorescent microplate reader (Biotek, Vermont, U.S.A.) set at an emission/excitation range of 530/560 nm.

2.10 Growth factor ELISAs

Samples were prepared for the ELISA assay by seeding DPCs at 2 x 10^3 into each well of a 96 well plate and were allowed to adhere overnight. Cells were then treated with 0, 1 or 100 nM of DHT and incubated at either low (2%) O_2 or atmospheric (21%) O_2 for 24 h and then media supernates were collected for ELISA quantification.

Growth factor secretions were quantified using Quantikine® assay kits (R&D, Abingdon, U.K.) according to the protocol provided. Some steps vary between kits, for further details of differing steps see **Table 2.5**. Assay diluent was added to the microplate provided, followed by 50 µl of supernate sample, standard curve control (31.25, 62.5, 125, 250, 500 and 1000 pg/ml for TGF-β1, - β2 and DKK-1 and 0.094, 0.188, 0.375, 0.750, 1.5, 3 and 6 ng/ml for IGF-1) or media blank. Plates were then incubated on an orbital microplate shaker then washed 4 times using the wash buffer provided. Growth factor antibody conjugate was then added to each well and plates were incubated on an orbital microplate shaker then washed 4 times using the wash buffer provided. Finally, the substrate solution was added incubated in the dark for a period of time before terminating the reaction with the stop solution.

Plates were then read using a Synergy HT fluorescent microplate reader (Biotek, Vermont, U.S.A.) measuring absorbance at 450 nm with wavelength correction set to 540 nm to account for the absorbance of the microplate plastic.

Samples being tested for TGF-β had an additional activation step before pipetting the supernatants onto the plate. Both TGF-β1 and - β2 exist as a inactive bound form carried by the latent TGF-β binding protein (LTBP) when secreted from the cells, which is undetectable by the Quantikine® kit's antibodies. To release the active

growth factor samples must first be acidified by adding 1 N HCl to the supernate (1:5), incubating for 15 min followed by neutralisation with 1.2 N Sodium hydroxide (NaOH) (1:5).

Assay	Diluent	Sample, Standard or Blank	Incubation Time A	Growth Factor Conjugate	Incubation Time B	Substrate Solution	Stop Solution
TGF-β1	RD1-21 50 µl	50 µl	2 h	100 µl	2 h	100 µl 30 min	100 µl
TGF-β2	RD1-17 100 µl	100 µl	2 h	200 µl	2 h	200 µl 20 min	50 µl
DKK-1	RD1W 100 µl	100 µl	2 h	200 µl	2 h	200 µl 30 min	50 µl
IGF-1	RD1-53 150 µl	50 µl	2 h 2-8°C	200 µl	1 h 2-8°C	200 µl 30 min	50 µl

Table 2.5: Varying steps for Quantikine® ELISA kits. Assays were conducted according to the manufacturer's protocol.

2.11 Cell Motility Assay

DPCs were seeded at 1 x 10^4 into 6 well plates. Plate was placed on a robotically controlled platform on an inverted light microscope (Nikon, Richmond, U.K.) inside a thermostatically controlled (37°C) chamber maintained at atmospheric oxygen (74% N_2, 5% CO_2, 21% O_2) conditions. DPCs were treated with 10 ng/ml of TGF-β1 or 3% BSA vehicle control at the start of each experiment.

Ten randomly selected points were chosen from each well and photographed using Metamorph software (Molecular Devices Ltd., Wokingham, U.K.). The software then recorded images at these chosen points every 10 minutes moving between them using the robotically controlled platform for 100 cycles.

The resultant images were then sequenced into a time-lapse video, and image analysis was carried out using Metamorph software to assess the velocity of individual cells' movements.

2.12 Statistical Analyses

Statistical analysis was determined using an unpaired Student's t test, one-way analysis of variance (ANOVA) followed by a Tukey *post-hoc* test or two-way ANOVA with Bonferroni *post-hoc* test depending on the number of variables being between test samples, i.e.:- one, two or three, respectively. All statistical evaluations were performed using GraphPad Prism 4.0 software (San Diego, CA, U.S.A.). Significance was assessed in all experiments as a probability value of $*P < 0.05$, $**P < 0.01$, $***P < 0.001$ or non significant (NS) $P > 0.05$. All statistical analyses were carried out using Graphpad Prism 5 Software.

Chapter 3

Effect of oxygen on dermal papilla proliferation and senescence

3.1 Introduction

Recent studies into the pathology of ageing of the hair follicle have begun to focus on the role of oxidative stress. Known instigators of oxidative stress, such as smoking or U.V. radiation have been associated with hair follicle greying (Van Neste and Tobin, 2004) (Arck *et al.*, 2006, Kauser *et al.*, 2010). It has been hypothesised that the pathophysiology of the balding follicle may also be related to the "free-radical" theory of ageing (Trueb, 2009), but as yet there have been no studies carried out investigating the role of oxidative stress in androgenic (AGA).

Previously, our group reported that cultured DPCs taken from balding frontal scalp hair follicles senesced much quicker *in vitro* than DPCs from non-balding occipital scalp follicles (Bahta et al 2008). Moreover, this senescence was associated with elevated expression of $p16^{INK4a}$, known to mediate cell cycle arrest in response to environmental stress. Balding DP also expressed higher levels of stress-response proteins such as heat shock protein 27 (HSP27), super oxide dismutase 1 (SOD1) and catalase. It was therefore proposed that balding DPCs may be more sensitive to environmental stress including oxidative stress and that this may play a role in AGA (Bahta et al 2008).

Under standard laboratory cell culture conditions cells are grown in an atmosphere of CO_2 and air (Freshney, 2005). Under such conditions the oxygen concentration 21%. However, despite its integral role in the physiology of higher eukaryotes, oxygen is in fact toxic to cells at too high a concentration producing an array of harmful reactive oxygen species (ROS). This phenomenon is known as the "oxygen paradox" (Davies, 1995). In the dermal layer of the skin Wang *et al.* (2003) have shown that oxygen is present at around 1-5%, dependent on the proximity to the blood supply of

the capillary network of the sub-papillary plexus and the highly vascularise hair follicles (Wang *et al.*, 2003, Wang *et al.*, 2005). Therefore, culturing cells at low (1-5%) oxygen reduces the toxic effects of oxygen and its production of ROS. As an example of this, growing human fibroblasts under low (3%) oxygen reduces cell stress (as determined by DNA damage), decreases the number of senescent cells and results in a quicker rate of proliferation (Chen *et al.*, 1995). To date, there have been no published reports investigating the effects of low oxygen culture on DPCs.

The primary aim of this chapter was to investigate the effects of oxygen on the growth and senescence of human DPCs from balding and non-balding scalp. To carry out these experiments matched balding and non-balding biopsies were obtained from hair transplant surgery. DPCs were cultured under low oxygen at 2% and atmospheric oxygen at 21% as described in the materials and methods (Chapter 2). The effects of oxygen on DPC viability and cell proliferation were studied using an Alamar Blue cell viability assay and population doublings based on counting cell numbers. Senescence was characterised by cell morphology, senescence associated β-galactosidase (SA-β-Gal) activity and by western blotting for stress-induced senescence markers p16, pRB and BMI-1.

DHT induces different effects within different follicles in a paradoxical manner (Randall, 2007). In the hair follicles of the beard DHT is able to induce the secretion of IGF-1 from the dermal papilla (Itami *et al.*, 1995). IGF-1 is known to stimulate proliferation of the ORS keratinocytes (Itami *et al.*, 1995, Batch *et al.*, 1996). However, in the hair follicles of the balding scalp, DHT has been shown to induce the secretion of TGF-β1 (Inui *et al.*, 2002, Inui *et al.*, 2003, Hibino and Nishiyama, 2004) and DKK-1 (Kwack *et al.*, 2012, Kwack *et al.*, 2008), which induce apoptosis in the ORS keratinocytes, triggering the onset of catagen.

3.2 Aim

To investigate the effect of oxygen on the growth and senescence of human DPCs from balding and occipital (non-balding) scalp.

3.3 Results

3.3.1 Effects of oxygen culture conditions on DPC proliferation – Alamar Blue

The effects of oxygen conditions on human DPC proliferation were investigated by culturing cells from balding and non balding scalp in response to both 2% and 21% oxygen conditions. DPCs were explanted from patient matched balding and non-balding occipital DPCs at 21% oxygen for between 14-21 days and were then passaged and expanded under conditions of 21% oxygen for a further passage as described in **Chapter 2** – Materials and Methods. DPCs were then split between 21% oxygen and 2% oxygen at passage 2 and used for the experiments described below. Alamar Blue was used as a surrogate marker of proliferation.

Figure 3.1 demonstrates that over the course of 10 days occipital DPCs grown at 2% oxygen showed a 16.11 ± 1.42 fold increase in Alamar blue metabolism, while those grown at 21% oxygen underwent 10.18 ± 0.47 fold increase in metabolism. Balding DPCs grown at 2% oxygen showed a 5.63 ± 0.55 fold increase in Alamar blue metabolism, while those grown at 21% oxygen showed a 4.12 ± 0.08 fold increase. Statistical analyses using one-way ANOVA with Tukey *post-hoc* test showed that at 2% oxygen there was a significant increase in both occipital and balding DPCs' proliferation when compared to those grown at 21% oxygen ($P < 0.001$).

These data also confirm previous reports that occipital DPCs proliferate at a consistently higher rate than balding DPCs. Occipital DPCs demonstrated over a threefold increase in proliferation rate compared to balding DPCs at 21% oxygen ($P < 0.001$). In addition, it was found that this effect was also seen at 2% oxygen, with occipital DPCs proliferating at over twofold the rate of balding DPCs ($P < 0.001$).

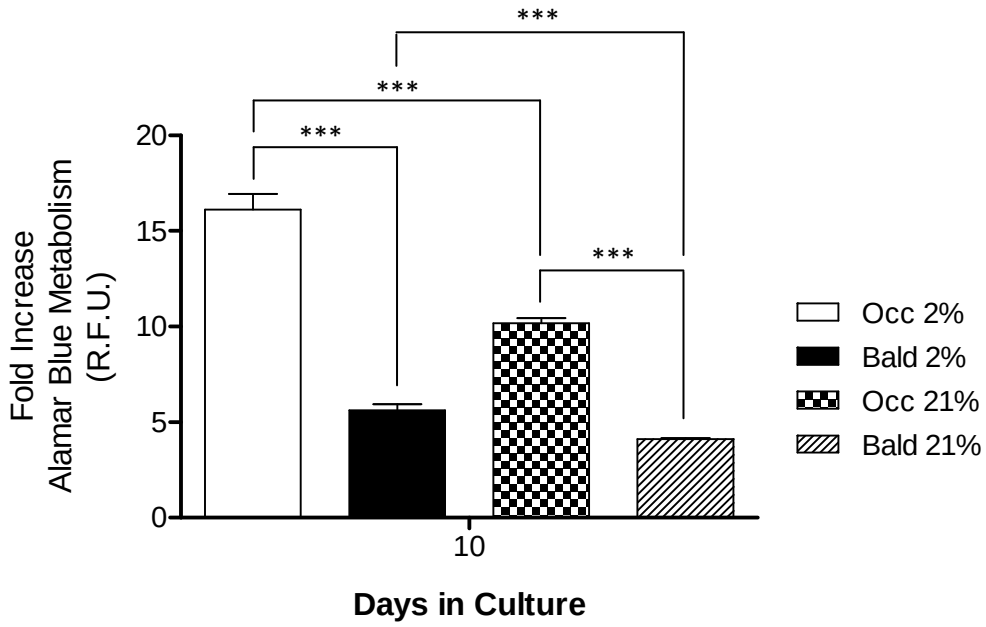

Figure 3.1: Effect of oxygen on DPC proliferation measured by Alamar Blue. Occipital and balding DPCs grown at 2% and 21% oxygen. Proliferation measured as fold increase in metabolism of Alamar blue substrate. DPCs were seeded on day -1. Alamar Blue metabolism was first measured on day 0 and subsequently on day 10. Alamar Blue metabolism was then normalised against the day 0 reading to calculate fold increase in DPCs' growth. Statistical analyses carried out using one-way ANOVA with Tukey *post-hoc* test. ***P < 0.001. Results presented as the mean ± S.E.M. for n = 5 (matched DPC samples from 5 different patients).

3.3.2 Effects of oxygen on DPC proliferation as measured by population doubling

In order to further clarify the effects of 2% and 21% oxygen on the DPCs' proliferation an alternative method was used wherein cell counts were taken at each passage. Cell counter Nucleocassettes were used to measure DPC populations at each passage over a total of 7 passages. Graphing this data gave an effective visualisation of the point at which proliferation rate plateaued indicating loss of proliferative capacity.

Figure 3.2A shows overall proliferation rate of occipital DPCs occurred at a quicker rate and underwent a higher number of population doubling as compared to the balding DPCs (**Figure 3.2B**). For both occipital and balding DPCs, 2% oxygen was shown to maintain a greater proliferation rate compared to 21% oxygen with occipital DPCs undergoing 16.1 ± 0.8 populations doublings at 2% oxygen compared to just 8.2 ± 0.4 population doublings at 21% oxygen. Similarly, balding DPCs cultured at 2% oxygen underwent 12.2 ± 0.4 population doublings compared to only 4.9 ± 0.3 at 21% oxygen.

These data also demonstrate that occipital DPCs undergo a higher number of population doublings under identical conditions compared to balding DPC. Occipital DPCs cultured at 2% oxygen underwent 16.1 ± 0.8 population doublings compared to balding DPCs which underwent 12.2 ± 0.4. Occipital DPCs cultured at 21% oxygen underwent 8.2 ± 0.4 population doublings compared to 4.9 ± 0.3 for balding DPC.

In addition **Figure 3.2** also shows the effects on population doubling of moving cells from 2% to 21% oxygen and from 21% to 2% oxygen. **Figure 3.2A** shows that

occipital DPCs that are initially cultured at 21% oxygen and then switched to 2% are able to recover and begin to undergo a quicker rate of population doubling. However, population doublings were decreased when occipital DPCs were initially grown at 2% oxygen and switched to 21% indicated in a fall in population doublings from 16.1 ± 0.8 when maintained at 2% to 13.5 ± 0.3 when switched to 21% oxygen. Occipital DPCs which were switched from 21% to 2% were able to achieve 9.5 ± 0.4 population doublings compared to 8.2 ± 0.4 of those maintained under 21% throughout their culture.

A similar finding was also observed for balding DPCs (**Figure 3.2B**) switched from 2% oxygen to 21%, where the number of population doublings fell from 12.2 ± 0.4 when maintained at 2% to 9.5 ± 0.04 when switched to 21% oxygen. Balding DPCs which were switched from 21% to 2% underwent 8.2 ± 0.4 population doublings compared to just 4.9 ± 0.3 of those maintained under 21% throughout their culture.

These data confirm that oxygen has an important effect on the proliferation of DPCs *in vitro* with much higher growth rates being observed at 2% oxygen compared to 21%. Moreover, they show that DPCs from occipital scalp consistently proliferate faster than those from balding scalp under identical oxygen conditions.

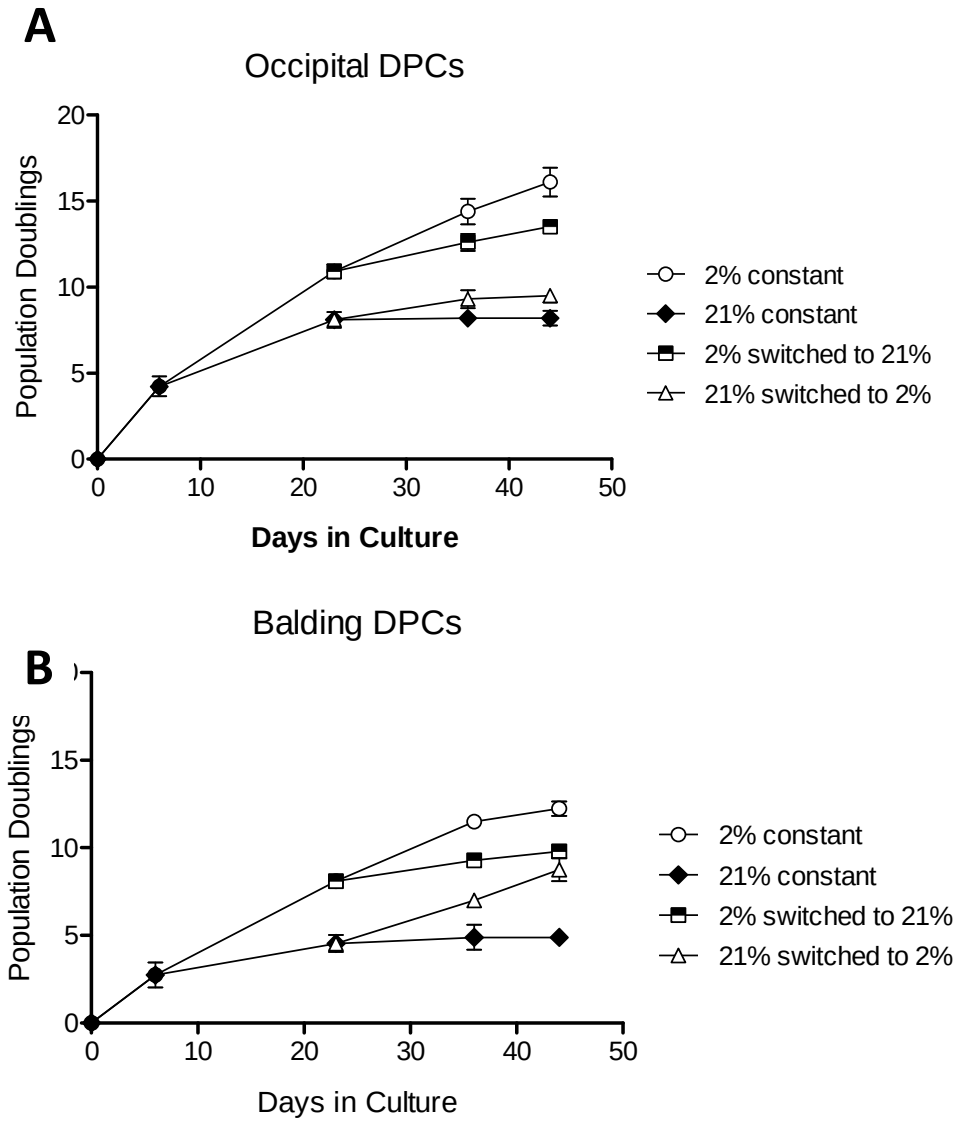

Figure 3.2: Growth of DPCs under different oxygen conditions. Population doublings of occipital (A) and balding (B) DPCs grown at varying oxygen conditions over time. Proliferation was calculated counting the number of cells after each passage. DPCs' proliferation was measured from their initial explantation through to their eventual senescence. DPCs were initially grown at 21% oxygen before being equally split between 2% and 21% oxygen incubators at passage 2. Cultures were then maintained for a further two passages before being split again, this time being either kept under the same oxygen conditions or switched to the opposite oxygen condition. Results are presented as the mean ± S.E.M. for n = 3 (matched DPC samples from 3 different patients).

3.3.3 Effects of oxygen culture conditions on DPC morphology

Morphological differences between balding and occipital DPCs grown under the both oxygen conditions were also apparent at passage 3. Balding DPCs grew in a dispersed, disorganised fashion (**Figure 3.3A and 3.3B**), with those grown at 21% oxygen demonstrating a flattened "fried egg" morphology (arrow 'a') characteristic of senescent cells (**Figure 3.3A**). Balding DPCs cultured at 2% oxygen maintained a spindly morphology (arrow 'b') typical of healthily proliferating fibroblasts.

The occipital phenotype DPCs grew in a more organised, clustered formation (**Figure 3.3C** and **3.3D**). **Figure 3.3C** shows occipital DPCs cultured at 21% oxygen had a flattened morphology, although they notably were not yet demonstrating the "fried egg" senescent appearance, but still clustered in an organised fashion (arrow 'c'). **Figure 3.3D** shows occipital DPCs grown at 2% oxygen arranged to form spindle-like cells, in a clustered pattern with clearly defined pseudopapillae (arrow 'd').

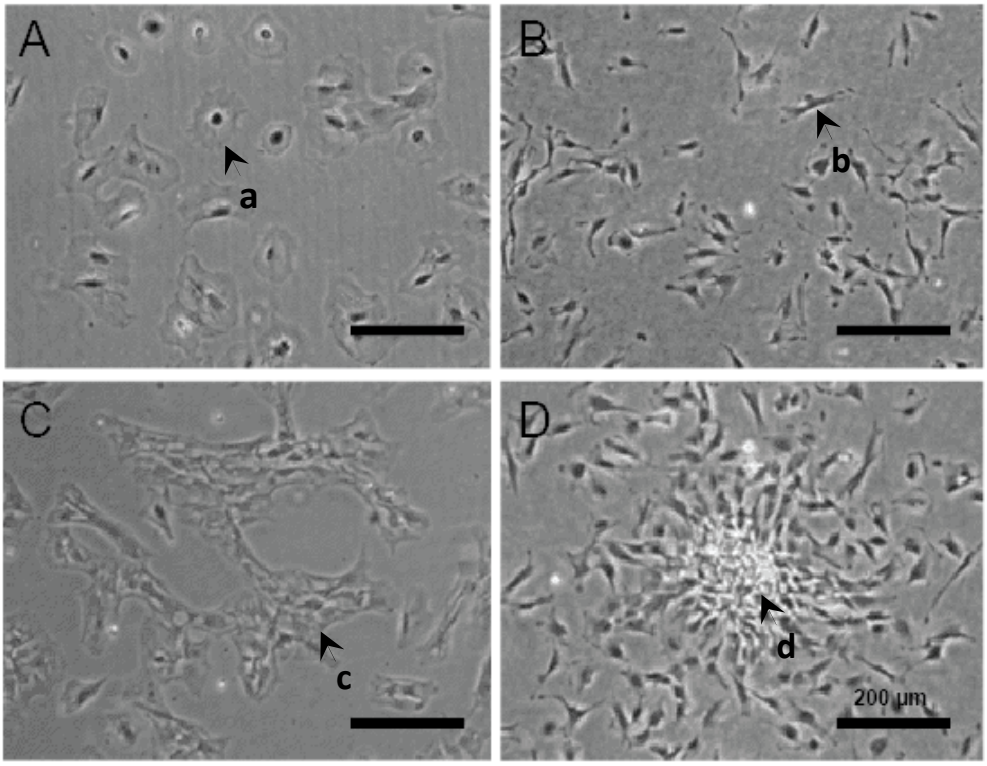

Figure 3.3: Demonstrative morphology and arrangement of DPCs. Balding DPCs at 21% oxygen (A); Balding DPCs at 2% oxygen (B); Occipital DPCs at 21% oxygen (C); Occipital DPCs at 2% oxygen (D). Arrow 'a' – Senescent, 'fried egg', unclustered balding DPC; Arrow 'b' – Spindle-like, unclustered balding DPC; Arrow 'c' – Senescent, 'fried egg', clustered occipital DPCs; Arrow 'd' – raised pseudopapilla formed from spindle-like occipital DPCs. Figures representative of generalised trend of cell morphology.

3.3.4 Effects of oxygen culture conditions on DPC senescence

As shown in **Section 3.3.3**, oxygen had a marked effect on the proliferation of occipital and balding DPCs as determined by total population doublings. In addition, balding DPCs had a much slower growth rate compared to occipital DPCs. To characterise this further, the DPCs analysed for population doublings in **Figure 3.2** were also investigated for cell senescence.

In order to quantify the levels of senescence for both occipital and balding DPCs cultured at both 2% and 21% oxygen conditions senescence associated β-galactosidase (SA-β-Gal) activity at pH 6.0 using 4-MU-Gal was quantified (see **Chapter 2** for description of method).

The data from these experiments has been analysed in two ways. In **Figure 3.4A** and **3.4B** the data have been presented to show DPCs whose early passage (P1-4) began at either 2% (**Figure 3.4A**) or 21% (**Figure 3.4B**) oxygen. This allowed statistical comparison of the differences between occipital (O) and balding (B) DPCs cultured under the culture conditions described above.

In **Figure 3.4C** and **3.4D** the data have been presented to show occipital (**Figure 3.4C**) and balding (**Figure 3.4D**) DPCs. This allowed statistical comparison of the effect of altering the oxygen environment of the DPCs.

From **Figure 3.4A** it can be seen that both occipital and balding DPCs maintained across 6 passages at 2% oxygen had low levels of senescence as shown by the R.F.U. for SA-β-Gal activity of 0.18 ± 0.006 for both occipital and balding DPC. In contrast when balding and occipital DPCs were maintained at 2% oxygen for passage 1-4 and then transferred to 21% oxygen for passage 5 and 6 a marked

increase in DPCs' senescence was observed. From **Figure 3.4A** it can be seen however, that there was a significantly higher ($P < 0.05$) level of senescence in balding DPCs (1.17 ± 0.19 R.F.U.) compared to occipital DPCs (0.68 ± 0.06 R.F.U.).

In **Figure 3.4B** it can be seen that both balding and occipital DPCs maintained at 21% oxygen for passage 1-4 and then switched to 2% oxygen for passage 5 and 6 showed low levels of senesce (0.18 ± 0.006 R.F.U.) that were comparable to cells maintained for all 6 passages at 2% oxygen (**Figure 3.4A**). In contrast, when either balding or occipital DPCs were maintained for all 6 passages at 21% oxygen there was a much higher level of cell senescence (0.8 ± 0.003 R.F.U. and 0.66 ± 0.02 R.F.U., respectively). However, as seen for cells initially maintained at 2% oxygen and then moved to 21% (**Figure 3.4A**) significantly higher levels of senescence ($P < 0.05$) were seen in balding DPCs compared to occipital. From these data it can be concluded that lower levels of senescence are observed in both balding and occipital DPCs when grown at 2% oxygen compared to 21% oxygen.

In **Figure 3.4C** it can be seen that occipital DPCs grown at 2% oxygen for all 6 passages demonstrates significantly lower levels of senescence compared to those grown at 21% oxygen for all 6 passages ($P < 0.001$). Moreover, occipital DPCs which were grown at 2% oxygen during early passage and switched to 21% oxygen during late passage also showed significantly higher levels of senescence (0.68 ± 0.06 R.F.U.) compared to occipital DPCs cultured at 2% oxygen for all 6 passages (0.18 ± 0.007 R.F.U.) ($P < 0.001$). Furthermore, occipital DPCs which were initially cultured at 21% oxygen during early passage and subsequently switched to 2% oxygen at late passage showed significantly lower levels of senescence (0.18 ± 0.009 R.F.U.) as compared to those grown at 21% oxygen for all 6 passages (0.66 ± 0.02 R.F.U.) ($P < 0.001$).

In **Figure 3.4D** it can be seen that balding DPCs grown at 2% oxygen for all 6 passages demonstrates significantly lower levels of senescence compared to those grown at 21% oxygen for all 6 passages ($P < 0.001$). Moreover, balding DPCs which were grown at 2% oxygen during early passage and switched to 21% oxygen during late passage also showed significantly higher levels of senescence (1.17 ± 0.19 R.F.U.) compared to occipital DPCs cultured at 2% oxygen for all 6 passages (0.19 ± 0.011 R.F.U.) ($P < 0.001$). Furthermore, occipital DPCs which were initially cultured at 21% oxygen during early passage and subsequently switched to 2% oxygen at late passage showed significantly lower levels of senescence (0.18 ± 0.004 R.F.U.) as compared to those grown at 21% oxygen for all 6 passages (0.66 ± 0.015 R.F.U.) ($P < 0.001$). Surprisingly, balding DPCs which were initially cultured at 2% oxygen during early passage and then switched to 21% oxygen during late passage showed higher levels of senescence (1.17 ± 0.19 R.F.U.) than balding DPCs grown at 21% oxygen for all 6 passages (0.8 ± 0.003 R.F.U.) ($P < 0.01$).

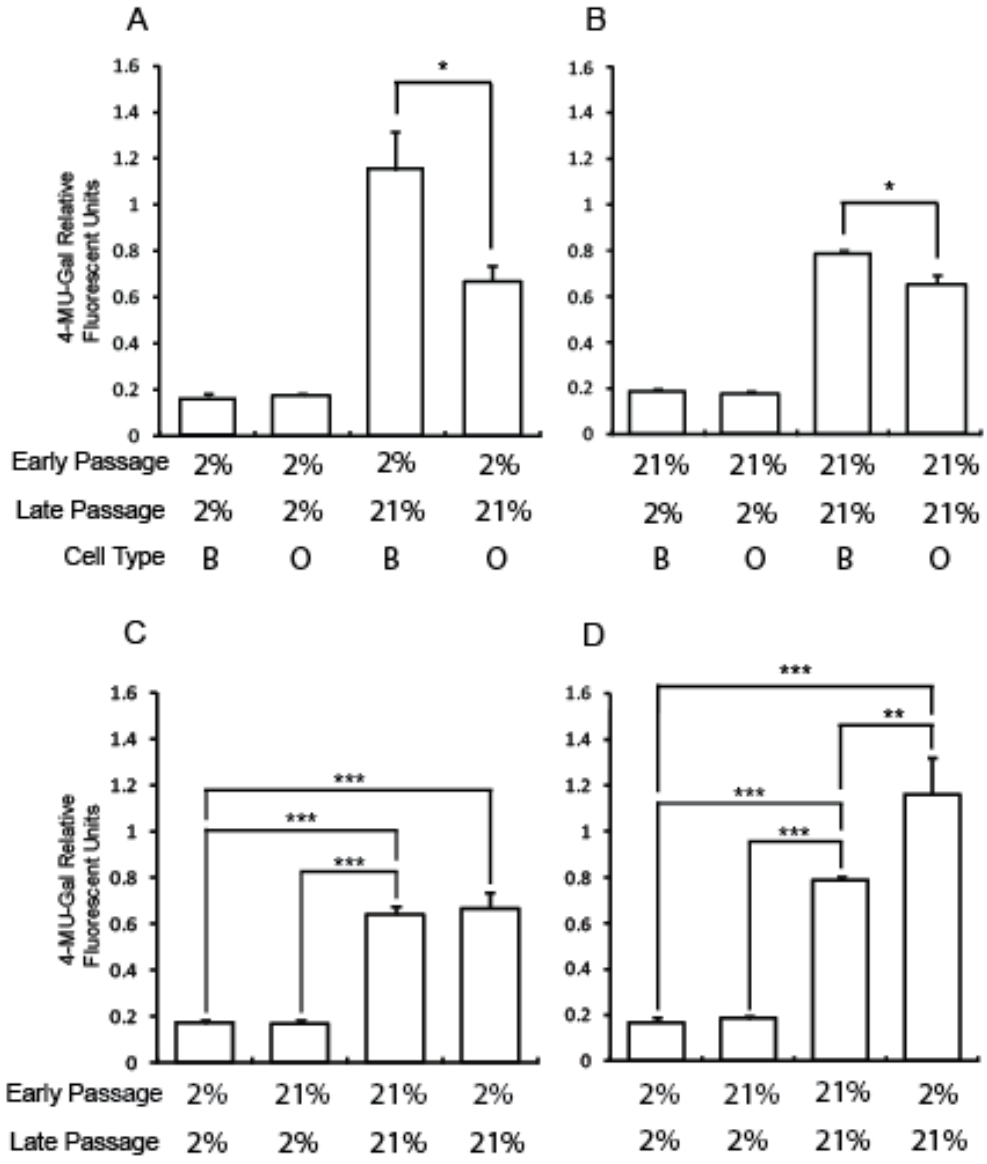

Figure 3.4: Relative levels of senescence in DPCs with varied combinations of oxygen over early (P1-4) and late (P5-6) passage. Senescence quantified using 4-MU-Gal at the end of passage 6 non-balding and balding DPCs first cultured at 2% oxygen (A) or 21% oxygen (B). Data are presented alternately in terms of occipital DPCs (C) and balding DPCs (D) to allow statistical comparison of varying oxygen conditions. Statistical analyses were carried out using one-way ANOVA with Tukey's *post-hoc* test * $P < 0.05$; ** $P < 0.01$; *** $P < 0.001$; Results presented as the mean ± S.E.M. for n = 3 (matched DPC samples from 3 different patients.

3.3.5 Expression of senescence associated proteins

In order to further establish the intracellular mechanism by which senescence was occurring immunocytochemistry and western blot analysis was conducted to confirm the role of stress-induced senescent markers in DPCs under both oxygen conditions. **Figures 3.5A, 3.5C** and **3.5E** show balding DPCs cultured at 2% oxygen exhibited minimal levels of $P16^{INK4a}$ and pRB protein, but a higher expression of BMI-1. Conversely, **Figures 3.5B, 3.5D** and **3.5F** show balding DPCs cultured at 21% oxygen expressed both $P16^{INK4a}$ and pRB protein, with a reduced expression of BMI-1.

Densitometry analysis of the western blots in **Figure 3.6** demonstrates that balding DPCs cultured at 2% oxygen express lower levels of $P16^{INK4a}$ (0.6 A.U.) and pRB (0.4 A.U.) compared to those cultured at 21% oxygen (1.4 and 0.7 A.U., respectively) at early passage (P2). Similarly, the same figure also shows that occipital DPCs expressed lower levels of $P16^{INK4a}$ (0.3 A.U.) and pRB (0.1 A.U.) at 2% oxygen compared to those cultured at 21% oxygen (0.7 and 1.1 A.U., respectively) at early passage (P2). Occipital DPCs also expressed lower levels of $P16^{INK4a}$ and pRB protein when compared to balding DPCs. However, by P4 $P16^{INK4a}$ and pRB protein expression appeared to plateau in both cell types and both conditions, apart from occipital DPCs cultured at 2% oxygen, which had a lower expression of $P16^{INK4a}$ (0.8 compared to 1.0-1.4 A.U.).

Figure 3.7 shows simultaneous immunofluorescence staining for $P16^{INK4a}$ and BMI-1. Occipital DPCs expressed little to no $P16^{INK4a}$ with higher expression of BMI-1 observed in those grown at 2% oxygen. The balding DPCs expressed $P16^{INK4a}$ under

both oxygen conditions, though BMI-1 was still markedly expressed in those grown at 2% oxygen, reflecting that seen with DAB staining. These data confirm that the senescence quantified in **Section 3.3.4** is associated with upregulation of $P16^{INK4a}$.

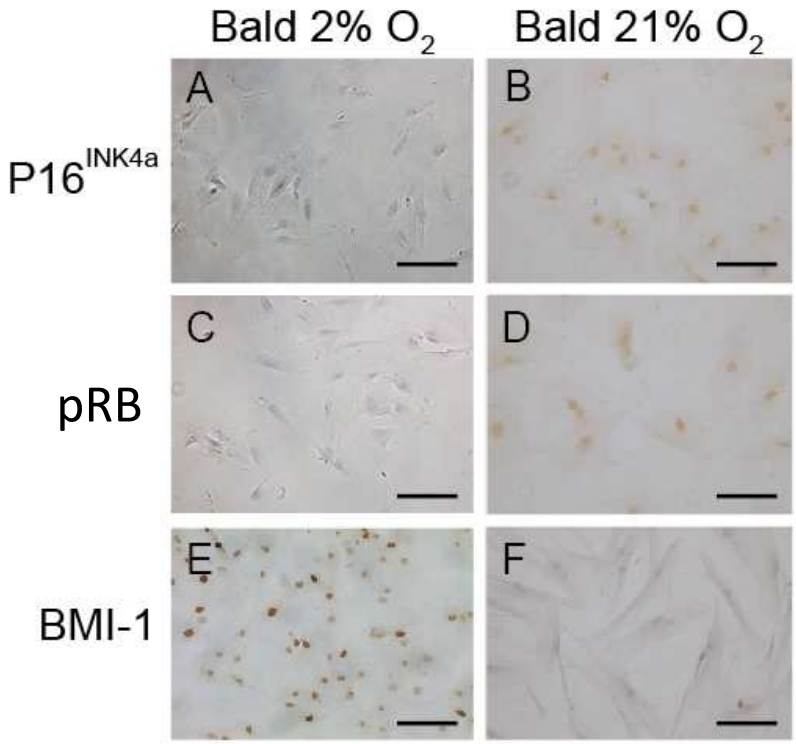

Figure 3.5: DAB Immunocytochemistry staining for P16INK4A, pRB, and BMI-1 in balding DPCs cultured at 2% and 21% oxygen. DPCs were cultured for 3 days prior to fixation and immunostaining. Images are representative of three separate experiments. Scale bar = 50 µm.

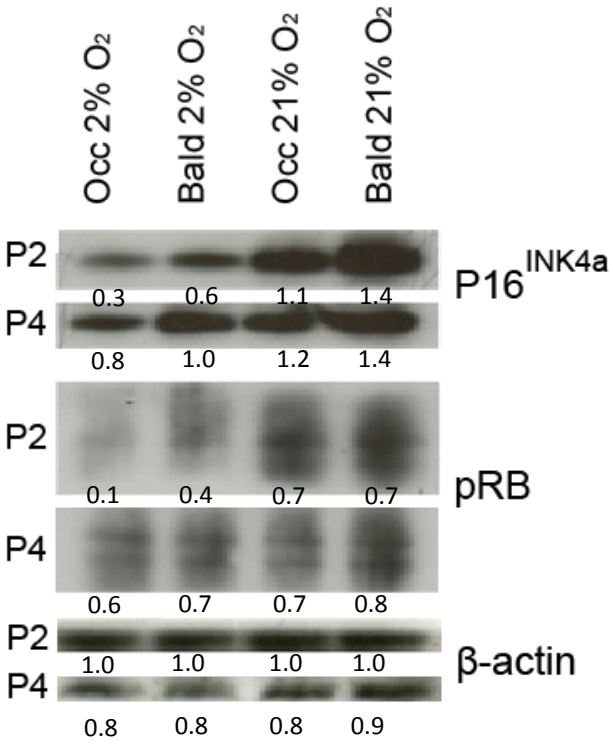

Figure 3.6: Western blot analysis of P16^{INK4a} and pRB protein expression in occipital and balding DPCs cultured at 2% oxygen and 21% oxygen at passages 2 and 4. Protein was isolated from occipital and balding DPCs cultured for 3 days at 2% or 21% oxygen. DPCs were lysed using RIPA buffer, normalised according to total protein concentration and 20 µg of each lysate was run on a Sigma Nu-page electrophoresis gel. β-Actin was used to determine equal protein loading. Blots representative of n = 3 patients. Densitometry values calculated using Image-J software for mean of all 3 blots expressed as a fraction of β-actin control presented below each lane.

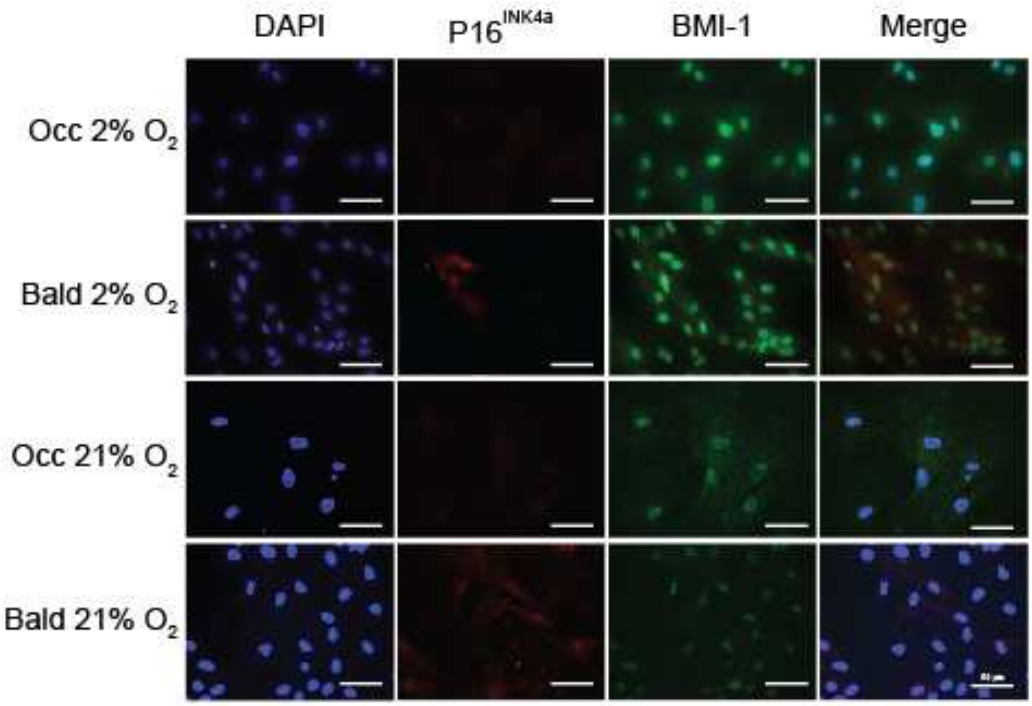

Figure 3.7: Immunofluorescence staining for p16^{INK4a} and BMI-1 in occipital and balding DPCs grown at 2% oxygen and 21% oxygen. DPCs were cultured for 3 days prior to fixation and immunofluorescence staining. Images are representative of three separate experiments. Scale bar = 50 µm.

3.3.6 Effects of oxygen on TGF-β isoform secretion in balding and occipital DPCs

The previous data showed that oxygen conditions can have a profound effect on proliferation and senescence of the DPCs. Therefore oxygen conditions may also have an effect on the dermal papilla's key function – the secretion of growth factors. ELISA kits were used to quantify secretions into the DPC culture media in order to determine the effects of oxygen on secretion of TGF-β isoforms.

Previous studies (Inui *et al.*, 2002) have shown that balding but not occipital DPCs secrete TGF-β in response to DHT stimulation. Therefore, the experiments carried out in this section were done in either the absence or presence of DHT (1 or 100 nM).

Figure 3.8 shows the effects of 2% and 21% oxygen on secretion of TGF-β1 and TGF-β2 isoforms by both occipital and balding DPCs in the presence and absence of DHT. Balding DPCs cultured at 21% oxygen showed a significant stimulation of TGF-β1 secretion when treated with 100nM DHT ($P < 0.01$) although 1 nM DHT had no significant effect ($P > 0.05$)(**Figure 3.8A**). Interestingly, occipital DPCs at 21% oxygen also showed a significant increase in TGF-β1 secretion with 100nM DHT ($P < 0.01$) however 1 nM DHT caused a significant decrease in TGF-β1 secretion ($P < 0.01$). Perhaps more striking was the observation that at 2% oxygen DHT had the opposite effect on balding DPCs at 2% oxygen demonstrating a significant dose-dependent decrease ($P < 0.001$) in TGF-β1 secretion. Similar results were also observed for occipital DPCs with a significant decrease in TGF-β1 secretion at 1 nM ($P < 0.01$) and 100nM DHT ($P < 0.05$).

Figure 3.8B shows that for balding and occipital DPCs cultured at 21% oxygen DHT at 100nM significantly stimulated secretion of TGF-β2 ($P < 0.01$) but at 1nM had no significant effect. However, in contrast to the data seen for TGF-β1 DPCs cultured at 2% oxygen showed no significant stimulation of TGF-β2 in response to either 1nM or 100nM DHT. These data show that oxygen has a significant effect on TGF-β1 and TGF-β2 secretion by both balding and occipital DPCs and suggests that TGF-β secretion may occur in response to conditions of oxidative stress, but only in the presence of 100nM DHT.

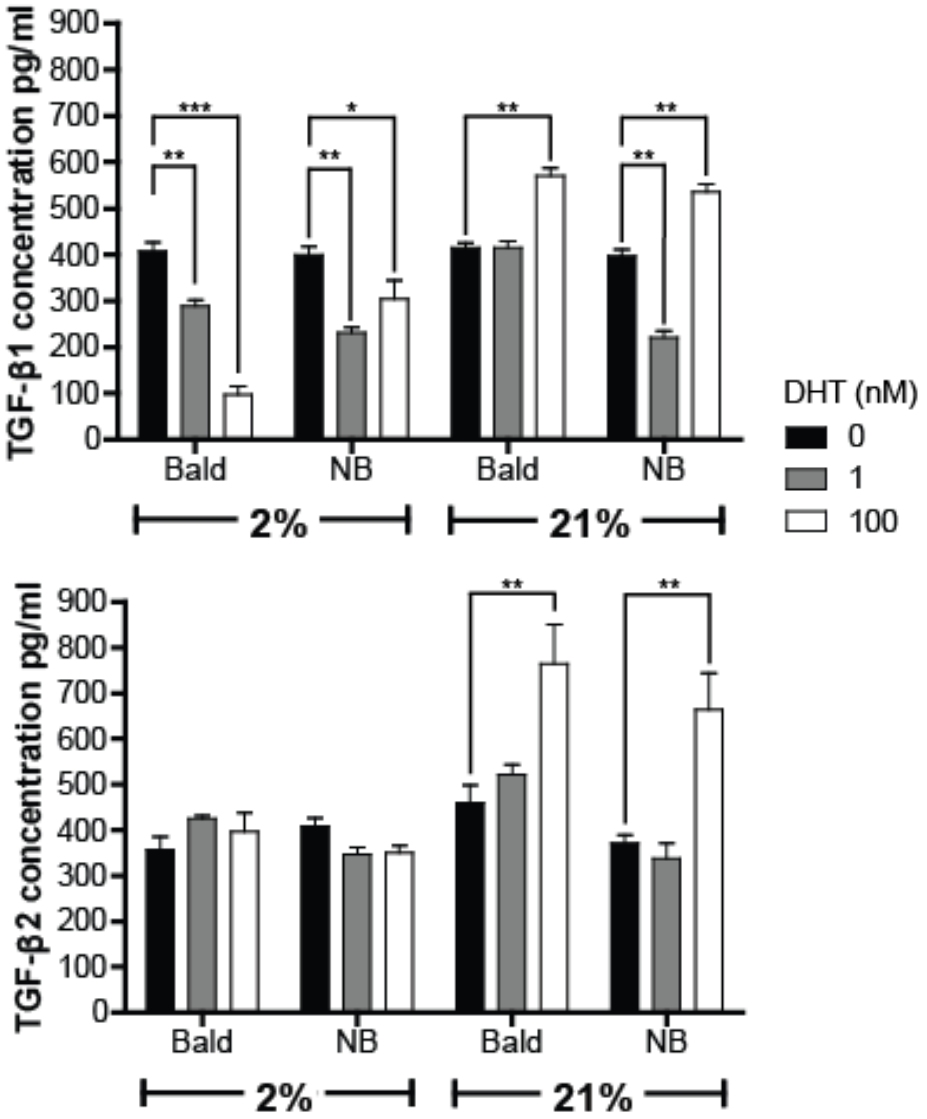

Figure 3.8: ELISAs for TGF-β1 (A) and TGF-β2 (B) secretion by balding and occipital DPCs cultured at 2% and 21% oxygen. DPCs ($2x10^3$ per well) were cultured for 24 h at 2% or 21% oxygen conditions. Cells were treated with 0, 1 or 100 nM of DHT.The culture media were then analysed by R&D Quantikine ELISA kits. Experiments were carried out in duplicate on DPCs from 3 separate patients. Statistical analysis was carried out using one-way ANOVA; * $P < 0.05$; ** $P < 0.01$; *** $P < 0.001$; Results presented as the mean ± S.E.M. for n = 4 (matched DPC samples from 4 different patients).

3.3.7 Effect of oxygen on DKK-1 secretion by cultured DPCs

DKK-1 is another growth factor used as a marker of catagen, therefore the effect of different oxygen conditions on DKK-1 secretion was measured using an ELISA.

Figure 3.9 shows that with 2% oxygen conditions there was no significant difference in DKK-1 secretions between balding and occipital DPCs. However, at 21% oxygen DKK-1 secretions were significantly higher in balding DPCs (323 pg/ml) compared to occipital DPCs (217 pg/ml)($P < 0.05$). Notably there was not a significant change in DKK-1 secretion by either balding or occipital DPCs when comparing between oxygen states, but rather a trend towards a raise in secretion in the balding and a reduction in secretion by the occipital which resulted in the significant difference overall at 21% oxygen.

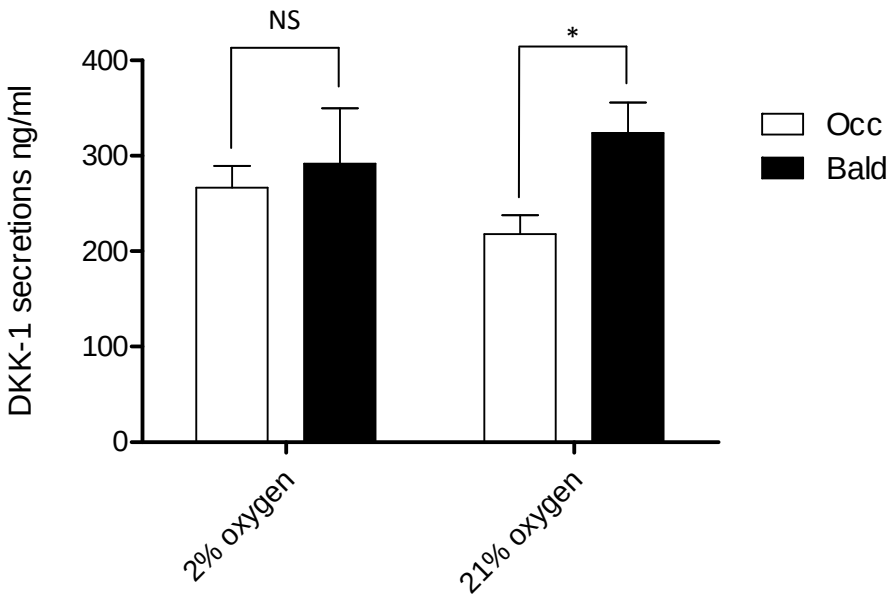

Figure 3.9: ELISA for DKK-1 secretion by balding and occipital DPCs cultured at 2% and 21% oxygen. DPCs ($2x10^3$ per well) were cultured for 24 h at 2% or 21% oxygen. The culture media were then analysed for DKK-1 secretion by ELISA. Measurements were carried out in duplicate in 3 separate patients. Statistical analysis was carried out using one-way ANOVA; * $P < 0.05$, NS $P > 0.05$; Results presented as the mean ± S.E.M. for n = 3 (matched DPC samples from 3 different patients).

3.3.8 Effect of oxygen on IGF-1 secretion by cultured DPCs

IGF-1 is a growth factor associated with the initiation of the anagen growth phase, stimulating the proliferation of the follicular epithelial cells, therefore the effect of different oxygen conditions on DKK-1 secretion was measured using an ELISA.

Figure 3.10 shows that at 2% oxygen conditions occipital DPCs secreted a higher concentration of IGF-1 (347 pg/ml) compared to those cultured at 21% (187 pg/ml)($P < 0.01$). **Figure 3.10** also there was a significant, though not as pronounced increase in IGF-1 in the balding DPCs cultured at 2% oxygen (257 pg/ml) compared to those cultured at 21% oxygen (172 pg/ml) ($P < 0.05$). Overall the occipital DPCs were shown to secrete a significantly higher concentration of IGF-1 than balding DPCs at 2% oxygen ($P < 0.05$), but no significant difference was observed at 21% oxygen.

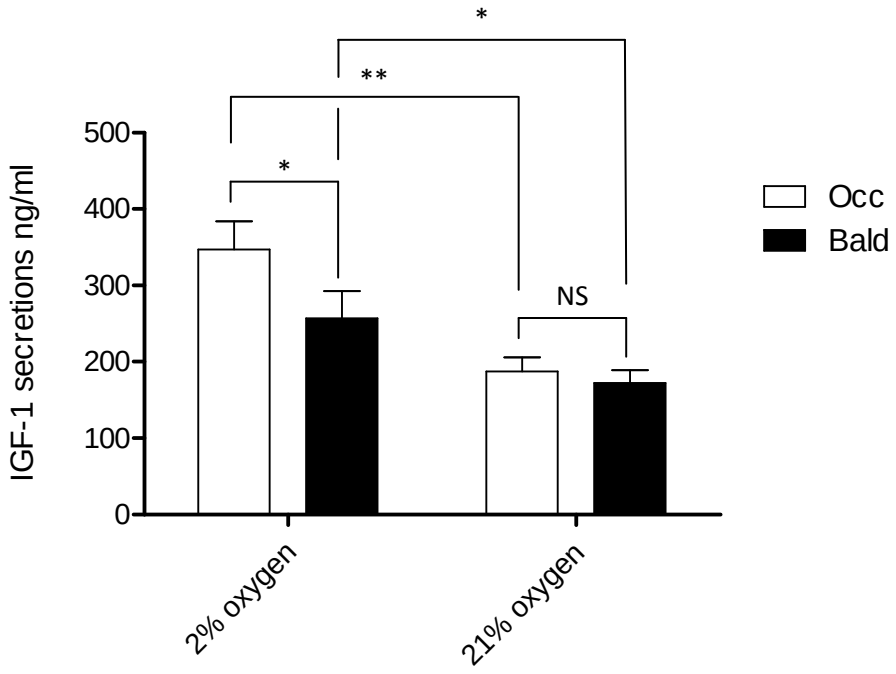

Figure 3.10: ELISA for IGF-1 secretion by balding and occipital DPCs cultured at 2% and 21% oxygen. DPCs ($2x10^3$ per well) were cultured for 24 h at 2% or 21% oxygen. The culture media were then analysed for IGF-1 secretion by ELISA. Measurements were carried out in duplicate in 3 separate patients. Statistical analysis was carried out using one-way ANOVA; * $P < 0.05$, ** $P < 0.01$, NS $P > 0.05$; Results presented as the mean ± S.E.M. for n = 3 (matched DPC samples from 3 different patients).

3.4 Discussion

The findings reported in this chapter highlight two major differences in DPCs with regards to proliferation and senescence. Firstly; as previously reported by our group, balding DPCs proliferate at a slower rate and senesce after fewer passages compared to occipital DPCs (Bahta *et al.*, 2008). Secondly; it was found that low oxygen culture was able to increase proliferation rate of both balding and occipital DPCs as well as delay their senescence. This finding supports previous reports showing that low oxygen culture was able to delay the onset of senescence in human diploid fibroblasts (Chen *et al.*, 1995, Chen *et al.*, 2000, Chen, 2000).

Though many steps may be taken to replicate the *in vivo* hair follicle microenvironment in an *in vitro* model, there are numerous shortcomings which impede the overall health of the DPCs. One such limitation is the cells' exposure to oxygen which is harmful to cells at atmospheric (21%) levels (Davies, 1995). In the case of the cells of the dermal papilla's microenvironment the normal physiological partial pressure of oxygen ranges somewhere between 1-6% (Wang, 2003), while standard cell culture takes place at normal atmospheric levels of 21% oxygen. Carbon dioxide levels were identical in both incubators (5%), while nitrogen effectively accounts for the total remaining air in both. For this study, this affords us an effective model – wherein the normal cell culture conditions at 21% acts as an oxidative stress condition compared to the more physiologically comparable environment of 2% oxygen. This method also allows us to investigate and characterise the use of 2% oxygen for DPCs culture – a method which is yet to be tested for research or clinical use.

One major observation with regards to differences between balding vs. occipital and 21% vs 2% oxygen is ability of cultures to form pseudopapillae. Balding DPCs grow in a disorganised pattern, while the occipital DPCs arrange into clusters. Of the occipital DPCs, it is only those grown at 2% oxygen, which form raised pseudopapillary structures indicative of the maintenance of the DPC's *in vivo* properties (Almond-Roesler *et al.*, 1997).

With regards to the cellular morphology and arrangement of the DPCs, pseudopapillae formation is indicative of the *in vitro* DPCs resemblance of their *in vivo* morphology via their maintenance of cell surface to extracellular matrix (ECM) interaction proteins integrins beta 1, alpha 1, and alpha 5 (Almond-Roesler *et al.*, 1997). Expression of these integrins appears to be imperative to the DPCs' function, as dermal fibroblasts (DF) from the skin lack expression and fail to form pseudopapillae as a result. Furthermore, it has been shown that pseudopapilla formation is associated with expression of alkaline phosphatase (Almond-Roesler *et al.*, 1997), Alkaline phosphatase is an established marker for cell viability as well as a vital component for *de novo* follicle induction by *in vitro* DPCs (McElwee *et al.*, 2003). These findings further support the hypothesis that 2% oxygen helps maintain viability of the DPCs and that occipital DPCs have a functional advantage over balding DPCs under cell culture conditions.

Loss of proliferative capacity and a flattened morphology are both indicators of cellular senescence. Therefore, senescence in the DPCs was measured using the 4-MU-Gal assay (Gary and Kindell, 2005). This assay showed that either balding or occipital DPCs taken at passage 6 from 2% oxygen (whether maintained there for the whole span of their cell culture or merely transferring them during their late passage) would exhibit a low level (0.18 R.F.U. ± 0.006) of SA-β-Gal activity. This suggests

that 2% oxygen can both prevent as well as rescue DPCs from senescence during later passage.

Occipital DPCs exhibited higher levels of SA-β-Gal activity (0.66 R.F.U. ± 0.06), though there was no significant difference between those which were either cultured constantly at 21% oxygen or transferred to 21% oxygen at later passage.

Interestingly, balding DPCs which were cultured at 2% oxygen during early passage but were then transferred to 21% oxygen exhibited a higher level of SA-β-Gal activity (1.17 R.F.U. ± 0.19) compared to balding DPCs grown at 21% oxygen for the entire duration of their cell culture (0.8 R.F.U. ± 0.003). It has been previously reported that although cells grown under low oxygen have a lower accumulation of oxidative damage, they are in fact more sensitised to acute changes in oxygen, either via alteration of their oxygen environment or through treatment with hydrogen peroxide (H_2O_2) (Davies, 1999). In turn cells grown at 21% oxygen, adapt accordingly via upregulation of antioxidants which protect them from entering premature senescence. The data presented here would suggest that the occipital DPCs are more adaptive than the balding DPCs to a change in from 2% to 21%.

To compliment these findings the protein modulators of stress induced senescence were examined. Using immunocytology, it was found that expression of $p16^{INK4a}$ and pRB – established markers of stress-induced senescence (Chen, 2000) – was higher in balding DPCs cultured at 21% oxygen conditions compared with passage-matched samples grown at 2% oxygen conditions. This showed an inverse correlation with expression of BMI-1 – a polycomb transcriptional regulator of $p16^{INK4a}$, whose expression was maintained for longer in balding DPCs cultured at 2% oxygen conditions.

Conversely, balding DPCs grown at 21% oxygen exhibited strong positive staining for both $P16^{INK4A}$ and pRB and showed loss of BMI-1 expression. Furthermore, BMI-1 staining was shown to be maintained at high levels in occipital DPCs under both oxygen conditons.

These findings correlate with the quantitative analysis of senescence levels as measured using the 4-MU-Gal supporting to our group's previous finding of the senescence in balding DPCs being a stress-induced, $P16^{INK4a}$ associated phenomenon (Bahta *et al.*, 2008). Furthermore, these findings are indicative of the fact that $P16^{INK4A}$ and pRB are exaserbated by oxidative stress, with the balding DPCs demonstrated a higher sensitivity.

An important consideration for these findings is that the dermal papilla *in vivo* is not a notably proliferative sub-cellular compartment. Indeed when compared to the epithelial keratinocytes whose cell number fluctuates as the result of rapid proliferation during anagen (Stenn and Paus, 2001) and apoptosis during catagen (Lindner *et al.*, 1997) the number of cells within the DP is relatively stable during the hair follicle growth cycle and the majority of fluctuations in cell number is thought to be accounted for by migration fibroblasts to and from the peripheral CTS (Tobin *et al.*, 2003).

Despite this, the dermal papilla still undergoes marked morphological transformation during the hair cycle (Tobin *et al.*, 2003). Furthermore, the morphology of the balding dermal papilla (small, rounded) *in vivo* is easily distinguished from that of its healthy occipital counterpart (large, "pear"-shaped) (Miranda *et al.*, 2010).

The key changes that occur in the remodelling of the dermal papillae occur as the result of altered an altered extracellular matrix (Messenger *et al.*, 1991b) and migration of the DPCs to and from the adjacent CTS (Tobin *et al.*, 2003).

However, under *in vitro* conditions the DPCs can be rapidly explanted and expanded (Jahoda and Oliver, 1981) at proliferation rates different to their behaviour *in vivo*. This divergence is largely overlooked and in fact it is widely held fact that high proliferation rates equate to healthy, viable cells.

As well as demonstrating the cause of balding DPCs senescence, the up-regulation of $P16^{INK4a}$ and pRB is also of functional importance. pRB has been shown to be a crucial regulator of growth factor secretion in human fibroblasts (Frippiat *et al.*, 2001). Hence, there is a concomitant induction of senescence with an alteration in the cells' growth factor secretions.

A key function of DPCs which is seen in both *in vivo* and *in vitro* conditions is the secretion of growth factors. The induction of catagen thought to occur via the secretion of TGF-β isoforms (Foitzik *et al.*, 2000). Studies using the treatment of androgen analogue R-1881 on balding DPCs caused an increase in both TGF-β1 (Inui *et al.*, 2003) and TGF-β2 (Hibino and Nishiyama, 2004) secretions. The major endogenous androgen responsible for mediating function in the dermal papilla is DHT. For these experiments, when quantifying TGF-β secretions, DPCs were tested in the presence and absence of 1 or 100 nM of DHT.

It was demonstrated that, through modifying the DPCs' oxygen environment, it is possible to regulate TGF-β1 and -β2 when stimulated with DHT (1, 100 nM). Balding DPCs secrete increased TGF-β1 and -β2 when stimulated with 100 nM at 21% oxygen conditions, concurring with previous findings by other groups (Inui *et*

al., 2003, Hibino and Nishiyama, 2004). Culturing the balding DPCs at 2% oxygen was able to negate any increase in DHT-stimulated TGF-β2 secretion (no significant difference between vehicle control and DHT treated cells). Even more notably, balding DPCs cultured at 2% oxygen exhibited a reduced secretion of TGF-β1 as compared to the vehicle control, with the higher dose of DHT (100 nM) conferring a greater decrease in secretion.

Occipital DPCs secrete also demonstrated an increase in TGF-β1 and TGF-β2 when stimulated with 100 nM at 21% oxygen conditions. Conversely, the lower dosage of DHT (1 nM) conferred a decrease in TGF-β1 secretion. Culturing the occipital DPCs at 2% oxygen was able to negate any increase in DHT-stimulated TGF-β2 secretion (no significant difference between vehicle control and DHT treated cells). A 1 nM dose of DHT caused a decrease in TGF-β1 secretion regardless of the oxygen environment, however with the 100 nM dosage of DHT occipital DPCs at 21% oxygen saw an increase in TGF-β1 secretion while at 2% oxygen TGF-β1 secretion decreased.

Taken together these findings suggest that DHT-stimulated TGF-β secretion can be viewed as a form of stress-response when DPCs are under the oxidative-stress inducing environment of 21% oxygen. Simultaneously, 2% oxygen is able to negate or even reduce TGF-β secretion in an isoform specific manner in the presence of DHT. TGF-β is secreted as a stress-response to oxidative stress in a number of other pathophysiological mechanisms, such as pulmonary fibrosis (Cui *et al.*, 2011) heart disease (Yeh *et al.*, 2011) or photo-ageing of the skin (Debacq-Chainiaux *et al.*, 2005).

DKK-1 is also instrumental in regulating catagen (Kwack *et al.*, 2012). For both occipital and balding DPCs changing the oxygen conditions exerted no significant change in DKK-1 secretion. Moreover, at 2% oxygen, there was no significant difference in DKK-1 secretion. However, at 21% oxygen balding DPCs secreted significantly higher levels of DKK-1 compared to occipital DPCs. This demonstrates occipital DPCs lower proclivity towards DKK-1 expression and secretion under a cell stress state, giving further evidence of catagen-inducing growth factors being secreted as a form of stress response.

IGF-1 is an established stimulus for ORS keratinocyte growth (Batch *et al.*, 1996). In this chapter it was shown that at 2% oxygen, IGF-1 expression is higher in both occipital and balding DPCs, with a significantly higher secretion in the occipital DPCs. This demonstrates that occipital DPCs are conferred a greater advantage when under physiological conditions as IGF-1 helps to maintain the hair follicle in its anagen growth phase.

These findings may go some way towards elucidating the paradoxical effects of the androgens on the DPCs wherein different growth factors are secreted by the dermal papilla in response to androgens depending on the hair follicle type (Randall, 2007). It is conceivable that *in vivo* the dermal papilla's growth factor secretion is regulated according to the conditions of the tissue microenvironment. This model of balding as an oxidative-stress induced condition of senescence can be compared to the model of oxidative-stress induced ageing of the skin wherein the DF senesce, alter growth factor secretion and alter their surrounding ECM as a result of increased oxidative stress over time (Reed *et al.*, 1994) (Debacq-Chainiaux *et al.*, 2005).

There is also a potential molecular link between oxidative-stress induced senescence and growth factor secretion. Two possible pathways for pRB-mediated TGF-β upregulation have been shown. pRB is known to regulate the Sp-1 transcription factor (Udvadia *et al.*, 1993) which is a TGF-β1 promoter (Geiser *et al.*, 1993). pRB also mediates the E2F transcription factor which is both responsible for inducing cellular senescence mechanism as well as binding to the TGF-β1 promoter region (Thatikunta *et al.*, 1997). It has been previously shown that H_2O_2-induced oxidative stress of fibroblasts causes a sustained overexpression of TGF-β1 via a pRB regulated pathway (Frippiat *et al.*, 2001). Notably, these cells also senesce, in a pRB-dependent manner as the result of the induced oxidative stress.

In this chapter and in previous work by this group (Bahta *et al.*, 2008) it has been demonstrated that balding cells secrete TGF-β1 and -β2 as well as expressing elevated pRB compared to occipital DPCs. Furthermore, it was demonstrated that culturing both occipital and balding DPCs at low oxygen reduced pRB expression and could either negate or reduce TGF-β1 or -β2 secretion. There is therefore evidence of a concomitant induction of senescence with an upregulation of TGF-β isoforms in the DPCs, however further work must be carried out to confirm whether pRB confers the mediation of TGF-β promoters.

In summary, we confirm the previous finding that balding DPCs proliferate slower and senesce more rapidly than occipital DPCs. Furthermore it was found that low oxygen was able to increase proliferation and delay senescence in both balding and occipital DPCs. Switching cells to 21% oxygen caused senescence after just two passages in both balding and occipital DPCs, with a more pronounced effect seen in the balding DPCs, indicating a higher sensitivity to oxidative stress. Low oxygen caused cells to form in clustered formations and in the case of occipital DPCs, form

pseudopapilla. Levels of senescence correlated with pRB and P16INK4a expression at the protein level as well as in cytochemical analysis. This expression demonstrated an inverse expression pattern to BMI-1 expression. Oxygen conditions were also shown to modulate growth factor secretions with low oxygen, negating or lowering DHT-stimulated TGF-β1 and -β2 secretions. Low oxygen also induced an increase in IGF-1 secretion in both balding and occipital DPCs.

Chapter 4

Effect of oxygen on dermal papilla ROS levels and antioxidant response

4.1 Introduction

Oxidative stress can cause deleterious effects to cells, causing protein misfolding, altering cellular signal transduction and causing DNA double strand breaks (Finkel and Holbrook, 2000). The mitochondria are a major source of oxidative stress (Turrens, 1997). Reactive oxygen species (ROS) are formed as a bi-product of the oxidisation reactions which occur in the electron transport chain (ETC) of the mitochondria. Inefficient activity in the ETC leads to "leakage" of electrons either via cytochrome bc1 or nicotinamide adenine dinucleotide dehydrogenase (Turrens, 1997) which react with oxygen molecules to form superoxide. Superoxides cause a chain reaction of highly volatile molecules containing one or more unpaired electrons. The altered charge on the molecules can then result in malformed protein conformations, with a resultant loss of function.

In vivo, multicellular organisms are able to respond to elevated levels of ROS through upregulated expression of antioxidant proteins and peptides, however this response is gradually lost as a result of the ageing process (reviewed in Wei *et al.*, 2001). Our group has previously shown that balding DPC exhibit a higher expression of stress-response proteins including heat shock protein 27 (HSP27), super oxide dismutase 1 (SOD1) and catalase (Bahta *et al.*, 2008).

Catalase and glutathione are two critical components in which protect cells from the deleterious effects of ROS production. Catalase is responsible for the enzymatic conversion of H_2O_2 into H_2O and O_2 and as such is critical for the reduction of superoxides from the cell (Lin *et al.*, 1995). Active glutathione (GSH) is a reduced sulfhydryl-containing peptide, which can be oxidised to form a homo-dimer – reduced glutathione disulphide (GSSG). This oxidation process requires a free

electron, which it may accept from the unpaired, free-radical electron from a ROS (Maher, 2005). GSSH can be recycled to form two new GSH molecules via the enzyme glutathione reductase. Therefore the most important factor in glutathione metabolism is the active fraction of GSH.

The previous chapter demonstrated that balding DPCs enter senescence more rapidly compared to occipital DPCs, and alter their growth factor secretory function when cultured at 21% oxygen compared to 2% oxygen.

As discussed in **Chapter 3**, the dermal layer of the skin which surrounds the proximal tip of the hair follicle is typically exposed to lower concentrations of oxygen (1-6%) (Wang, 2005) as compared to the normoxic levels of oxygen (20%) used in DPC cell culture (Messenger, 1984).

As discussed in chapter 3, the DHT-TGF-β axis has been proposed as a possible mechanism in the pathology of AGA (Inui *et al.*, 2002). Both DHT (Pathak *et al.*, 2008, Lee *et al.*, 2008) and TGF-β (Senturk *et al.*, 2010, Rhyu *et al.*, 2005) are well established mediators of cellular redox homeostasis. To date no reports have been published examining the relative ROS levels within the balding and occipital DPCs or the effects of DHT and TGF-β on ROS and antioxidants in DPCs.

4.2 Aim

To investigate the levels of ROS and the antioxidants catalase and glutathione in human DPCs from balding and occipital (non-balding) scalp in response to oxygen environment and in response to exogenous DHT and TGF-β.

4.3 Results

4.3.1 Effect of H_2O_2 on ROS levels in cultured DPCs

In order to test the effectiveness of the dichlorodihydrofluorescein diacetate (H_2DCFDA) assay and to determine whether oxidative stress could be induced in balding DPCs. DPCs were treated with acute dosages (0, 10, 100 and 1000 µM) of hydrogen peroxide (H_2O_2) for 30 min. **Figure 4.1** shows the relative levels of ROS in balding DPCs. A low concentration of H_2O_2 (10 µM) exerted no change in ROS levels above the basal level measured with a DPBS vehicle control. At 100 µM H_2O_2 was able to induce a 4.14 fold increase in ROS levels ($P < 0.05$). A higher concentration of 1000 µM H_2O_2 was also tested, but this concentration caused cells to lose adherence from the well plate, therefore this dosage was deemed too toxic for DPCs. Therefore, the H_2DCFDA assay was established as being an effective means of measuring ROS production under oxidative stress conditions.

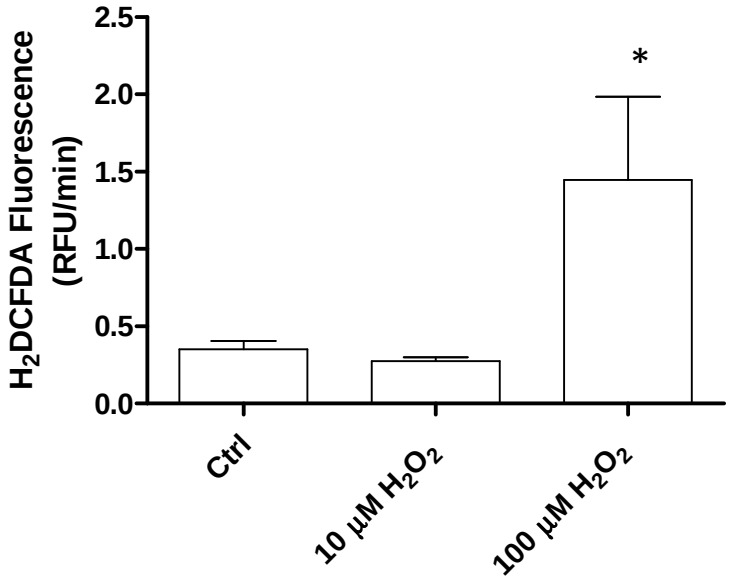

Figure 4.1: H_2DCFDA assay measuring levels of intracellular ROS in balding DPC in response to H_2O_2. DPCs were treated with an acute dose of H_2O_2 for 30 minutes prior to the ROS assay prior to incubating the H_2DCFDA dye 1 h. H_2DCFDA fluorescence was quantified on a heated (37°C) multiwell plate reader with relative fluorescent units (R.F.U.) being measured at 5 minute intervals over 30 minutes. Figures show data expressed as R.F.U./min. Statistical analysis was carried out using Student's t test; * $P < 0.05$; results presented as the mean ± S.E.M. for n = 3 (matched DPC samples from 3 different patients).

4.3.2 Effect of oxygen and passaging on ROS levels in the balding and occipital DPCs

In order to determine the basal levels of ROS within the balding and occipital DPCs, the H_2DCFDA assay was conducted in DPCs cultured at both 2% and 21% oxygen. Measurements were also taken over progressive passages in order to confirm whether oxidative stress had a cumulative effect over the lifespan of the DPC cultures. DPCs were assayed from passage 3 onwards as the volume of cells required for the assay could not be met by cells at passage 2.

Figure 4.2 shows that at early passage there was no statistically significant difference between balding and occipital DPCs cultured at either 2% or 21% oxygen (P3). There was however a 1.98 fold increase (0.276 to 0.449 R.F.U./min) in the level of ROS in the balding DPCs grown at 21% oxygen ($P < 0.01$) as well as a 2.21 fold increase (0.245 to 0.517 R.F.U./min) in the level of ROS in the occipital DPCs grown at 21% oxygen ($P < 0.01$).

At late passage (P4) there was a 3.25 fold increase (0.088 to 0.263 R.F.U./min) in the levels of ROS in balding DPCs compared with occipital DPCs cultured at 2% oxygen ($P < 0.001$) as well as a 0.27 fold increase (0.592 to 0.793 R.F.U./min) in the levels of ROS in balding DPCs compared with occipital DPCs cultured at 21% oxygen ($P < 0.01$). There was also a 3.12 fold increase (0.263 to 0.793 R.F.U./min) in the level of ROS in the balding DPCs grown at 21% oxygen compared to those cultured at 2% oxygen ($P < 0.001$) as well as a 7.63 fold increase (0.88 to 0.592 R.F.U./min) in the level of ROS in the occipital DPCs grown at 21% oxygen compared to those cultured at 2% oxygen ($P < 0.0001$).

At late passage (P5) there was a 0.33 fold increase (0.9 to 1.194 R.F.U./min) in the levels of ROS in balding DPCs compared with occipital DPCs cultured at 21% oxygen ($P < 0.01$). There was no significant difference in ROS levels between balding and occipital DPCs cultured at 2% oxygen. There was also a 0.64 fold increase (0.687 to 1.194 R.F.U./min) in the level of ROS in the balding DPCs grown at 21% oxygen compared to those cultured at 2% oxygen ($P < 0.01$) as well as a 0.37 fold increase (0.635 to 0.9) in the level of ROS in the occipital DPCs grown at 21% oxygen compared to those cultured at 2% oxygen ($P < 0.01$).

The results of these experiments show that oxygen stimulates an increase in ROS in both balding and occipital DPCs. However, with the exception of early passage (P3) cells the increase in ROS is much higher in balding than occipital DPCs.

These data also show a marked effect of cell passage on levels of ROS in both balding and occipital DPCs. At 2% oxygen the increase in ROS is similar with increasing passage between balding and occipital DPCs. However, at 21% oxygen the difference in ROS levels is more marked between balding and occipital DPC at the later passages (P4, P5) with significantly higher levels of ROS in the balding DPC ($P < 0.001$).

These data therefore show that balding DPC are more sensitive to oxygen than occipital DPC with regard to ROS production.

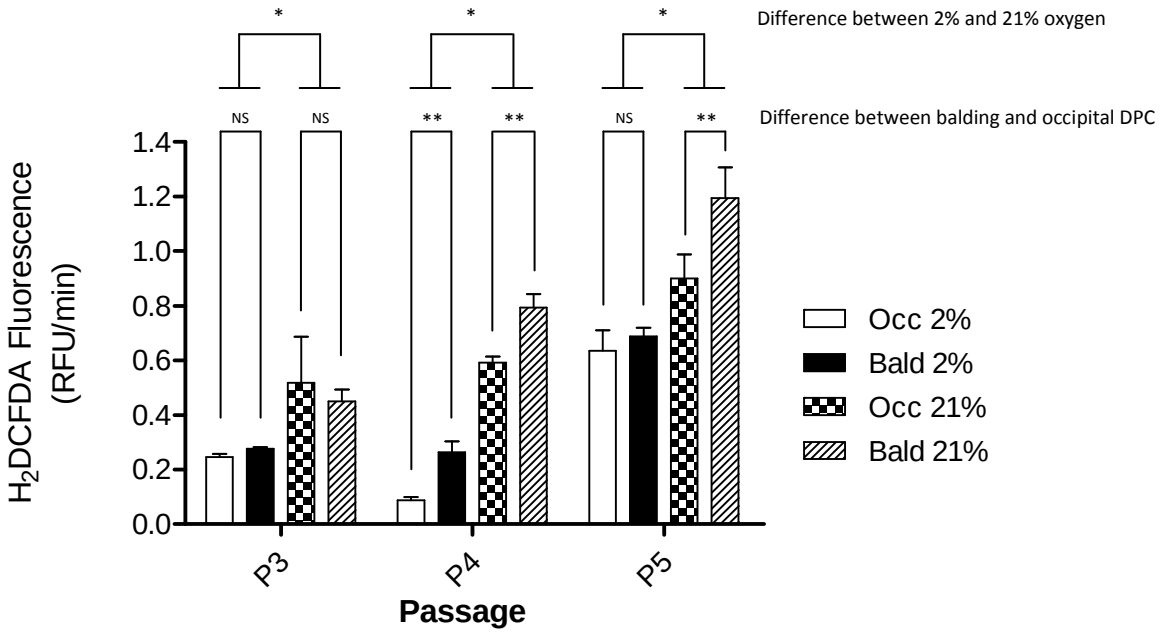

Figure 4.2: Levels of intracellular ROS in balding and occipital DPC over passage at 2% or 21% oxygen over passage 3, 4 and 5. ROS levels, as quantified using the H_2DCFDA assay, were conducted in balding and occipital DPCs cultured at 2% and 21% oxygen. Measurements were taken at each passage from P3 to P5. DPCs were incubated with media containing H_2DCFDA in the dark for 1 h. After 1 h the cells were imaged on a heated (37°C) multiwell plate reader with fluorescence readings (R.F.U.) being taken at 5 minute intervals over 30 minutes. Figures show data expressed as R.F.U./min. Statistical analysis was carried out using Two-way ANOVA with Bonferroni post-test; ** $P < 0.01$, NS indicates $P > 0.05$; Results presented as the mean ± S.E.M. for n = 3 (matched DPC samples from 3 different patients).

4.3.3 Effect of TGF-β1 on ROS levels in the balding and non-balding DPCs.

TGF-β1 is an established mediator of catagen in the hair follicle (Foitzik *et al.*, 2000). It has also been indicated in the modulation of ROS in a range of different cell types (Senturk *et al.*, 2010, Rhyu *et al.*, 2005). Therefore intracellular ROS production in response to a supraphysiological dose of TGF-β1 (10ng/ml) was measured in balding and occipital DPCs. The findings are presented in **Figure 4.3**.

Using two-way ANOVA analysis with Bonferroni post-test there was no significant change in ROS production in response to TGF-β1 compared to DPBS vehicle control in balding or occipital DPCs at either 2% or 21% oxygen. These data indicate that the modulatory effect of TGF-β1 on ROS production observed in other cell types is not applicable in DPCs.

Two-way ANOVA analysis with Bonferroni *post-hoc* test indicated a significantly higher ($P < 0.001$) level of ROS in DPCs grown at 21% oxygen compared to those grown at 2% oxygen. Moreover, it was found that balding DPCs produced significantly higher levels of ROS compared to occipital DPCs at 21% ($P < 0.05$), but not 2% oxygen ($P > 0.05$). These data concur with that presented in **Figure 4.2** supporting the findings and acting as a positive control for the H_2DCFDA assay's effectiveness. The two-way ANOVA indicated a non-significant ($P > 0.05$) interaction effect between the variables of oxygen condition and TGF-β1 treatment.

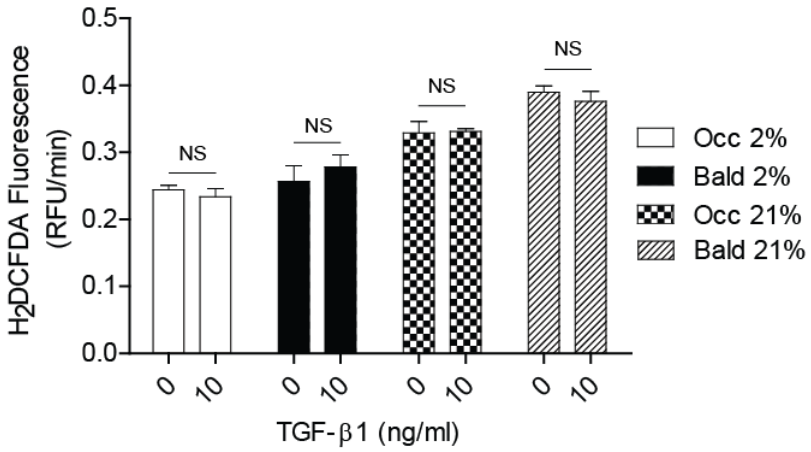

Figure 4.3: ROS levels of in balding and occipital DPC in response to TGF-β1 at 2% and 21% oxygen conditions. Using the H_2DCFDA assay, ROS-levels were measured in passage 3 balding and occipital DPCs in the presence or absence of 10 ng/ml TGF-β1 at 2% (A) or 21% (B) oxygen. DPCs were incubated with TGF-β1 for 1 h, following which H_2DCFDA dye was added to the media and cells were incubated at 37°C in the dark for 1 h. Cells were subsequently imaged on a heated (37°C) multiwell plate reader with fluorescence readings (R.F.U.) being taken at 5 minute intervals over 30 minutes. Figures show data expressed as R.F.U./min. Measurements carried out in duplicate in samples from 3 different patients. Statistical analyses were carried out using two-way ANOVA between cell type with Bonferroni post-test; NS indicates no significant difference; Results presented as the mean ± S.E.M. for n = 3 (matched DPC samples from 3 different patients).

4.3.4 Effect of DHT on ROS levels in the balding and non-balding DPCs

DHT plays a critical role in the pathogenesis of AGA and is also an established modulator of ROS in androgen sensitive tissues such as mouse embryonic stem cells (Pathak *et al.*, 2008, Lee *et al.*, 2008). To date there have been no published reports investigating the effect of DHT on ROS levels in DPCs. To establish whether DHT also affected ROS production in DPCs balding and occipital DPCs were incubated with DHT (1, 100 nM) for 1 h and then internal ROS production was measured using H_2DCFDA.

Using the two-way ANOVA with Bonferroni post-test **Figure 4.4** shows that DHT caused no significant increase in ROS levels in occipital DPCs cultured at 2% oxygen, however DHT was able to induce a dose responsive decrease in ROS levels in balding DPCs cultured at 2% oxygen at 1 and 100 nM ($P < 0.01$ and $P < 0.001$, respectively). **Figure 4.4** also shows that DHT did not induce an effect on ROS levels in either balding or occipital DPCs cultured at 21% oxygen. There was, however, a significant difference in ROS between balding and occipital DPCs and between cells grown at 2% or 21% oxygen.

The two-way ANOVA indicated a significant difference ($P < 0.001$) in the expression of ROS between both cell types when cultured at 2% or 21% oxygen, thus concurring with the data presented in **Figure 3.2** showing oxygen conditions affected intracellular ROS levels. This finding also acts as a positive control for the H_2DCFDA assay's effectiveness.

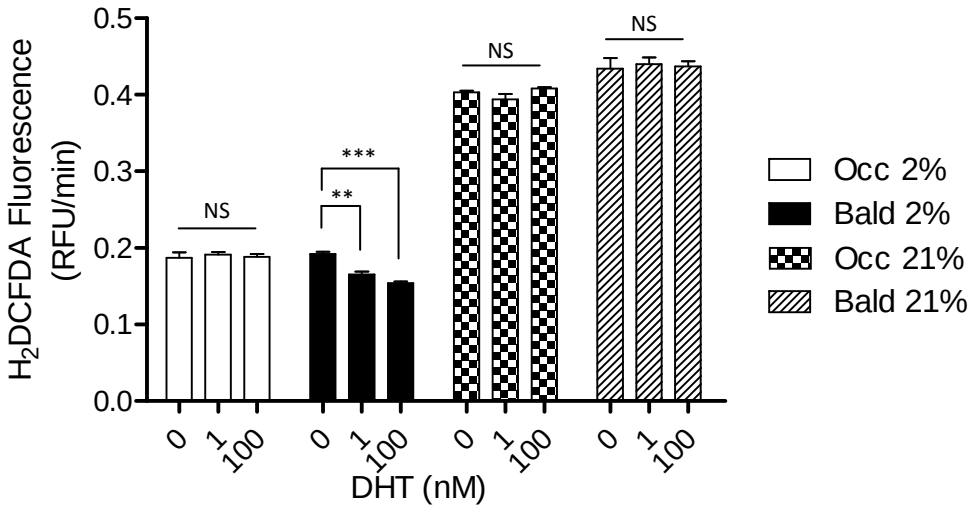

Figure 4.4: ROS levels of in balding and occipital DPC in response to DHT cultured at 2% and 21% oxygen. Using the H_2DCFDA assay, ROS-levels were measured in passage 3 balding and occipital DPCs with a treatment of 0, 1 or 100 nM of DHT cultured at 2% (A) or 21% (B) oxygen. Measurements were taken at passage 3. DPCs were incubated with DHT for 1 h, following which H_2DCFDA dye was added to the media and cells were incubated at 37°C in the dark for 1 h. Cells were subsequently imaged on a heated (37°C) multiwell plate reader with fluorescence readings (R.F.U.) being taken at 5 minute intervals over 30 minutes. Figures show data expressed as R.F.U./min. Measurements were conducted in duplicate in samples from 4 different patients. Statistical analyses were carried out using two-way ANOVA with Bonferroni t-test between cell type; ** $P < 0.01$, *** $P < 0.001$; NS indicates no significant difference. Results presented as the mean ± S.E.M. for n = 4 (matched DPC samples from 4 different patients).

4.3.5 Catalase expression in balding and occipital DPCs cultured at 2% and 21% oxygen

Catalase is responsible for the enzymatic conversion of H_2O_2 into H_2O and O_2 and as such is critical for the reduction of superoxides from the cell (Lin *et al.*, 1995).

Densitometry analysis of the western blot in **Figure 4.5** demonstrates that balding DPCs cultured at 2% oxygen express lower levels of catalase (0.4 A.U.) compared to those cultured at 21% oxygen (1.1 A.U) at early passage (P2). Similarly, the same figure also shows that occipital DPCs expressed only trace levels of catalase at 2% oxygen (< 0.1 A.U.) compared to those cultured at 21% oxygen (0.9 A.U). Occipital DPCs also expressed lower levels of catalase when compared to balding DPCs. From **Figure 4.5** it can also be seen that catalase expression appears to plateau by late passage (P4), in both cell types, under both conditions (1.1-1.2 A.U.).

These findings correlate with the data shown in **Figure 4.2** demonstrating that higher catalase expression was observed in those cells which had a higher level of ROS i.e.:- balding DPCs or DPCs cultured at 21% oxygen. This suggests a homeostatic response of catalase to help regulate ROS; however it is important to note that despite catalase expression it appears to be unable to maintain ROS levels at those seen in the occipital DPCs.

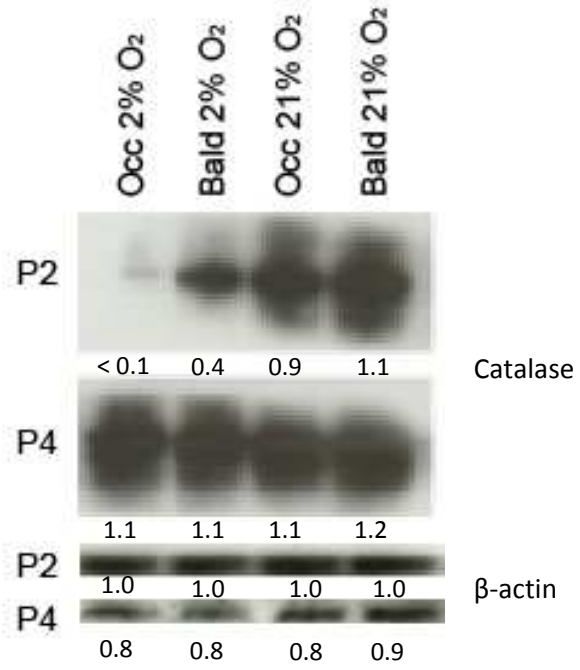

Figure 4.5: Western blot analysis of catalase expression in occipital and balding DPCs cultured at 2% or 21% oxygen at passages 2 and 4. Protein was isolated from occipital and balding DPCs cultured for 3 days at 2% or 21% oxygen. DPCs were lysed using RIPA buffer, normalised according to total protein count via the Bradford assay and 20 µg of each lysate was run on a Sigma Nu-page electrophoresis gel. β-actin was used to confirm equal protein loading. Densitometry values calculated using Image-J software for mean of all 3 blots expressed as a fraction of β-actin control presented below each lane.

4.3.6 Functional analysis of catalase in balding and occipital DPCs

A functional catalase assay was used to further establish the difference in catalase expression in balding and occipital DPCs cultured at both oxygen conditions. In addition to this, based on the findings detailed in **Figure 4.4** catalase activity in response to DHT (100 nM) was tested. Assays were conducted on early passage (P2) DPCs before the plateau effect observed in **Figure 4.5** in order to detect the most biologically significant differences.

Figure 4.6 shows catalase activity in was higher in balding DPCs (40.8 nM/min) compared to occipital DPCs (25.8 nM/min) cultured at 2% oxygen ($P < 0.01$). Catalase activity was also higher in balding DPCs (71.7 nM/min) compared to occipital DPCs (47.3 nM/min) cultured at 21% oxygen ($P < 0.01$). Overall catalase activity was higher in both balding and occipital DPCs when cultured at 21% oxygen compared to 2% oxygen ($P < 0.01$ for both cell types). These data concur with the western blot analysis shown in **Figure 4.5** confirming that increased catalase expression directly correlates with its increased activity.

DPCs were treated with DHT (100 nM) at either 2% or 21% oxygen. **Figure 4.6** shows that DHT was able to increase catalase activity in DPCs grown at 2% oxygen. Balding DPCs saw an increase in catalase activity from 40.8 nM/min in control treated cells to 61.9 nM/min when treated with DHT (100 nM) ($P < 0.01$). Similarly, occipital DPCs saw an increase in catalase activity from 25.8 nM/min in control treated cells to 38.5 nM/min when treated with DHT (100 nM) ($P < 0.01$). DHT (100 nM) exerted no significant effect ($P > 0.05$) on balding or occipital DPCs when cultured at 21% oxygen.

These data taken with the findings in **Figure 4.4**, wherein it was shown that DHT could reduce ROS production in balding DPCs cultured at 2% oxygen, indicate DHT as having a role in protecting the balding DPCs from oxidative stress via modulating catalase and its resultant antioxidative function.

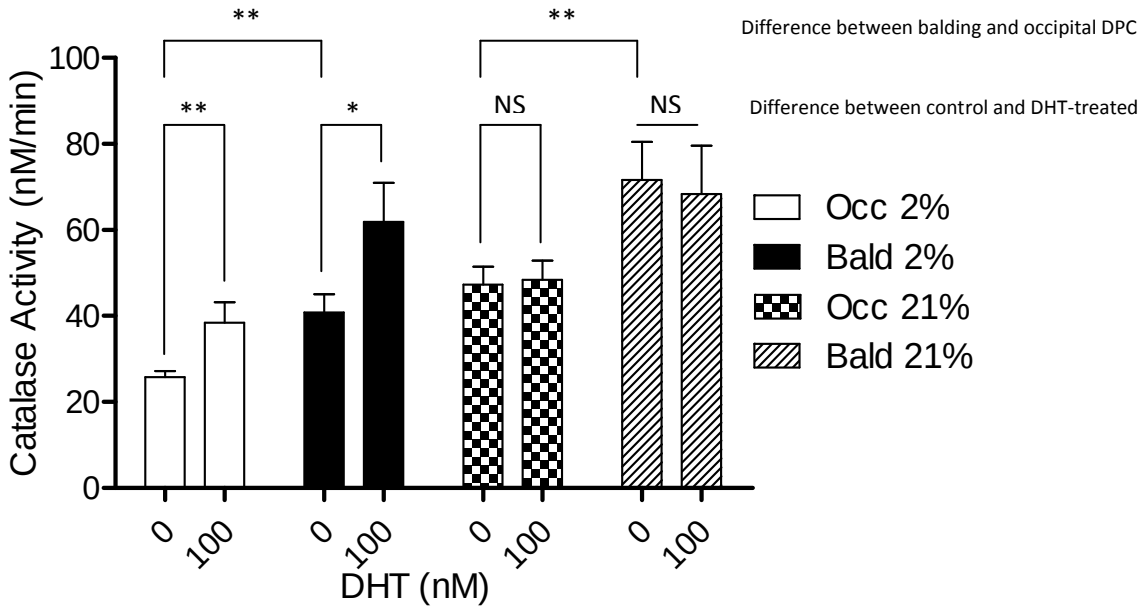

Figure 4.6: Activity of catalase in balding and occipital DPC cultured at 2% and 21% oxygen in response to DHT (100 nM).

Balding and occipital DPCs cultured at 2% or 21% oxygen were pre-treated with 0.001% (v/v) ethanol vehicle control or DHT for 1 h. Cells were subsequently lysed and normalised by Bradford total protein assay and measured for catalase activity using Amplex Red assay. Experiments were carried out in duplicate on DPCs from 3 separate patients. Statistical analyses was carried out using two-way ANOVA with Bonferroni post-test; * $P < 0.05$, ** $P < 0.01$; Results presented as the mean ± S.E.M. for n = 3 (matched DPC samples from 3 different patients).

4.3.7 Functional analysis of glutathione in balding and occipital DPCs at 2% and 21% oxygen

Glutathione plays a critical role in the elimination of ROS within all cell types (Maher, 2005). Using the 5,5'-dithiobis-(2-nitrobenzoic acid) (DTNB) reaction assay (see **Chapter 2**) total glutathione, and its respective fractions of its reduced and oxidised forms (GSH + GSSG), was quantified in balding and occipital DPCs cultured at 2% and 21% oxygen. **Figure 4.7** shows the reduced and oxidised glutathione concentrations in balding and occipital DPCs cultured at 2% oxygen were not significantly different ($P > 0.05$). Balding DPCs cultured at 21% saw a significantly increased expression of total glutathione (3.413 µM) compared to occipital DPCs (2.72 µM) ($P < 0.001$). However, the fraction of total glutathione which was in its active reduced form (GSH) was significantly lower in balding DPCs (0.743 µM) compared to occipital DPCs (0.914 µM) ($P < 0.05$).

The overall trend in these data can be best analysed by observing the relative fraction of active glutathione (GSH) as presented in **Table 4.1**. Although culture at 2% oxygen confers a lower expression of total glutathione (2.304 µM in both occipital and balding DPCs) the overall fraction of active GSH to oxidised GSSG remains relatively high for occipital (41.1%) and balding (36.7%) DPCs. Comparatively, GSH to GSSG fractions are much lower when DPCs are cultured at 21% oxygen, with occipital DPCs exhibiting 33.5% GSH and balding DPCs exhibiting an even lower 21.8% GSH.

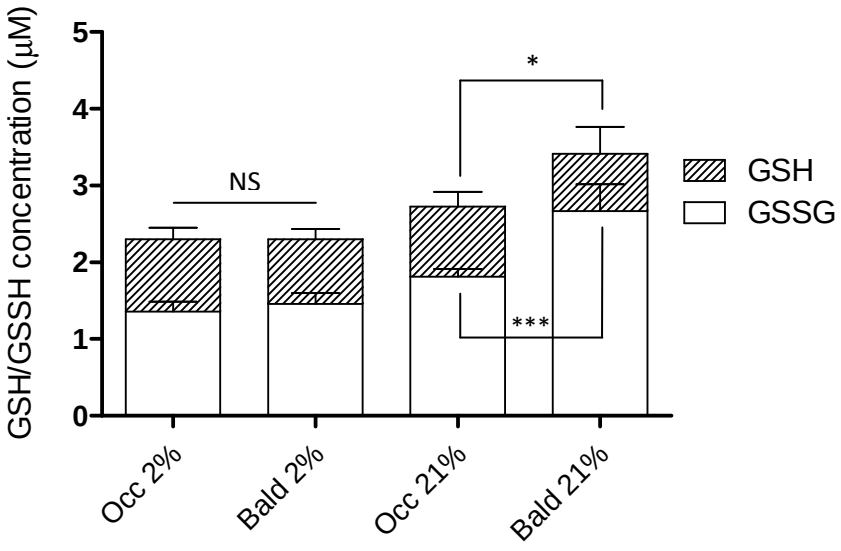

Figure 4.7: Total glutathione concentration showing reduced (GSH) and oxidised (GSSG) fractions in balding and occipital DPC cultured at 2% and 21% oxygen.

Balding and occipital DPCs cultured at 2% or 21% oxygen were lysed and normalised by Bradford total protein assay and measured for total glutathione concentration using the DTNB assay. Experiments were carried out in duplicate on DPCs from 3 separate patients. Statistical analyses was carried out using Student's t test; * $P < 0.05$, *** $P < 0.001$, NS $P > 0.05$; Results presented as the mean ± S.E.M. for n = 3 (matched DPC samples from 3 different patients).

	Total Glutathione GSH+GSSG (µM)	Reduced Glutathione GSH (µM)	Oxidised Glutathione GSSG (µM)	Active Glutathione Fraction GSH:Total
Occ 2%	2.304 ± 0.12	0.948 ± 0.14	1.356 ± 0.03	41.1%
Bald 2%	2.304 ± 0.09	0.846 ± 0.11	1.458 ± 0.04	36.7%
Occ 21%	2.727 ± 0.12	0.914 ± 0.19	1.813 ± 0.01	33.5%
Bald 21%	3.413 ± 0.2	0.743 ± 0.25	2.67 ± 0.35	27.7%

Table 4.1: Relative fractions of reduced/oxidised glutathione in balding and occipital DPCs at 2% and 21% oxygen. Data from Figure 4.7 presented in table form to highlight the relative ratios of active glutathione between balding and occipital DPCs at 2% and 21% oxygen.

4.4 Discussion

Standard laboratory cell culture conditions grow cells in an atmosphere of 5%-10% CO_2 and air. Under such conditions the oxygen concentration is 21%. However, in the dermal layer of the skin, where the dermal papilla is located, the oxygen concentration is between 1 and 5%, dependent on the proximity to the blood supply of the capillary network of the sub-papillary plexus and the highly vascularise hair follicles (Wang *et al.*, 2003, Wang *et al.*, 2005). Therefore, under standard laboratory conditions, DPCs are not cultured at their physiological oxygen concentration and this could promote a stress phenotype (Davies, 1995).

The data in this chapter show that 21% oxygen and progressive passaging both significantly increase the levels of ROS in DPCs. Most importantly, the data demonstrate that balding DPCs produce more ROS under both oxygen conditions compared to occipital DPCs, with a more pronounced effect seen at 21% oxygen. Oxidative stress is the most probable cause of the increased stress-related senescence seen in the balding DPCs at 21% oxygen conditions, as demonstrated in the **Chapter 3**. Other groups have demonstrated the link between oxidative stress and senescence in other types of fibroblast cells. Under atmospheric cell culture, IMR-90 fibroblasts have been shown to senesce after fewer passages than those grown under low oxygen (Chen *et al.*, 1995). In addition, hyperoxia (40% oxygen) induced rapid senescence in lung fibroblasts (von Zglinicki *et al.*, 1995) similar to the senescence inducing effect seen with an acute concentration of H_2O_2 (Frippiat *et al.*, 2002).

Our group has previously shown that the increased sensitivity to oxidative stress in balding DPCs was associated with higher expression of stress response proteins including catalase (Bahta *et al.*, 2008). Catalase is involved in the mitigation of

oxidative stress, conferring a cell protective effect against oxidative stress (Bai *et al.*, 1999). The data in this chapter further confirm these findings, showing catalase expression and activity is higher in balding DPCs compared to occipital DPCs, and that its expression and activity is reduced at 2% oxygen relative to 21% oxygen in both balding and occipital DPCs. This reduced catalase activity occurs in conjunction with the reduced ROS levels seen at 2% oxygen and in occipital DPCs demonstrating catalase as an important stress-response protein in the DPCs.

Catalase has been found to play an important role in hair follicle ageing within the melanocytes (Kauser *et al.*, 2010). For example greying hair follicles have a lower expression of catalase compared to healthy, pigmented follicles (Wood *et al.*, 2009). These data contrast with the findings shown in this chapter, where the catalase expression is higher in the balding DPCs. This potentially highlights a fundamental difference between the relative pathogeneses of graying and balding. In balding follicles the stress response is active, but may not be able to cope with the higher levels of ROS being produced. In greyness this stress response is already lost.

TGF-β1 is known to be important in hair follicle growth cycling (Foitzik *et al.*, 2000). TGF-β isoforms are also known regulators of ROS production in various cell types, such as hepatocyte carcinoma (Senturk *et al.*, 2010) lung fibroblasts (Cui *et al.*, 2011) or renal epithelial cells (Rhyu *et al.*, 2005). It has also been found that DPC secreted growth factors were able to act upon the DPC itself in autocrine regulatory manner (Hamada and Randall, 2006). Therefore TGF-β1 was exogenously applied to DPCs cultured at 2% and 21% oxygen to determine whether they affected ROS production. The data presented here show that TGF-β1 does not induce an effect on ROS production in the DPCs. It is important to note that DPCs

were only exposed to TGF-β1 for 1 hour and a longer exposure may be required to observe an effect.

DHT is an established agonist of the dermal papilla cells (Inui *et al.*, 2002). Androgen receptors are found in balding and occipital DPCs, with balding cells expressing a higher number of receptors (Hibberts *et al.*, 1998). DHT's action as an inhibitor of ROS production has been demonstrated in murine embryonic stem cells (Pathak *et al.*, 2008, Lee *et al.*, 2008). The data in this chapter indicate a novel role for DHT in the DPC wherein ROS production was reduced in a dose-response manner in the balding DPCs. This function was also associated with an upregulation of the antioxidant enzyme catalase in response to DHT in both balding and occipital DPCs. This effect was only observed when cells were cultured at 2% oxygen and not 21% oxygen. All previous studies of DHT on DPCs *in vitro* have been conducted at 21% oxygen suggesting this effect is prevented under high levels of oxygen.

One potentially important observation in this chapter is that normal cell culture conditions of 21% oxygen may mask the beneficial effects of DHT reducing ROS in balding DPCs. A similar action with regards to DHT inhibiting ROS has also been observed in murine embryonic stem cells ((Pathak *et al.*, 2008, Lee *et al.*, 2008). In **Chapter 3** it was demonstrated how different oxygen conditions could significantly modulate the secretory output in balding and occipital DPCs. Here we see another example of altered function within the DPCs under low oxygen whereby low oxygen enables DHT to stimulate upregulation of catalase potentially resulting in a further reduction of ROS levels. This highlights a potential positive feedback loop wherein DPCs whose microenvironment confers a reduction in ROS levels can maintain these low levels through further DHT stimulation. This effect would then be lost in

cells whose microenvironment conferred a higher ROS build up, for example the DPCs of the poorly vascularised balding scalp.

DHT also promoted catalase activity in occipital DPCs cultured at 2% oxygen, however unlike balding DPCs this was not associated with a reduction of ROS levels. The next step to elucidating DHT's role in ROS regulation would be to analyse androgen sensitive follicles from the beard, pubis or axillary to determine whether catalase and ROS are regulated via the same DHT-dependent mechanism.

Regulating ROS within the cell is a tightly controlled homeostatic equilibrium that plays a major role in intracellular signalling (Ray *et al.*, 2012). For example ROS can cause the upregulation of HSP27 and ATM both of which, as well as acting to mitigate cell damage by protein misfolding, as in the case of HSP27 (Mymrikov *et al.*, 2011), or DNA double-strand breaks, in the case of ATM (Hawkins *et al.*, 2011), concomitantly act as intracellular signalling modulators themselves.

In this chapter it has been demonstrated that glutathione, is also regulated by oxygen conditions along with different levels of expression between balding and occipital DPCs. Glutathione can also act as an intracellular signalling molecule, affecting transcription via a number of mechanism (Maher, 2005).

Glutathione is upregulated at 21% oxygen compared to 2% oxygen conditions, in a similar manner to catalase, and a significantly higher expression is seen in balding DPCs compared to occipital DPCs at 21% oxygen. However, the fraction of glutathione which remains in its active, reduced form (GSH) is significantly lower in balding DPCs compared to occipital DPCs cultured at 21% oxygen. The oxidised form of glutathione (GSSG) can be recycled to GSH via the enzyme glutathione reductase (Maher, 2005). Therefore glutathione reductase is the critical rate-

determing step dictating the levels of GSH in the cells and is a more accurate indicator of the cells' ability to regulate ROS (Maher, 2005).

Active GSH also regulates intracellular signalling by blocking the promoter binding sites of AP-1 and SP-1 (Vayalil *et al.*, 2007). SP-1 is a known target of the androgen receptor and binding between them can be blocked with glutathione (Curtin *et al.*, 2001). GSSG does not affect the same pathways as GSH therefore the relative balance between these two oxidative states may confer in glutathione the ability to act as a ROS sensitive signal modulator. There is therefore scope for further examination of the role of GSH signalling and whether it is able to modulate DHT signalling. Notably, TGF-β can auto-induce the transcription of itself via the AP-1 and SP-1 promoters via the intracellular Smad signalling (Geiser *et al.*, 1993, Van Obberghen-Schilling *et al.*, 1988), the potential relevance of which is explored further in **Chapter 5**.

In summary, at low oxygen the levels of ROS in both balding and occipital DPCs are reduced. Balding DPCs exhibit a consistently higher level of ROS compared to occipital DPCs, however they also appear to be more responsive to DHT induced catalase upregulation which is associated with a reduction in ROS levels, an effect that is only observed at 2% oxygen. Balding DPCs also express higher levels of total glutathione, but the active GSH fraction is lower compared to occipital DPCs.

Chapter 5

Expression of TGF-β receptors and effects of TGF-β on occipital and balding DPCs

5.1 Introduction

The primary function of the dermal papilla is thought to be the control of hair follicle cycling by secreting growth factors that regulate growth, differentiation and apoptosis of the surrounding hair follicle epithelium (Stenn and Paus, 2001). During the growth cycle, the hair follicle undergoes complex tissue remodelling which changes the size and shape of the dermal papilla via migration and alteration of the hair follicle extra cellular matrix (Tobin *et al.*, 2003, Messenger *et al.*, 1991a, Elliott *et al.*, 1999). In contrast to occipital DP, the macrophysiology of balding DP is smaller, rounder and do not penetrate as deeply into the hair matrix (Miranda *et al.*, 2010).

The possibility of autocrine regulation in the dermal papilla has been explored in a report by Hamada and Randall (2006), in which media taken from balding DPCs inhibited the growth of occipital DPCs, but the specific growth factors responsible for this autocrine regulation were not elucidated. TGF-β isoforms can inhibit proliferation and act an autocrine fashion in lung fibroblasts (Moses *et al.*, 1987). TGF-β1 and -β2 signalling have been reported as playing an important role in signalling within the hair follicle, although these studies have concentrated on their effects on inducing apoptosis in the ORS at the onset of catagen (Foitzik *et al.*, 2000, Foitzik *et al.*, 1999).

TGF-β signalling occurs via the TGF-β receptors. The TGF-β receptor exists as three different serine/threonine kinase subunits TGF-βRI (also referred to as Alk5), TGF-βRII and TGF-βRIII (Wrana *et al.*, 1992). Within the pilo-sebacious unit only the TGF-βRI and TGF-βRII subunits are expressed (Paus *et al.*, 1997). The TGF-βRI and -βRII subunits combine to form a functional heterodimer. TGF-βRII receptor

first can bind either of the TGF-β ligands within the extracellular space, the ligand-bound TGF-βRII subunit then activates TGF-βRI via phosphorylation (Wrana *et al.*, 1992). Phosphorylated TGF-βRI then initiates cytoplasmic signalling by phosphorylating Smads 1, 2, 3 or 5, which subsequently translocate to the nucleus to regulate the transcription of target genes (Miyazono *et al.*, 2000). TGF-β signalling can be blocked by using the inhibitor SB-431542, a compound which specifically blocks the action of the TGF-βRI subunit (Inman *et al.*, 2002)

TGF-β must be bound by latent TGF-β binding proteins (LTBPs) 1, 3 or 4 in order for the protein to be secreted to the extracellular domain (Saharinen *et al.*, 1999). The LTBPs are able to bind to ECM components such as fibronectin or fibrillin, whereupon they release the active TGF-β ligand (Hyytiainen and Keski-Oja, 2003, Hyytiainen *et al.*, 2004). This mechanism allows the TGF-β ligands to be targeted to tissues with specific ECM. Unlike LTBP1, 3 and 4, LTBP2 is unable to bind TGF-β but acts as a competitive antagonist to isoforms 1, 3 and 4 for the fibronectin and fibrillin binding sites (Hirani *et al.*, 2007). TGF-β is released from the LTBPs through enzymatic cleavage by plasmin, thrombin and MT1-MMP (Taipale *et al.*, 1992, Tatti *et al.*, 2008). A number of other factors, including pH and the presence of reactive oxygen species, can increase the rate at which this cleavage occurs (Koli *et al.*, 2001). The overall activity of TGF-β is therefore controlled by the rate at which it can be secreted with and subsequently released from the LTBPs.

Based on the previous data (**Chapter 3**) demonstrating TGF-β1 and -β2 are secreted from both balding and occipital DPCs this chapter explores the potential role for TGF-β isoforms as autocrine regulators in the dermal papilla.

5.2 Aim

To investigate the potential role of TGF-β1 and β2 as autocrine growth regulators of the dermal papilla.

5.3 Results

5.3.1 Expression analysis of TGF-β receptors in DPCs

In order to establish whether TGF-β signalling could be transduced by DPCs, mRNA of TGF-β signalling components were analysed by PCR. **Figure 5.1** shows balding DPCs expressed higher levels of TGF-βRI mRNA relative to occipital DPCs. Balding DPCs also expressed TGF-βRII mRNA while the occipital DPCs only expressed only trace levels.

LTBP1 activates, whereas LTBP2 inhibits TGF-β ligand binding activity, therefore LTBP isoforms were also analysed by PCR. The data show higher levels of LTBP1 mRNA in the balding DPCs compared to occipital DPCs. Conversely, the occipital DPCs expressed higher levels of LTBP2 mRNA compared to balding DPCs. Thus the LTBP mRNA profile would facilitate TGF-β signalling in balding DPCs but inhibit the TGF-β pathway in occipital DPCs.

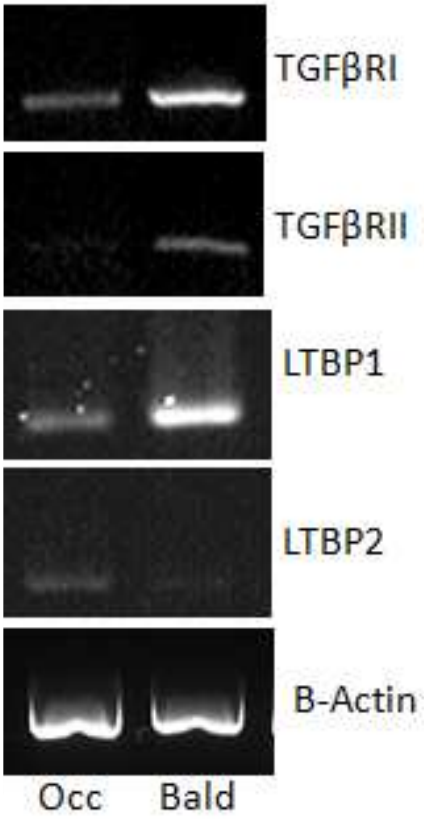

Figure 5.1: PCR for TGF-β signalling components in DPCs. Expression of TGF-β receptors I and II and binding proteins LTBP1 and LTBP2 in occipital and balding DPCs cultured at 21% oxygen. A single PCR product was detected in each lane matching the predicted product size for TGF-βRI (301 b.p.), TGF-βRII (400 b.p.), LTBP1 (207 b.p.), LTBP2 (399 b.p.) or β-actin (516 b.p.) The figure is a representative of three separate experiments.

The protein expression profiles of TGF-β receptors in DPCs were also analysed. **Figure 5.2** shows that both TGF-βRI and TGF-βRII were expressed in the DPCs. Densitometry analysis showed expression in the balding DPCs was higher for both receptor subunits (TGF-βRI = 1.2 A.U.; TGF-βRII = 1.4 A.U.) compared to occipital DPCs (TGF-βRI = 0.4 A.U.; TGF-βRII = 0.3 A.U.) correlating with the mRNA given in **Figure 5.1**. Notably the trace levels of TGF-βRII mRNA seen in the occipital did transcribe signal as expression of the subunit could be observed at the protein level.

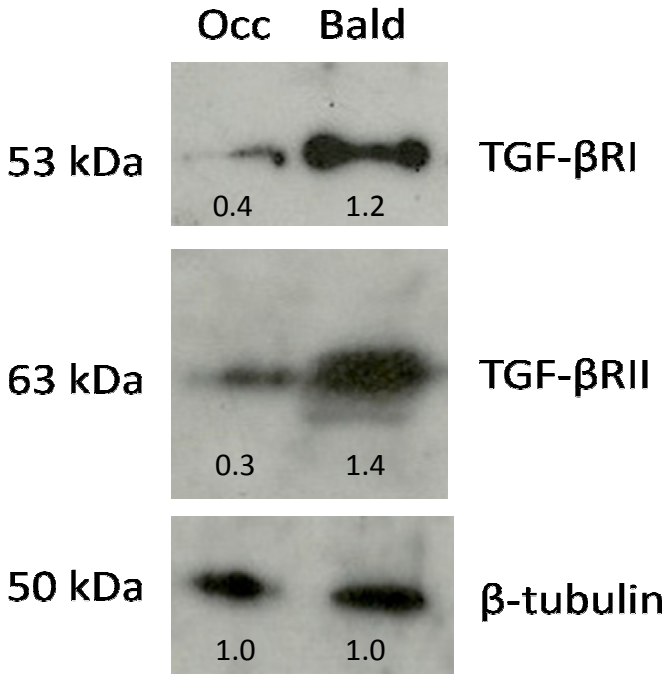

Figure 5.2: Western blot analysis of TGF-βRI and TGF-βRII protein expression in occipital and balding DPCs at passage 2. Protein was isolated from occipital and balding DPCs cultured for 3 days at 21% oxygen. DPCs were lysed using RIPA buffer, normalised according to total protein count and 20 µg of each lysate was separated by SDS-PAGE then detected by using the appropriate antibodies (see **Table 2.2**). Equal protein loading protein loading was confirmed by β-tubulin. Representative images from immunoblots taken for n = 3 separate patients. Densitometry values calculated using Image-J software for mean of all 3 blots expressed as a fraction of β-tubulin control presented below each lane.

5.3.2 Smad3 phosphorylation in DPCs

TGF-β signalling affects cellular function by activating Smad transcription factors though phosphorylation. Therefore, to assess TGF-β receptor activity, levels of phosphorylated Smad3 (pSmad3) was analysed by immunoblotting in the presence or absence of recombinant TGF-β1.

Densitometry analysis of the western blots **in Figure 5.3** shows that TGF-β1 induced phosphorylation of Smad3 in both occipital (0.3 A.U.) and balding DPCs (0.6 A.U.), while no phosphorylation of Smad3 was seen in either balding or occipital DPCs in the absence of TGF-β1. Balding DPCs exhibited a higher degree of phosphorylation compared to the occipital DPCs.

These data demonstrate that DPCs express functionally active TGF-β receptors that are able to phosphorylate Smad3. Balding DPCs would have the requisite components for autocrine TGF-β signalling, via higher expression of TGF-β receptors and through the ability to secrete more TGF-β with higher expression of LTBP1 and lower expression of the inhibitory LTBP2.

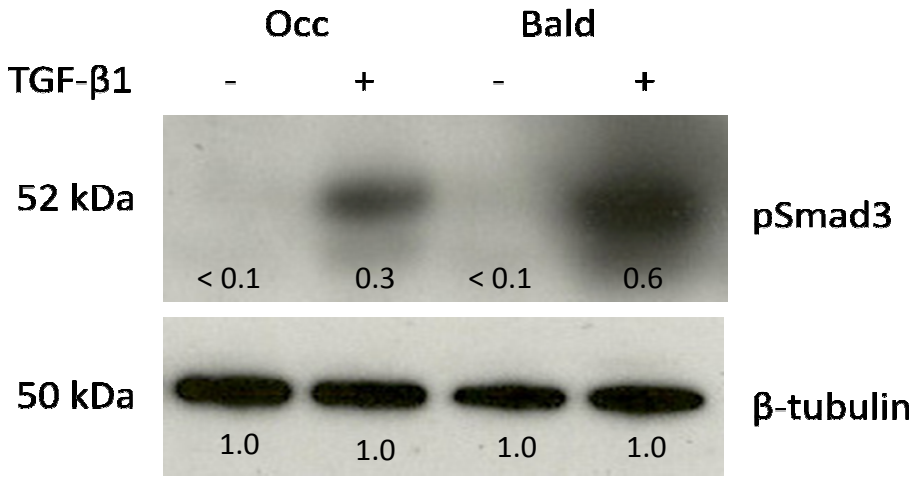

Figure 5.3: Western blot analysis of phosphorylation of Smad3 in balding and occipital DPCs. Protein was isolated from occipital and balding DPCs treated with BSA control or 10 ng/ml TGF-β1. DPCs were lysed using RIPA buffer, normalised according to total protein concentration and 20 µg of each protein lysate was separated by SDS-PAGE then detected by using the appropriate antibodies (see **Table 2.2**). Equal protein loading protein loading was confirmed by β-tubulin. Representative images from immunoblots taken for n = 3 separate patients. Densitometry values calculated using Image-J software for mean of all 3 blots expressed as a fraction of β-tubulin control presented below each lane.

5.3.3 The effect of TGF-β on DPC proliferation

In order to ascertain whether TGF-β could induce a functional effect on the DPCs by inhibiting cell growth, an Alamar Blue assay was conducted on balding and occipital DPCs treated with TGF-β1, -β2 or BSA vehicle control over a period of seven days.

Alamar blue analysis showed balding and occipital DPC proliferation rates were inhibited by both isoforms of TGF-β (**Figure 5.4**). However, balding DPC proliferation was more severely compromised than occipital DPC proliferation by TGF-β1 and 2. Occipital DPCs underwent 87.3% ± 2.8 ($P < 0.05$) proliferation, whereas balding DPCs underwent 61.2% ± 12.6 ($P < 0.01$) proliferation when treated with TGF-β1. Occipital DPCs proliferation rate reduced to 90.4% ± 3.5 ($P < 0.05$) were as balding DPCs proliferation was significantly reduced to 63.1% ±7.6 ($P < 0.001$) when treated with TGF-β2. There was no significant difference in inhibition of growth in either balding or occipital DPCs between the TGF-β1 and -β2 isoforms. These data appear to correlate with the previous findings demonstrating that balding DPCs express TGF-β receptors to a higher degree, as can be seen via the increased inhibitory effect on the cell function of proliferation.

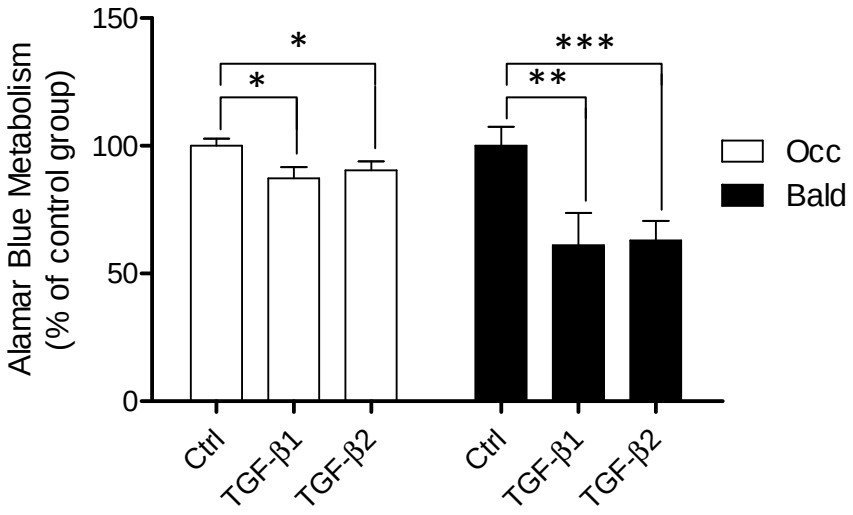

Figure 5.4: Effect of TGF-β1 and -β2 on the proliferation of balding and occipital DPCs. Alamar Blue metabolism was measured at day 0 and day 7, R.F.U. Balding and occipital DPCs were treated with BSA control or 10 ng/ml TGF-β1 or -β2. Measurements for TGF-β1 or -β2 treated DPCs were normalised against BSA treated controls for each cell type. Statistical analysis was carried out using one-way ANOVA; * $P < 0.05$, ** $P < 0.01$, *** $P < 0.001$; results presented as the mean ± S.E.M. for n = 3 (matched DPC samples from 3 different patients).

5.3.4 The effect of TGF-β1 on DPC migration

Migration of the DPCs is thought to play an important role in the cell-cycle remodelling of the dermal papilla's morphology. Analysis was carried out to determine whether TGF-β could affect DPC migration. **Figure 5.5** shows the average motility velocities of balding and occipital DPCs in the presence and absence of 10 ng/ml TGF-β1.

There was no significant difference in motility between occipital and balding DPCs in the absence of TGF-β1 (**Figure 5.5**). TGF-β1 did not significantly inhibit occipital DPCs' motility ($P > 0.05$), however TGF-β1 significantly reduced cell motility in balding DPCs, falling from a velocity of 0.76 µm/min under control conditions to 0.50 µm/min ($P < 0.05$) when treated with TGF-β1. These data correlate with the findings detailed in the previous sections showing TGF-β isoforms as having a greater effect on balding DPCs.

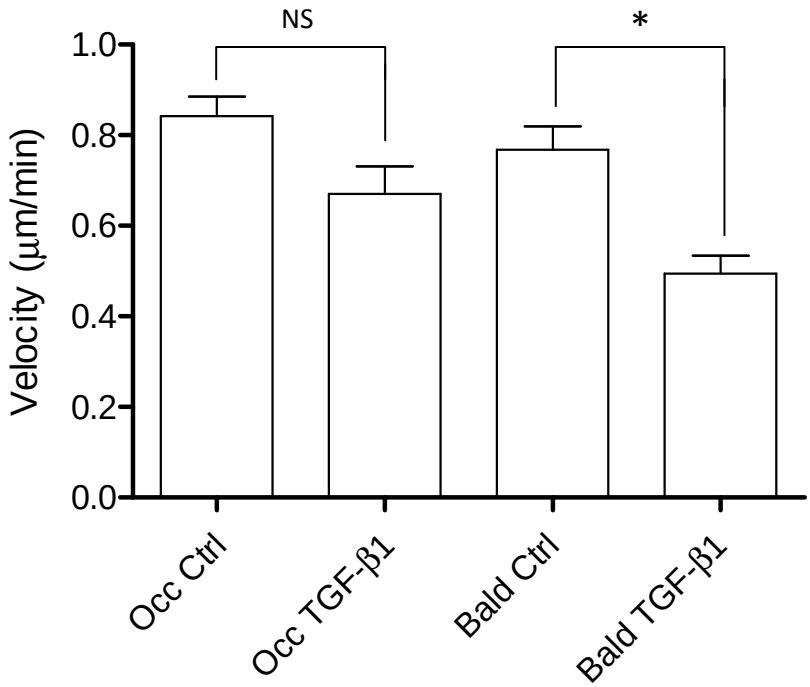

Figure 5.5: Motility of balding and occipital DPCs with TGF-β1 treatment. DPC motility was measured using timelapse photography (every 10 min for 24 h) at 21% oxygen. Balding and occipital DPCs were treated with BSA control or 10 ng/ml TGF-β1. Statistical analysis was carried out using Student's t test; * $P < 0.05$, NS > 0.05; results presented as the mean ± S.E.M. for n = 3 (matched DPC samples from 3 different patients).

In conclusion, the data presented here show the expression and functional activity of TGF-β receptors in DPCs *in vitro*. Furthermore, TGF-β1 is able to reduce cell motility in balding DPCs. The components required for TGF-β signalling – binding proteins and receptors) are expressed at higher levels in the balding DPCs compared to the occipital DPCs and this translates to balding DPCs having a markedly higher sensitivity to TGF-β1 with regards to the cell functions of proliferation and motility. This data taken with the previous observation that DPCs secrete TGF-β isoforms suggests that TGF-β isoforms may act as growth inhibitory autocrine factors in a manner hypothesised by Hamada et. al (2004), although importantly it must be noted that these findings only prove TGF-β's effect as an exogenous treatment.

5.4 Discussion

The majority of studies examining growth factor signalling within the hair follicle concentrate on the paracrine secretions of the dermal papilla and the effect these factors induce in the surrounding epithelial keratinocytes of the germinative epithelium, hair matrix and outer root sheath (Stenn and Paus, 2001). However, little is known about what growth factors affect the remodelling of the dermal papilla itself.

Such growth factors may be systemic, possible candidates include glucocorticoids (Thornton *et al.*, 2006), adenosine (Hwang *et al.*, 2012), and androgens (Elliott *et al.*, 1999). The possibility of localised control by growth factors secreted by the dermal papilla itself has been hypothesised and proven in principal (Thornton *et al.*, 1998, Hamada and Randall, 2006).

The data presented in this chapter show TGF-β1 and -β2 as potential candidates for such autocrine growth regulation through confirmation of expression of functional TGF-β receptor heterodimer, phosphorylation of intacellular Smad3 and functional assays. A critical question is then whether this proven *in vitro* mechanism can be applied to the *in vivo* hair follicle.

Expression of TGF-β receptors within the human hair follicle is predominantly localised to the epithelial cells, however a near-constant expression of TGF-βRI is maintained in the dermal papilla throughout the hair cycle in mice while TGF-βRII is expressed almost exclusively during catagen (Paus *et al.*, 1997). TGF-β receptors expression at all stages of the human hair cycle has not been conducted therefore their expression in the dermal papilla cannot be ruled out. Both receptor subunits must be expressed in order to form a fully functional heterodimer, therefore

presenting a difference in the expression pattern of the receptors between *in vivo* and *in vitro* DPCs. The two possible explanations for this are that: a) TGF-β receptor expression in the human dermal papilla differs to that of the mouse, or b) that expression of the TGF-β receptor is an artefact of *in vitro* cell culture.

There is the possibility that TGF-β receptors are only expressed *in vitro*. Cells undergo changes in protein expression during the process of dedifferentiation which occurs during cell culture. It has been reported that human dermal fibroblasts which express TGF-β receptors when cultured in monolayer downregulate TGF-β receptor expression when cultured in 3D collagen spheroid matrices (Kunz-Schughart *et al.*, 2003). Such findings demonstrate the dynamic nature of growth factor signalling and its inextricable link to cellular remodelling.

Nonetheless the findings reported in this chapter give new evidence that support the theory of autocrine regulatory pathway in cell cultured DPCs (Hamada and Randall, 2006) and go further to highlight TGF-β1 and -β2 as key components of this pathway.

The Alamar Blue proliferation assay was carried out to confirm and extend the findings of Hamada *et al.* (2006). However, as discussed in **Chapter 3**, the dermal papilla does not proliferate or apoptose to a substanitial degree *in vivo*, instead relying on alteration in ECM composition and cell migration during tissue remodelling (Elliott *et al.*, 1999, Tobin *et al.*). For this reason, the migration assay is a more suitable indicator of DPC function than proliferation.

The timelapse method was chosen to quantify migration instead of the more commonly used “scratch assay” due to the nature of fibroblast movement. Compared to epithelial cells, which move as a unified migratory front in a scratch assay

(Fitsialos *et al.*, 2007), fibroblasts movements are more individual and varied, thus net movement into a scratch is not an effective assay. Using the timelapse allowed data to be collected on a large number of individual cells.

Another key functional effect of TGF-β is the ability to modulate ECM protein expression. TGF-β isoforms have been shown to initiate secretion of tissue remodelling enzymes such as plasmin activator inhibitor-1 (PAI-1) in fibroblasts collagen and fibronectin (Keski-Oja *et al.*, 1988, Raghow *et al.*, 1987, Vayalil *et al.*, 2005) as well as being indicated in modulating cell migration (Brenmoehl *et al.*, 2009) (Postlethwaite *et al.*, 1987). In turn TGF-β is targeted to specific tissues based on their ECM composition. LTBPs 1, 3 and 4, that regulate TGF-β release to target tissue, bind to fibronectin and fibrillin before releasing TGF-β (Saharinen *et al.*, 1999). In addition LTBP2, shown in this chapter to be expressed by balding DPCs, but not by occipital DPCs, acts as a competitive antagonist for the LTBP binding sites, inhibiting the targeting of TGF-β isoforms to the ECM and therefore inhibiting TGF-β release (Hyytiainen and Keski-Oja, 2003) (Hirani *et al.*, 2007). Notably, the rate of release of TGF-β from the LTBP in the extracellular domain is also increased in the presence of ROS, (Koli *et al.*, 2001) which as shown in the previous chapter are produced at higher levels in the balding DPCs which may therefore lead to an increase rate of TGF-β signalling.

ROS have also been shown to regulate TGF-β signalling in the intracellular domain as well as the extracellular domain. Data in the previous chapter showed that TGF-β1 was unable to affect ROS production in either balding or occipital DPCs, therefore suggesting that the regulation of TGF-β signalling is downstream to ROS activity. One potential mechanism for this downstream regulation is via ROS' affect

on reduced glutathione levels within the cell. Previous studies in mouse 3T3 fibroblasts have shown that TGF-β mediated alteration of ECM formation is a process which is controlled by intracellular glutathione levels (Vayalil *et al.*, 2007, Vayalil *et al.*, 2005). The latter study showed that this mechanism occurred via the SP-1 promoter (TGF-β signalling target), which also autoregulates the transcription TGF-βRI (Periyasamy *et al.*, 2000) and TGF-βRII (Ammanamanchi *et al.*, 1998). TGF-β is also known to regulate its own expression by positive feedback (Van Obberghen-Schilling *et al.*, 1988). Therefore TGF-β's self-regulatory behaviour along with its susceptibility to ROS and glutathione levels within cells may account for the higher expression of TGF-β receptors in the balding DPCs.

In summary, these data show that balding DPCs express greater levels of TGF-βRI and -βRII *in vitro*, which was translated to a functional affect of TGF-β1 and -β2 being able to suppress balding DPC proliferation and migration. Increased TGF-β signalling could therefore reduce the ability of the dermal papilla cells to migrate and from the connective tissue sheath. This would result in the smaller, rounder and poor remodelling ability that is observed in the balding follicle's dermal papilla. Since higher levels of TGF-β are secreted by balding DPCs (Inui *et al.*, 2002) the increased TGF-βR signalling capabilities observed in this chapter could explain the marked difference in the macrophysiology of the dermal papilla between follicle types.

Chapter 6

Role of oxidative stress in the balding dermal papilla

6.1 Discussion

The research presented in this thesis demonstrates novel mechanisms of DPC action in androgenic alopecia. The primary finding was that stress induced senescence is associated with oxidative stress and that ROS can affect the DHT-TGF-β signalling axis within balding and non-balding DPCs. Furthermore, it was found that balding DPCs showed a greater sensitivity to oxidative-stress induced senescence caused by transferring cells from 2% oxygen to 21% oxygen. The findings develop previously published research that showed that cultured balding DPCs senesced after fewer passages and had an upregulated expression of oxidative stress and senescence markers (Bahta *et al.* 2008).

The findings of this thesis demonstrate that balding DPCs express higher levels of ROS than occipital DPCs in a similar manner to the higher levels of ROS produced in ageing dermal fibroblasts (Poljsak and Dahmane, 2012, Trueb, 2009). Recent work in mice *in vivo* has shown that elevating ROS levels in the skin, through the knockdown of the ubiquitous antioxidant Sod2, caused elevated levels of DNA damage inducing cellular senescence and a resultant aged appearance of the skin (Velarde *et al.*, 2012).

Interestingly, it was found that balding DPCs expressed higher levels of catalase and glutathione when compared to occipital DPCs. This is in contrast to the theory of free-radical ageing, in which levels of ROS increase within organisms as their antioxidant functionality diminishes (Poljsak and Dahmane, 2012). In addition, in hair follicles it has been shown that greying hair follicles have a lower expression of catalase compared to healthy, pigmented follicles (Wood *et al.*, 2009).

Therefore, although greying and balding may share a common molecular mediator in the form of catalase, the mechanisms by which the pathogenesis of these conditions occur is likely to occur in a different manner, with regards to time frame over which the process occurs. Although the shedding of hair in male-pattern baldness may appear to be a gradual process, this is merely the net appearance of tens of thousands of acute events within each individual follicle. The follicle's terminal-to-vellus switch is thought to occur as an "abrupt change" over just a few, or perhaps even a single hair cycle (Whiting, 2001). The balding follicles used for these experiments are miniaturised but not yet full vellus hairs, therefore the finding that DPCs from these follicles express a higher level of catalase would support the theory of an "abrupt" terminal-to-vellus switch, in which the dermal papilla is mounting a reactionary response to an acute stress event. To date no studies have compared the levels of ROS between greying and pigmented follicles, and it remains to be elucidated as to which stress mechanisms lead to loss of pigmentation within the follicle.

It should also be noted that while catalase expression is higher in the balding DPCs, ROS levels are also higher demonstrating that the balding DPCs despite mounting an elevated response to increased ROS are unable to reduce them to a substantial degree. Evidence for this was also shown via the measurement of total and reduced glutathione, wherein despite total glutathione levels being higher in the balding DPCs the equilibrium of reduced to oxidised glutathione is weighed more towards the oxidised fraction when compared to occipital DPCs.

On a functional level, it was found that oxygen environment could affect the growth factor secretion of the DPCs, with 2% oxygen able to negate the DHT-induced TGF-β1 secretion observed at 21% oxygen in previous studies (Inui *et al.*, 2002, Inui *et*

al., 2003). It was found that culturing DPCs at low oxygen caused a marked increase in IGF-1 secretion, with a greater increase seen in occipital DPCs, IGF-1 being one of the key epithelial mitogenic stimuli required for hair follicle growth.

Previous work has shown that balding but not occipital DPCs respond to synthetic androgen R-1881 by producing TGF-β1 (Inui *et al.*, 2002). Conversely our study demonstrated that occipital DPCs could also secrete TGF-β1 and -β2 in response to DHT. In addition it was found that DHT was able to increase expression of catalase in both balding and occipital DPCs, resulting in a decrease in ROS levels in the balding DPCs. Occipital DPCs are classically described as androgen-insensitive, however their insensitivity stems from a lack of 5α-reductase which converts testosterone from the blood into DHT, rather than from a lack of androgen receptors (AR). To support this, it has been previously demonstrated that occipital DPCs do express AR, but at lower expression levels that the balding DPCs (Hibberts *et al.*, 1998). The addition of exogenous DHT in culture systems therefore bypasses the crucial step of DHT synthesis via 5α-reductase testosterone metabolism. The fact that similar effects can be induced in balding and occipital DPCs with DHT supports the theory that androgen sensitivity in the dermal papilla is predominantly controlled by 5α-reductase (Kaufman, 1996).

The role of ROS in the causation of baldness is a paradigm shift in the way in which we think of the pathophysiology of androgenic alopecia. Androgenic alopecia is well established as a polygenic condition whose onset and patterning is influenced by a large number of different genes (Hoffmann, 2002). The follicles of the balding scalp are genetically predisposed to undergo transformation into the smaller, unpigmented vellus follicles (Paus and Cotsarelis, 1999). The factors affecting an individual's

propensity towards free-radical induced ageing are also likely to be influenced by hereditary factors – such as reduced expression of antioxidants or increased expression of factors within the stress-induced senescence pathways. The differences between the frontal and occipital follicles may be due to developmental differences. The frontal parietal regions of the scalp develop in the embryo from the neural crest cells, while the occipital scalp forms from the mesoderm (Van Neste D, 1996) resulting in dermal papillae which are phenotypically dissimilar and express a different array of proteins. Equally, consideration must also be given the overall effect on the follicles by environmental factors, be they diet, alcohol, drug or tobacco consumption, physical or emotional stress or UV-exposure (Trueb, 2009). The work in this thesis helps to draw a link between these intrinsic (different antioxidant expression) and extrinsic (different oxygen environments) factors. Low oxygen was able to delay senescence of both occipital and balding DPCs and this effect was associated with a reduction in ROS production. In addition it was discovered that culturing DPCs at low oxygen could alter their secretions of the growth factors TGF-β1 –β2, DKK1 and IGF-I.

One theory which may unite intrinsic and extrinsic factors *in vivo* is that the patterning of androgenic alopecia is based on the anabolic effects of DHT on bone formation in the skull (Taylor, 2009). The continued growth of the skull in adult males forces a remodelling of the skin with a net reduction in the vascularisation. This theory is supported by the fact that balding follicles are poorly vascularised compared to occipital follicles (Miranda *et al.,* 2010). Reduced vascularisation is a well established cause of skin ageing (Chung and Eun, 2007). Moreover, one of the most effective known treatments for male pattern baldness is through the use of minoxidil which stimulates cutaneous blood flow when applied directly to balding

scalp (Wester *et al.*, 1984). It achieves this via activation of the ATP-sensitive potassium channels of the arterial smooth muscle cells, hyperpolarising the membrane to prevent calcium influx via the voltage gated calcium channels. This causes a drop in cytosolic calcium which is required to activate contraction of the arterial smooth muscle. The relaxed resistance arteries then allow a greater volume of blood to the scalp (Cohn et al., 2011).

Unlike the *in vitro* model, wherein lower oxygen concentration leads to a reduction in ROS through the reduction in oxygen exposure (Davies, 1995) it has been reported that *in vivo* that hypoxia may in fact lead to an increase in ROS (Turrens, 1997). The proposed mechanism for this is that under hypoxic, vasoconstricted conditions where oxygen levels to the tissues are greatly reduced, transfer of electrons in the Kreb's cycle is switched at ubi-semiquinone step to create H_2O_2 leading to the generation of ROS. Therefore, in the context of the balding scalp, reduced vascularisation resulting in hypoxia of the localised tissue causing the necessary switch in the Kreb's cycle to cause an increase in ROS. Work to study the effects of low oxygen on the growth of whole follicles using the "Philpott model" may also lead towards a greater understanding of the different effects of hypoxia between the *in vivo* and *in vitro* models of hair growth.

The tissue microenvironment of the balding hair follicles, particularly with regards to vasculature and the resultant levels of oxygen diffusion may play a critical role in pathogenesis of the balding phenotype. Interestingly, hair follicles which are transplanted from the occipital region to balding frontal scalp become well established and grow healthily just as they would within the occipital regions (Hwang *et al.*, 2009). This suggests occipital follicles contain an intrinsic ability to alter the peripheral tissue microenvironment possibly through the processes of ECM

remodelling or angiogenesis. TGF-β1 is known to modulate the components of the ECM (Vayalil *et al.*, 2005), therefore follicles with DPs which secrete reduced TGF-β1 (such as those of the occipital scalp) could result in an altered ECM of the balding scalp they are transplanted to. Further work to establish the tissue remodelling of balding scalp region before and after hair transplantation, as well as analysis of the levels of ROS within this region would help to further understand the observations seen by Hwang *et al.* (2009).

Despite the fact that higher eukaryotic aerobic organisms cannot exist without oxygen, oxygen itself is inherently dangerous to their existence, causing the formation of ROS which can be deleterious to the cell at high levels. This phenomena is known as the "oxygen paradox" (Davies, 1995). Low oxygen culture is able to mitigate this effect by reducing the cells' exposure to oxygen, thus reducing their production of ROS. The tissue culture incubator effectively mimics the physiological microenviroment of the DPCs. In this respect low (2%) oxygen incubator is analogous to well-vascularised healthy occipital scalp, while the normal atmospheric (21%) oxygen incubator is analogous to the poorly vascularised skin of the frontal balding scalp. The findings detailed in this thesis demonstrating the alteration of the growth factor secretion profile of both the occipital and balding DPCs grown at different oxygen conditions would support this analogy and go some way towards explaining the scalp-site-specific differences in dermal papilla function. In addition to this low oxygen culture of DPCs has wide implications for the fields of research, hair-transplantation and industry.

DPCs *in vitro* culture systems attempt to model conditions that closely resemble physiological conditions. For example, DPCs are cultured in media that has been optimised for their specific nutrient requirements (Messenger, 1984). One of the best

established methods for *in vitro* hair follicle study is the "Philpott model" in which whole follicles may be grown in media, thus maintaining the DPCs and surrounding tissues in their normal physiological arrangement (Philpott *et al.*, 1990). More recently, it has been found that DPC culture can be optimised through the use of collagen spheroid matrices which act as a more suitable model of the papilla structure and allow DPCs to maintain their *in vivo* properties for longer (Higgins *et al.*, 2010).

The use of low oxygen culture would serve as a valuable addition to the list of parameters for optimised DPC culture. Low oxygen would provide a more physiologically relevant model for growing DPCs as well as prolonging the number of passages for which cells remain viable for experimentation.

Another important application of low oxygen culture would be in the field of *de novo* follicle synthesis, wherein new whole follicles may be formed using implanted DPCs taken from an existing hair follicle (Reynolds and Jahoda, 1992). Current hair transplantation methods rely on transplantation of whole follicular units from the occipital to the balding regions of the scalp (Barrera, 2003). There are a finite number of available follicles which can be used for this process and the operation itself requires highly invasive removal of the scalp. The potential to take a relatively less invasive biopsy from a single follicular unit which may then have its DPCs expanded under cell culture conditions to form the necessary tissue for new follicles has obvious benefits for both patients and surgeons.

Low oxygen culture of biopsied cells would grant numerous benefits for this process. The maximum yield of cells which could be expanded would be greatly increased as shown by the higher replicative capacity of DPCs grown under low oxygen. A

quicker rate of proliferation would also mean faster turnaround times for surgeons to treat patients. In addition low oxygen culture potentially maintains the DPCs inductive capacity, as DPCs grown under low oxygen maintain their ability to form pseudopapilla, a marker of the cells' maintenance of dermal papilla specific function.

The role of ROS and antioxidants in mediating the balding DPC phenotype represents a pathway that could potentially be targeted to prevent the balding hair follicle phenotype. The majority of established mediators of hair follicle cycling secreted by the DP are growth factors such as TGF-β, DKK-1 and IGF-1, all of which represent contentious drug targets due to the range of effects they may induce in cells. Intervention of the growth factor signalling pathways is likely to affect downstream pathways in the follicle and surrounding skin and would be logistically difficult to localise to the dermal papilla alone. Antioxidants may therefore represent a more viable, less side-effect prone target for prophylactic therapy of baldness.

The findings of this thesis also showed that TGF-β receptors were expressed in DPCs *in vitro* at 21% oxygen and that these allowed for TGF-β1 and -β2 to inhibit the proliferation and migration of cells , moreover this effect was more marked in balding DPCs. This is in contrast to a previous report that showed mouse dermal papilla has not been reported to express full TGF-β receptors in mice *in vivo* (Paus *et al.*, 1997). There is a possibility that TGF-β receptor expression is an artefact of cell culture, perhaps related to oxidative stress as well. To elucidate this there is a need to confirm expression of the TGF-β receptors within human follicles *in vivo* and to repeat the TGF-β functional assays at 2% oxygen conditions.

In summary, oxidative stress appears to play a major role in the mediation of proliferation, senescence, migration and growth factor secretion in the dermal papilla

with the balding DPCs demonstrating a markedly higher sensitivity to the build up of ROS within the cell, as seen by an elevated stress-response of elevated antioxidants. Cross-talk between these antioxidants, ROS, cell senescence mediators and the growth factor pathways may go some way towards explaining the different behaviour seen in the balding follicles' dermal papillae when compared to those of the occipital hair follicle.

6.2 Study Overview

An overview of the major findings of this and the thesis and how they fit with the currently established model of DHT-stimulated TGF-β secretion in the balding DPCs can be viewed below (**Figure 6.1**).

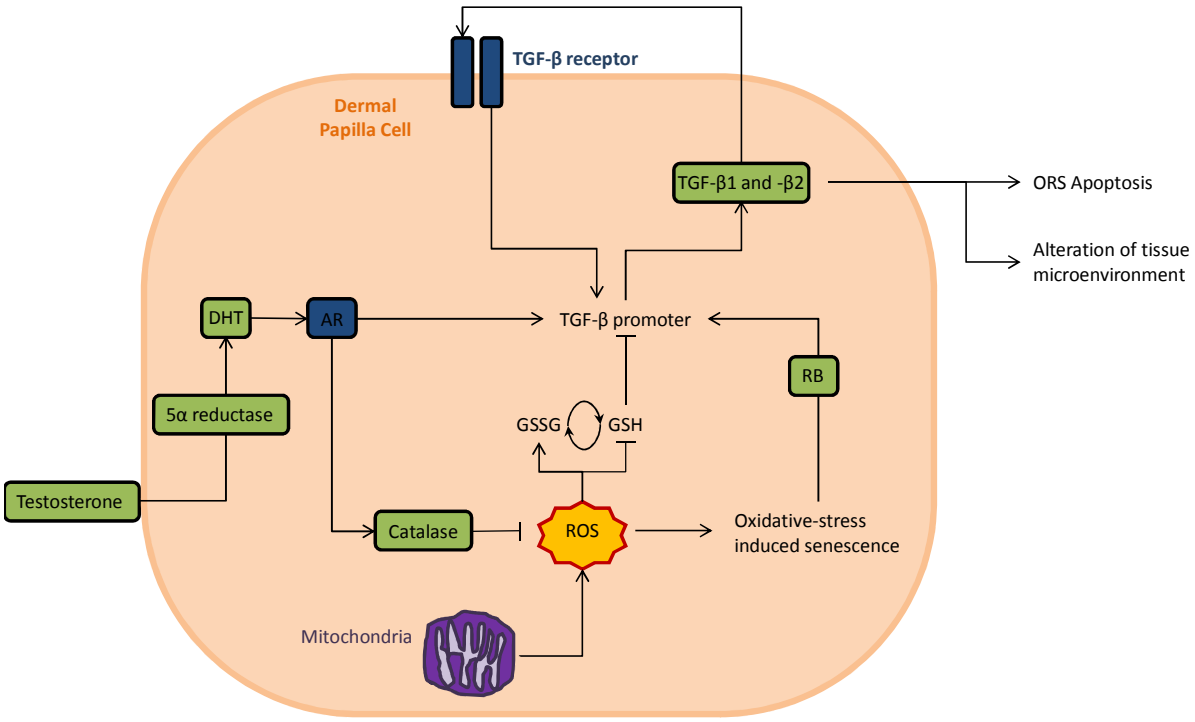

Figure 6.1: Model of DHT-TGF-β-axis in the DPC incorporating ROS, senescence and autocrine pathways. 1) Experiments carried out using DHT, unlike the synthetic androgen R-1881, was able to induce a response in both balding and occipital DPCs. 2) DHT was found to stimulate catalase expression with an associated decrease in ROS levels in balding DPCs, but only at 2% oxygen. The transcription factors mediating this process were not investigated and it was not established what other antioxidants were affected by DHT stimulation. 3) Further work is required to establish the factors controlling the production of ROS within the mitochondria, predominantly the NADPH isoforms. 4) There are established differences in the levels of total and active glutathione between balding and occipital DPCs, further work is required to understand the effect this may have on nuclear transcription. 5) The senescence mediator RB acts as a transcription factor for a number of growth factors, including the TGF-βs. Further work is required to establish whether this pathway is relevant in senescent DPCs. 6) Autocrine TGF-β signalling within the DPCs has been shown to function in principal at 21% oxygen. Further work is required to confirm whether this mechanism is an oxidative stress mediated effect and whether it is functional within the dermal papilla *in vivo*. 7) Further work is required to ascertain whether growth factor secretions from the dermal papilla are able to affect the perifollicular skin.

6.3 Future work

This study highlighted several areas for potential future work:

Explore the effects of DHT on antioxidants

While this study showed that DHT was able to increase the activity of catalase in the DPCs at 2% oxygen, this only led to a marked decrease in ROS in the balding DPCs. Therefore, it would be of interest to deliberate which other, if any, antioxidants are upregulated downstream of DHT. Moreover, as the beneficial reduction in ROS was only seen in the more androgen sensitive balding DPCs, the next step for this line of investigation would be to see whether androgen sensitive DPCs from the beard, axilla or pubis also upregulated antioxidant production with an associated reduction in ROS.

Investigate the factors controlling initial ROS production

While this study showed that balding DPCs had an elevated antioxidant response compared to occipital DPCs, it was shown that the balding DPCs still exhibited a higher level of intracellular ROS. Therefore further work elucidating the factors which control initial ROS production may help to gain a greater understanding of the redox equilibrium within the DPCs. The NADPH molecules of the mitochondria would be the most logical starting point for this line of investigation.

Investigate the role of the SP-1 transcription factor

SP-1 represents a common downstream target for TGF-β, glutathione, and pRB as well as acting as a transcription control upstream of TGF-β. The possibility that this transcription factor may represent a key focal-point to the control of the DPC function warrants further investigation.

Confirmation of TGF-β as an autocrine growth inhibitor of the dermal papilla

The work shown in this thesis demonstrated that TGF-β was able to act upon DPCs when applied exogenously, however further steps are required to confirm this as true autocrine regulation. This could be conducted by stimulating TGF-β secretion using DHT, as previously shown then transferring media to serum free cultured cells in the presence or absence of a TGF-β inhibitor such as SB431542. A suitable functional measurement for this assay would be the motility assay described in the previous chapter. Further to this expression of the TGF-β receptor within the DPCs must be further investigated. It would be of interest to ascertain whether the TGF-β receptor was expressed in DPCs cultured at 2% oxygen. In addition, histological analysis of balding and occipital dermal papillae *in vivo* would be key to gauging the importance of TGF-β as an autocrine regulator of the DP.

Bibliography

ALALUF, S., MUIR-HOWIE, H., HU, H. L., EVANS, A. & GREEN, M. R. 2000. Atmospheric oxygen accelerates the induction of a post-mitotic phenotype in human dermal fibroblasts: the key protective role of glutathione. *Differentiation,* 66**,** 147-55.

ALCORTA, D. A., XIONG, Y., PHELPS, D., HANNON, G., BEACH, D. & BARRETT, J. C. 1996. Involvement of the cyclin-dependent kinase inhibitor p16 (INK4a) in replicative senescence of normal human fibroblasts. *Proc Natl Acad Sci U S A,* 93**,** 13742-7.

ALMOND-ROESLER, B., SCHON, M., SCHON, M. P., BLUME-PEYTAVI, U., SOMMER, C., LOSTER, K. & ORFANOS, C. E. 1997. Cultured dermal papilla cells of the rat vibrissa follicle. Proliferative activity, adhesion properties and reorganization of the extracellular matrix in vitro. *Arch Dermatol Res,* 289**,** 698-704.

AMMANAMANCHI, S., KIM, S. J., SUN, L. Z. & BRATTAIN, M. G. 1998. Induction of transforming growth factor-beta receptor type II expression in estrogen receptor-positive breast cancer cells through SP1 activation by 5-aza-2'-deoxycytidine. *J Biol Chem,* 273**,** 16527-34.

ANDL, T., REDDY, S. T., GADDAPARA, T. & MILLAR, S. E. 2002. WNT signals are required for the initiation of hair follicle development. *Dev Cell,* 2**,** 643-53.

ARCK, P. C., OVERALL, R., SPATZ, K., LIEZMAN, C., HANDJISKI, B., KLAPP, B. F., BIRCH-MACHIN, M. A. & PETERS, E. M. 2006. Towards a "free radical theory of graying": melanocyte apoptosis in the aging human hair follicle is an indicator of oxidative stress induced tissue damage. *FASEB J,* 20**,** 1567-9.

BAHTA, A. W., FARJO, N., FARJO, B. & PHILPOTT, M. P. 2008. Premature senescence of balding dermal papilla cells in vitro is associated with p16(INK4a) expression. *J Invest Dermatol,* 128**,** 1088-94.

BAI, J. & CEDERBAUM, A. I. 2001. Mitochondrial catalase and oxidative injury. *Biol Signals Recept,* 10**,** 189-99.

BAI, J., RODRIGUEZ, A. M., MELENDEZ, J. A. & CEDERBAUM, A. I. 1999. Overexpression of catalase in cytosolic or mitochondrial compartment protects HepG2 cells against oxidative injury. *J Biol Chem,* 274**,** 26217-24.

BARRERA, A. 2003. Advances in aesthetic hair restoration. *Aesthet Surg J,* 23**,** 259-64.

BATCH, J. A., MERCURI, F. A. & WERTHER, G. A. 1996. Identification and localization of insulin-like growth factor-binding protein (IGFBP) messenger RNAs in human hair follicle dermal papilla. *J Invest Dermatol,* 106**,** 471-5.

BAYNE, E. K., FLANAGAN, J., EINSTEIN, M., AYALA, J., CHANG, B., AZZOLINA, B., WHITING, D. A., MUMFORD, R. A., THIBOUTOT, D., SINGER, II & HARRIS, G. 1999. Immunohistochemical localization of types 1 and 2 5alpha-reductase in human scalp. *Br J Dermatol,* 141**,** 481-91.

BEAUSEJOUR, C. M., KRTOLICA, A., GALIMI, F., NARITA, M., LOWE, S. W., YASWEN, P. & CAMPISI, J. 2003. Reversal of human cellular senescence: roles of the p53 and p16 pathways. *EMBO J,* 22**,** 4212-22.

BEN-PORATH, I. & WEINBERG, R. A. 2005. The signals and pathways activating cellular senescence. *Int J Biochem Cell Biol,* 37**,** 961-76.

BERGFELD, W. F. 1995. Androgenetic alopecia: an autosomal dominant disorder. *Am J Med,* 98**,** 95S-98S.

BIRCH, M. P. & MESSENGER, A. G. 2001. Genetic factors predispose to balding and non-balding in men. *Eur J Dermatol,* 11**,** 309-14.

BRADFORD, M. M. 1976. A rapid and sensitive method for the quantitation of microgram quantities of protein utilizing the principle of protein-dye binding. *Anal Biochem,* 72**,** 248-54.

BRENMOEHL, J., MILLER, S. N., HOFMANN, C., VOGL, D., FALK, W., SCHOLMERICH, J. & ROGLER, G. 2009. Transforming growth factor-beta 1 induces intestinal myofibroblast differentiation and modulates their migration. *World J Gastroenterol,* 15**,** 1431-42.

BRINGOLD, F. & SERRANO, M. 2000. Tumor suppressors and oncogenes in cellular senescence. *Exp Gerontol,* 35**,** 317-29.

BROWN, C. J., GOSS, S. J., LUBAHN, D. B., JOSEPH, D. R., WILSON, E. M., FRENCH, F. S. & WILLARD, H. F. 1989. Androgen receptor locus on the human X chromosome: regional localization to Xq11-12 and description of a DNA polymorphism. *Am J Hum Genet,* 44**,** 264-9.

BRUNK, U., ERICSSON, J. L., PONTEN, J. & WESTERMARK, B. 1973. Residual bodies and "aging" in cultured human glia cells. Effect of entrance into phase 3 and prolonged periods of confluence. *Exp Cell Res,* 79**,** 1-14.

BULL, J. J. 2002. Expression and putative functions of Myc superfamily and CCAAT/Enhancer binding protein transcription factors in the hair follicle. 29.

CAMPISI, J. 2001. Cellular senescence as a tumor-suppressor mechanism. *Trends Cell Biol,* 11**,** S27-31.

CHANCE, B. & OSHINO, N. 1971. Kinetics and mechanisms of catalase in peroxisomes of the mitochondrial fraction. *Biochem J,* 122**,** 225-33.

CHEN, Q. & AMES, B. N. 1994. Senescence-like growth arrest induced by hydrogen peroxide in human diploid fibroblast F65 cells. *Proc Natl Acad Sci U S A,* 91**,** 4130-4.

CHEN, Q., FISCHER, A., REAGAN, J. D., YAN, L. J. & AMES, B. N. 1995. Oxidative DNA damage and senescence of human diploid fibroblast cells. *Proc Natl Acad Sci U S A,* 92**,** 4337-41.

CHEN, Q. M. 2000. Replicative senescence and oxidant-induced premature senescence. Beyond the control of cell cycle checkpoints. *Ann N Y Acad Sci,* 908**,** 111-25.

CHEN, Q. M., TU, V. C., CATANIA, J., BURTON, M., TOUSSAINT, O. & DILLEY, T. 2000. Involvement of Rb family proteins, focal adhesion proteins and protein synthesis in senescent morphogenesis induced by hydrogen peroxide. *J Cell Sci,* 113 (Pt 22)**,** 4087-97.

CHOONG, C. S. & WILSON, E. M. 1998. Trinucleotide repeats in the human androgen receptor: a molecular basis for disease. *J Mol Endocrinol,* 21**,** 235-57.

CHOUDHRY, R., HODGINS, M. B., VAN DER KWAST, T. H., BRINKMANN, A. O. & BOERSMA, W. J. 1992. Localization of androgen receptors in human skin by immunohistochemistry: implications for the hormonal regulation of hair growth, sebaceous glands and sweat glands. *J Endocrinol,* 133**,** 467-75.

CHUNG, J. H. & EUN, H. C. 2007. Angiogenesis in skin aging and photoaging. *J Dermatol,* 34**,** 593-600.

COHN, J. N., MCINNES, G. T. & SHEPHERD, A. M. 2011. Direct-acting vasodilators. *J Clin Hypertens (Greenwich),* 13**,** 690-2.

COTSARELIS, G., SUN, T. T. & LAVKER, R. M. 1990. Label-retaining cells reside in the bulge area of pilosebaceous unit: implications for follicular stem cells, hair cycle, and skin carcinogenesis. *Cell,* 61**,** 1329-37.

COURTOIS, M., LOUSSOUARN, G., HOURSEAU, C. & GROLLIER, J. F. 1994. Hair cycle and alopecia. *Skin Pharmacol,* 7**,** 84-9.

COWIN, A. J., HOLMES, T. M., BROSNAN, P. & FERGUSON, M. W. 2001. Expression of TGF-beta and its receptors in murine fetal and adult dermal wounds. *Eur J Dermatol,* 11**,** 424-31.

CRISTOFALO, V. J., PIGNOLO, R. J., CIANCIARULO, F. L., DIPAOLO, B. R. & ROTENBERG, M. O. 1992. Changes in gene expression during senescence in culture. *Exp Gerontol,* 27**,** 429-32.

CUI, Y., ROBERTSON, J., MAHARAJ, S., WALDHAUSER, L., NIU, J., WANG, J., FARKAS, L., KOLB, M. & GAULDIE, J. 2011. Oxidative stress contributes to the induction and persistence of TGF-beta1 induced pulmonary fibrosis. *Int J Biochem Cell Biol,* 43**,** 1122-33.

CURTIN, D., JENKINS, S., FARMER, N., ANDERSON, A. C., HAISENLEDER, D. J., RISSMAN, E., WILSON, E. M. & SHUPNIK, M. A. 2001. Androgen suppression of GnRH-stimulated rat LHbeta gene transcription occurs through Sp1 sites in the distal GnRH-responsive promoter region. *Mol Endocrinol,* 15**,** 1906-17.

DANILENKO, D. M., RING, B. D. & PIERCE, G. F. 1996. Growth factors and cytokines in hair follicle development and cycling: recent insights from animal models and the potentials for clinical therapy. *Mol Med Today,* 2**,** 460-7.

DAOUSSIS, D. & ANDONOPOULOS, A. P. 2011. The emerging role of Dickkopf-1 in bone biology: is it the main switch controlling bone and joint remodeling? *Semin Arthritis Rheum,* 41**,** 170-7.

DAVIES, K. J. 1995. Oxidative stress: the paradox of aerobic life. *Biochem Soc Symp,* 61**,** 1-31.

DAVIES, K. J. 1999. The broad spectrum of responses to oxidants in proliferating cells: a new paradigm for oxidative stress. *IUBMB Life,* 48**,** 41-7.

DEBACQ-CHAINIAUX, F., BORLON, C., PASCAL, T., ROYER, V., ELIAERS, F., NINANE, N., CARRARD, G., FRIGUET, B., DE LONGUEVILLE, F., BOFFE, S., REMACLE, J. & TOUSSAINT, O. 2005. Repeated exposure of human skin fibroblasts to UVB at subcytotoxic level triggers premature senescence through the TGF-beta1 signaling pathway. *J Cell Sci,* 118**,** 743-58.

DIMRI, G. P., LEE, X., BASILE, G., ACOSTA, M., SCOTT, G., ROSKELLEY, C., MEDRANO, E. E., LINSKENS, M., RUBELJ, I., PEREIRA-SMITH, O. & ET AL. 1995. A biomarker that identifies senescent human cells in culture and in aging skin in vivo. *Proc Natl Acad Sci U S A,* 92**,** 9363-7.

EICHELER, W., HAPPLE, R. & HOFFMANN, R. 1998. 5 alpha-reductase activity in the human hair follicle concentrates in the dermal papilla. *Arch Dermatol Res,* 290**,** 126-32.

ELLIOTT, K., STEPHENSON, T. J. & MESSENGER, A. G. 1999. Differences in hair follicle dermal papilla volume are due to extracellular matrix volume and cell number: implications for the control of hair follicle size and androgen responses. *J Invest Dermatol,* 113**,** 873-7.

FITSIALOS, G., CHASSOT, A. A., TURCHI, L., DAYEM, M. A., LEBRIGAND, K., MOREILHON, C., MENEGUZZI, G., BUSCA, R., MARI, B., BARBRY, P. & PONZIO, G. 2007. Transcriptional signature of epidermal keratinocytes subjected to in vitro scratch wounding reveals selective roles for ERK1/2, p38, and phosphatidylinositol 3-kinase signaling pathways. *J Biol Chem,* 282**,** 15090-102.

FOITZIK, K., LINDNER, G., MUELLER-ROEVER, S., MAURER, M., BOTCHKAREVA, N., BOTCHKAREV, V., HANDJISKI, B., METZ, M., HIBINO, T., SOMA, T., DOTTO, G. P. & PAUS, R. 2000. Control of murine hair follicle regression (catagen) by TGF-beta1 in vivo. *FASEB J,* 14**,** 752-60.

FOITZIK, K., PAUS, R., DOETSCHMAN, T. & DOTTO, G. P. 1999. The TGF-beta2 isoform is both a required and sufficient inducer of murine hair follicle morphogenesis. *Dev Biol,* 212**,** 278-89.

FORSYTH, N. R., EVANS, A. P., SHAY, J. W. & WRIGHT, W. E. 2003. Developmental differences in the immortalization of lung fibroblasts by telomerase. *Aging Cell,* 2**,** 235-43.

FRIPPIAT, C., CHEN, Q. M., ZDANOV, S., MAGALHAES, J. P., REMACLE, J. & TOUSSAINT, O. 2001. Subcytotoxic H2O2 stress triggers a release of transforming growth factor-beta 1, which induces biomarkers of cellular senescence of human diploid fibroblasts. *J Biol Chem,* 276**,** 2531-7.

FRIPPIAT, C., DEWELLE, J., REMACLE, J. & TOUSSAINT, O. 2002. Signal transduction in H2O2-induced senescence-like phenotype in human diploid fibroblasts. *Free Radic Biol Med,* 33**,** 1334-46.

DRY, F. W., 1926. Coat of the mouse (*Mus Musculus*). *J Genetics,* 16**,** 287-340.

GAETANI, G. F., FERRARIS, A. M., ROLFO, M., MANGERINI, R., ARENA, S. & KIRKMAN, H. N. 1996. Predominant role of catalase in the disposal of hydrogen peroxide within human erythrocytes. *Blood,* 87**,** 1595-9.

GARY, R. K. & KINDELL, S. M. 2005. Quantitative assay of senescence-associated beta-galactosidase activity in mammalian cell extracts. *Anal Biochem,* 343**,** 329-34.

GEISER, A. G., BUSAM, K. J., KIM, S. J., LAFYATIS, R., O'REILLY, M. A., WEBBINK, R., ROBERTS, A. B. & SPORN, M. B. 1993. Regulation of the transforming growth factor-beta 1 and -beta 3 promoters by transcription factor Sp1. *Gene,* 129**,** 223-8.

GERLAND, L. M., PEYROL, S., LALLEMAND, C., BRANCHE, R., MAGAUD, J. P. & FFRENCH, M. 2003. Association of increased autophagic inclusions labeled for beta-galactosidase with fibroblastic aging. *Exp Gerontol,* 38**,** 887-95.

GEYFMAN, M. & ANDERSEN, B. 2010. Clock genes, hair growth and aging. *Aging (Albany NY),* 2**,** 122-8.

GUTTERIDGE, J. M. & QUINLAN, G. J. 1992. Antioxidant protection against organic and inorganic oxygen radicals by normal human plasma: the important primary role for iron-binding and iron-oxidising proteins. *Biochim Biophys Acta,* 1159**,** 248-54.

HAMADA, K. & RANDALL, V. A. 2006. Inhibitory autocrine factors produced by the mesenchyme-derived hair follicle dermal papilla may be a key to male pattern baldness. *Br J Dermatol,* 154**,** 609-18.

HAMADA, K., THORNTON, M. J., LAING, I., MESSENGER, A. G. & RANDALL, V. A. 1996. The metabolism of testosterone by dermal papilla cells cultured from human pubic and axillary hair follicles concurs with hair growth in 5 alpha-reductase deficiency. *J Invest Dermatol,* 106**,** 1017-22.

HAMILTON, J. B. 1951. Patterned loss of hair in man; types and incidence. *Ann N Y Acad Sci,* 53**,** 708-28.

HAMILTON, J. B. 1960. Effect of castration in adolescent and young adult males upon further changes in the proportions of bare and hairy scalp. *J Clin Endocrinol Metab,* 20**,** 1309-18.

HAMILTON, J. B., TERADA, H. & MESTLER, G. E. 1958. Studies of growth throughout the life span in Japanese. II. Beard growth in relation to age, sex, heredity, and other factors. *J Gerontol,* 13**,** 269-81.

HARA, E., SMITH, R., PARRY, D., TAHARA, H., STONE, S. & PETERS, G. 1996. Regulation of p16CDKN2 expression and its implications for cell immortalization and senescence. *Mol Cell Biol,* 16**,** 859-67.

HARMAN, D. 1991. The aging process: major risk factor for disease and death. *Proc Natl Acad Sci U S A,* 88**,** 5360-3.

HARMAN, D. 1992. Role of free radicals in aging and disease. *Ann N Y Acad Sci,* 673**,** 126-41.

HAUPT, Y., ALEXANDER, W. S., BARRI, G., KLINKEN, S. P. & ADAMS, J. M. 1991. Novel zinc finger gene implicated as myc collaborator by retrovirally accelerated lymphomagenesis in E mu-myc transgenic mice. *Cell,* 65**,** 753-63.

HAWKINS, A. J., GOLDING, S. E., KHALIL, A. & VALERIE, K. 2011. DNA double-strand break-induced pro-survival signaling. *Radiother Oncol,* 101**,** 13-7.

HAYFLICK, L. & MOORHEAD, P. S. 1961. The serial cultivation of human diploid cell strains. *Exp Cell Res,* 25**,** 585-621.

HENGARTNER, M. O. 2000. The biochemistry of apoptosis. *Nature,* 407**,** 770-6.

HERRERA, B., ALVAREZ, A. M., BELTRAN, J., VALDES, F., FABREGAT, I. & FERNANDEZ, M. 2004a. Resistance to TGF-beta-induced apoptosis in regenerating hepatocytes. *J Cell Physiol,* 201**,** 385-92.

HERRERA, B., ALVAREZ, A. M., SANCHEZ, A., FERNANDEZ, M., RONCERO, C., BENITO, M. & FABREGAT, I. 2001. Reactive oxygen species (ROS) mediates the mitochondrial-dependent apoptosis induced by transforming growth factor (beta) in fetal hepatocytes. *FASEB J,* 15**,** 741-51.

HERRERA, B., MURILLO, M. M., ALVAREZ-BARRIENTOS, A., BELTRAN, J., FERNANDEZ, M. & FABREGAT, I. 2004b. Source of early reactive oxygen species in the apoptosis induced by transforming growth factor-beta in fetal rat hepatocytes. *Free Radic Biol Med,* 36**,** 16-26.

HIBBERTS, N. A., HOWELL, A. E. & RANDALL, V. A. 1998. Balding hair follicle dermal papilla cells contain higher levels of androgen receptors than those from non-balding scalp. *J Endocrinol,* 156**,** 59-65.

HIBINO, T. & NISHIYAMA, T. 2004. Role of TGF-beta2 in the human hair cycle. *J Dermatol Sci,* 35**,** 9-18.

HIGGINS, C. A., RICHARDSON, G. D., FERDINANDO, D., WESTGATE, G. E. & JAHODA, C. A. 2010. Modelling the hair follicle dermal papilla using spheroid cell cultures. *Exp Dermatol,* 19**,** 546-8.

HIGGINS, C. A., RICHARDSON, G. D., WESTGATE, G. E. & JAHODA, C. A. 2009. Exogen involves gradual release of the hair club fibre in the vibrissa follicle model. *Exp Dermatol,* 18**,** 793-5.

HILLMER, A. M., HANNEKEN, S., RITZMANN, S., BECKER, T., FREUDENBERG, J., BROCKSCHMIDT, F. F., FLAQUER, A., FREUDENBERG-HUA, Y., JAMRA, R. A., METZEN, C., HEYN, U., SCHWEIGER, N., BETZ, R. C., BLAUMEISER, B., HAMPE, J., SCHREIBER, S., SCHULZE, T. G., HENNIES, H. C., SCHUMACHER, J., PROPPING, P., RUZICKA, T., CICHON, S., WIENKER, T. F., KRUSE, R. & NOTHEN, M. M. 2005. Genetic variation in the human androgen receptor gene is the major determinant of common early-onset androgenetic alopecia. *Am J Hum Genet,* 77**,** 140-8.

HINSON, J. P. & KHAN, M. 2004. Dehydroepiandrosterone sulphate (DHEAS) inhibits growth of human vascular endothelial cells. *Endocr Res,* 30**,** 667-71.

HIRANI, R., HANSSEN, E. & GIBSON, M. A. 2007. LTBP-2 specifically interacts with the amino-terminal region of fibrillin-1 and competes with LTBP-1 for binding to this microfibrillar protein. *Matrix Biol,* 26**,** 213-23.

HODAK, E., GOTTLIEB, A. B., COLEN, S., ANZILOTTI, M. & KRUEGER, J. G. 1996. In vivo expression of the insulin-like growth factor-I (IGF-I) receptor in congenital pigmented nevi. *J Cutan Pathol,* 23**,** 19-24.

HOFFMANN, R. 2002. Male androgenetic alopecia. *Clin Exp Dermatol,* 27**,** 373-82.

HWANG, K. A., HWANG, Y. L., LEE, M. H., KIM, N. R., ROH, S. S., LEE, Y., KIM, C. D., LEE, J. H. & CHOI, K. C. 2012. Adenosine stimulates growth of dermal papilla and lengthens the anagen phase by increasing the cysteine level via fibroblast growth factors 2 and 7 in an organ culture of mouse vibrissae hair follicles. *Int J Mol Med,* 29**,** 195-201.

HWANG, S. T., KIM, H. Y., LEE, S. J., LEE, W. J., KIM DO, W. & KIM, J. C. 2009. Recipient-site influence in hair transplantation: a confirmative study. *Dermatol Surg,* 35**,** 1011-4.

HYYTIAINEN, M. & KESKI-OJA, J. 2003. Latent TGF-beta binding protein LTBP-2 decreases fibroblast adhesion to fibronectin. *J Cell Biol,* 163**,** 1363-74.

HYYTIAINEN, M., PENTTINEN, C. & KESKI-OJA, J. 2004. Latent TGF-beta binding proteins: extracellular matrix association and roles in TGF-beta activation. *Crit Rev Clin Lab Sci,* 41**,** 233-64.

IMPERATO-MCGINLEY, J., GAUTIER, T., PICHARDO, M. & SHACKLETON, C. 1986. The diagnosis of 5 alpha-reductase deficiency in infancy. *J Clin Endocrinol Metab,* 63**,** 1313-8.

INMAN, G. J., NICOLAS, F. J., CALLAHAN, J. F., HARLING, J. D., GASTER, L. M., REITH, A. D., LAPING, N. J. & HILL, C. S. 2002. SB-431542 is a potent and specific inhibitor of transforming growth factor-beta superfamily type I activin receptor-like kinase (ALK) receptors ALK4, ALK5, and ALK7. *Mol Pharmacol,* 62**,** 65-74.

INUI, S., FUKUZATO, Y., NAKAJIMA, T., YOSHIKAWA, K. & ITAMI, S. 2002. Androgen-inducible TGF-beta1 from balding dermal papilla cells inhibits epithelial cell growth: a clue to understand paradoxical effects of androgen on human hair growth. *FASEB J,* 16**,** 1967-9.

INUI, S., FUKUZATO, Y., NAKAJIMA, T., YOSHIKAWA, K. & ITAMI, S. 2003. Identification of androgen-inducible TGF-beta1 derived from dermal papilla cells as a key mediator in androgenetic alopecia. *J Investig Dermatol Symp Proc,* 8**,** 69-71.

INUI, S., ITAMI, S., PAN, H. J. & CHANG, C. 2000. Lack of androgen receptor transcriptional activity in human keratinocytes. *J Dermatol Sci,* 23**,** 87-92.

ITAHANA, K., CAMPISI, J. & DIMRI, G. P. 2007. Methods to detect biomarkers of cellular senescence: the senescence-associated beta-galactosidase assay. *Methods Mol Biol,* 371**,** 21-31.

ITAHANA, K., DIMRI, G. & CAMPISI, J. 2001. Regulation of cellular senescence by p53. *Eur J Biochem,* 268**,** 2784-91.

ITAHANA, K., ZOU, Y., ITAHANA, Y., MARTINEZ, J. L., BEAUSEJOUR, C., JACOBS, J. J., VAN LOHUIZEN, M., BAND, V., CAMPISI, J. & DIMRI, G. P. 2003. Control of the replicative life span of human fibroblasts by p16 and the polycomb protein Bmi-1. *Mol Cell Biol,* 23**,** 389-401.

ITAMI, S. & INUI, S. 2005. Role of androgen in mesenchymal epithelial interactions in human hair follicle. *J Investig Dermatol Symp Proc,* 10**,** 209-11.

ITAMI, S., KURATA, S. & TAKAYASU, S. 1995. Androgen induction of follicular epithelial cell growth is mediated via insulin-like growth factor-I from dermal papilla cells. *Biochem Biophys Res Commun,* 212**,** 988-94.

JACKSON, E. A. 2000. Hair disorders. *Prim Care,* 27**,** 319-32.

JACOBS, J. J. & DE LANGE, T. 2004. Significant role for p16INK4a in p53-independent telomere-directed senescence. *Curr Biol,* 14**,** 2302-8.

JAHODA, C. & OLIVER, R. F. 1981. The growth of vibrissa dermal papilla cells in vitro. *Br J Dermatol,* 105**,** 623-7.

JAHODA, C. A., HORNE, K. A. & OLIVER, R. F. 1984. Induction of hair growth by implantation of cultured dermal papilla cells. *Nature,* 311**,** 560-2.

JAHODA, C. A. & REYNOLDS, A. J. 1996. Dermal-epidermal interactions. Adult follicle-derived cell populations and hair growth. *Dermatol Clin,* 14**,** 573-83.

JAWORSKY, C., KLIGMAN, A. M. & MURPHY, G. F. 1992. Characterization of inflammatory infiltrates in male pattern alopecia: implications for pathogenesis. *Br J Dermatol,* 127**,** 239-46.

KAUFMAN, K. D. 1996. Androgen metabolism as it affects hair growth in androgenetic alopecia. *Dermatol Clin,* 14**,** 697-711.

KAUSER, S., WESTGATE, G. E., GREEN, M. R. & TOBIN, D. J. 2010. Human Hair Follicle and Epidermal Melanocytes Exhibit Striking Differences in Their Aging Profile which Involves Catalase. *J Invest Dermatol*.

KESKI-OJA, J., RAGHOW, R., SAWDEY, M., LOSKUTOFF, D. J., POSTLETHWAITE, A. E., KANG, A. H. & MOSES, H. L. 1988. Regulation of mRNAs for type-1 plasminogen activator inhibitor, fibronectin, and type I procollagen by transforming growth factor-beta. Divergent responses in lung fibroblasts and carcinoma cells. *J Biol Chem,* 263**,** 3111-5.

KIYONO, T., FOSTER, S. A., KOOP, J. I., MCDOUGALL, J. K., GALLOWAY, D. A. & KLINGELHUTZ, A. J. 1998. Both Rb/p16INK4a inactivation and telomerase activity are required to immortalize human epithelial cells. *Nature,* 396**,** 84-8.

KLIGMAN, A. M. 1959. The human hair cycle. *J Invest Dermatol,* 33**,** 307-16.

KLIGMAN, A. M. 1988. The comparative histopathology of male-pattern baldness and senescent baldness. *Clin Dermatol,* 6**,** 108-18.

KOLI, K., SAHARINEN, J., HYYTIAINEN, M., PENTTINEN, C. & KESKI-OJA, J. 2001. Latency, activation, and binding proteins of TGF-beta. *Microsc Res Tech,* 52**,** 354-62.

KUNZ-SCHUGHART, L. A., WENNINGER, S., NEUMEIER, T., SEIDL, P. & KNUECHEL, R. 2003. Three-dimensional tissue structure affects sensitivity of fibroblasts to TGF-beta 1. *Am J Physiol Cell Physiol,* 284**,** C209-19.

KURZ, D. J., DECARY, S., HONG, Y. & ERUSALIMSKY, J. D. 2000. Senescence-associated (beta)-galactosidase reflects an increase in lysosomal mass during replicative ageing of human endothelial cells. *J Cell Sci,* 113 (Pt 20)**,** 3613-22.

KWACK, M. H., KIM, M. K., KIM, J. C. & SUNG, Y. K. 2012. Dickkopf 1 promotes regression of hair follicles. *J Invest Dermatol,* 132**,** 1554-60.

KWACK, M. H., SUNG, Y. K., CHUNG, E. J., IM, S. U., AHN, J. S., KIM, M. K. & KIM, J. C. 2008. Dihydrotestosterone-inducible dickkopf 1 from balding dermal papilla cells causes apoptosis in follicular keratinocytes. *J Invest Dermatol,* 128**,** 262-9.

LEE, M. N., LEE, S. H., LEE, M. Y., KIM, Y. H., PARK, J. H., RYU, J. M., YUN, S. P., LEE, Y. J., KIM, M. O., PARK, K. & HAN, H. J. 2008. Effect of dihydrotestosterone on mouse embryonic stem cells exposed to H2O2-induced oxidative stress. *J Vet Sci,* 9**,** 247-56.

LEWIS, D. A., TRAVERS, J. B. & SPANDAU, D. F. 2009. A new paradigm for the role of aging in the development of skin cancer. *J Invest Dermatol,* 129**,** 787-91.

LIN, F., JACKSON, V. E. & GIROTTI, A. W. 1995. Amplification and hyperexpression of the catalase gene in selenoperoxidase-deficient leukemia cells. *Arch Biochem Biophys,* 317**,** 7-18.

LINDNER, G., BOTCHKAREV, V. A., BOTCHKAREVA, N. V., LING, G., VAN DER VEEN, C. & PAUS, R. 1997. Analysis of apoptosis during hair follicle regression (catagen). *Am J Pathol,* 151**,** 1601-17.

LUBAHN, D. B., JOSEPH, D. R., SULLIVAN, P. M., WILLARD, H. F., FRENCH, F. S. & WILSON, E. M. 1988. Cloning of human androgen receptor complementary DNA and localization to the X chromosome. *Science,* 240**,** 327-30.

LUKAS, J., BARTKOVA, J., ROHDE, M., STRAUSS, M. & BARTEK, J. 1995. Cyclin D1 is dispensable for G1 control in retinoblastoma gene-deficient cells independently of cdk4 activity. *Mol Cell Biol,* 15**,** 2600-11.

LUTZ, M. & KNAUS, P. 2002. Integration of the TGF-beta pathway into the cellular signalling network. *Cell Signal,* 14**,** 977-88.

LYNFIELD, Y. L. 1960. Effect of pregnancy on the human hair cycle. *J Invest Dermatol,* 35**,** 323-7.

MAHER, P. 2005. The effects of stress and aging on glutathione metabolism. *Ageing Res Rev,* 4**,** 288-314.

MANGELSDORF, D. J., THUMMEL, C., BEATO, M., HERRLICH, P., SCHUTZ, G., UMESONO, K., BLUMBERG, B., KASTNER, P., MARK, M., CHAMBON, P. & EVANS, R. M. 1995. The nuclear receptor superfamily: the second decade. *Cell,* 83**,** 835-9.

MARSHALL, W. A. 1970. Sex differences at puberty. *J Biosoc Sci Suppl,* 2**,** 31-41.
MCELWEE, K. & HOFFMANN, R. 2000. Growth factors in early hair follicle morphogenesis. *Eur J Dermatol,* 10**,** 341-50.
MCELWEE, K. J., KISSLING, S., WENZEL, E., HUTH, A. & HOFFMANN, R. 2003. Cultured peribulbar dermal sheath cells can induce hair follicle development and contribute to the dermal sheath and dermal papilla. *J Invest Dermatol,* 121**,** 1267-75.
MESSENGER, A. G. 1984. The culture of dermal papilla cells from human hair follicles. *Br J Dermatol,* 110**,** 685-9.
MESSENGER, A. G. 1989. Isolation, culture and in vitro behaviour of cells isolated from papillae of the human hair follicle. . *Trends in Human Hair Growth and Alopecia Research* 57-67.
MESSENGER, A. G., ELLIOTT, K., TEMPLE, A. & RANDALL, V. A. 1991a. Expression of basement membrane proteins and interstitial collagens in dermal papillae of human hair follicles. *J Invest Dermatol,* 96**,** 93-7.
MESSENGER, A. G., ELLIOTT, K., WESTGATE, G. E. & GIBSON, W. T. 1991b. Distribution of extracellular matrix molecules in human hair follicles. *Ann N Y Acad Sci,* 642**,** 253-62.
MILNER, Y., SUDNIK, J., FILIPPI, M., KIZOULIS, M., KASHGARIAN, M. & STENN, K. 2002. Exogen, shedding phase of the hair growth cycle: characterization of a mouse model. *J Invest Dermatol,* 119**,** 639-44.
MIRANDA, B. H., TOBIN, D. J., SHARPE, D. T. & RANDALL, V. A. 2010. Intermediate hair follicles: a new more clinically relevant model for hair growth investigations. *Br J Dermatol,* 163**,** 287-95.
MIYAZONO, K., TEN DIJKE, P. & HELDIN, C. H. 2000. TGF-beta signaling by Smad proteins. *Adv Immunol,* 75**,** 115-57.
MOERMAN, D. E. 1988. The meaning of baldness and implications for treatment. *Clin Dermatol,* 6**,** 89-92.
MOSES, H. L., COFFEY, R. J., JR., LEOF, E. B., LYONS, R. M. & KESKI-OJA, J. 1987. Transforming growth factor beta regulation of cell proliferation. *J Cell Physiol Suppl,* Suppl 5**,** 1-7.
MYERS, R. J. & HAMILTON, J. B. 1951. Regeneration and rate of growth of hairs in man. *Ann N Y Acad Sci,* 53**,** 562-8.
MYMRIKOV, E. V., SEIT-NEBI, A. S. & GUSEV, N. B. 2011. Large potentials of small heat shock proteins. *Physiol Rev,* 91**,** 1123-59.
NAKAO, A., IMAMURA, T., SOUCHELNYTSKYI, S., KAWABATA, M., ISHISAKI, A., OEDA, E., TAMAKI, K., HANAI, J., HELDIN, C. H., MIYAZONO, K. & TEN DIJKE, P. 1997. TGF-beta receptor-mediated signalling through Smad2, Smad3 and Smad4. *EMBO J,* 16**,** 5353-62.
NIEHRS, C. & SHEN, J. 2010. Regulation of Lrp6 phosphorylation. *Cell Mol Life Sci,* 67**,** 2551-62.
NORLEN, L., NICANDER, I., LUNDH ROZELL, B., OLLMAR, S. & FORSLIND, B. 1999. Inter- and intra-individual differences in human stratum corneum lipid content related to physical parameters of skin barrier function in vivo. *J Invest Dermatol,* 112**,** 72-7.
NORWOOD, O. T. 1975. Male pattern baldness: classification and incidence. *South Med J,* 68**,** 1359-65.
OHTANI, N., ZEBEDEE, Z., HUOT, T. J., STINSON, J. A., SUGIMOTO, M., OHASHI, Y., SHARROCKS, A. D., PETERS, G. & HARA, E. 2001. Opposing effects of Ets and Id proteins on p16INK4a expression during cellular senescence. *Nature,* 409**,** 1067-70.
OLIVER, R. F. 1966. Histological studies of whisker regeneration in the hooded rat. *J Embryol Exp Morphol,* 16**,** 231-44.

OLIVER, R. F. 1967. The experimental induction of whisker growth in the hooded rat by implantation of dermal papillae. *J Embryol Exp Morphol,* 18**,** 43-51.

OLIVER, R. F. 1971. The dermal papilla and the development and growth of hair. *J Soc Cosmet Chem,* 22**,** 741-755.

OUJI, Y., YOSHIKAWA, M., MORIYA, K. & ISHIZAKA, S. 2007. Effects of Wnt-10b on hair shaft growth in hair follicle cultures. *Biochem Biophys Res Commun,* 359**,** 516-22.

PARAKKAL, P. F. 1970. Morphogenesis of the hair follicle during catagen. *Z Zellforsch Mikrosk Anat,* 107**,** 174-86.

PATHAK, S., SINGH, R., VERSCHOYLE, R. D., GREAVES, P., FARMER, P. B., STEWARD, W. P., MELLON, J. K., GESCHER, A. J. & SHARMA, R. A. 2008. Androgen manipulation alters oxidative DNA adduct levels in androgen-sensitive prostate cancer cells grown in vitro and in vivo. *Cancer Lett,* 261**,** 74-83.

PAUS, R. 1998. Principles of hair cycle control. *J Dermatol,* 25**,** 793-802.

PAUS, R. & COTSARELIS, G. 1999. The biology of hair follicles. *N Engl J Med,* 341**,** 491-7.

PAUS, R., FOITZIK, K., WELKER, P., BULFONE-PAUS, S. & EICHMULLER, S. 1997. Transforming growth factor-beta receptor type I and type II expression during murine hair follicle development and cycling. *J Invest Dermatol,* 109**,** 518-26.

PERIYASAMY, S., AMMANAMANCHI, S., TILLEKERATNE, M. P. & BRATTAIN, M. G. 2000. Repression of transforming growth factor-beta receptor type I promoter expression by Sp1 deficiency. *Oncogene,* 19**,** 4660-7.

PHILPOTT, M. P., GREEN, M. R. & KEALEY, T. 1990. Human hair growth in vitro. *J Cell Sci,* 97 (Pt 3)**,** 463-71.

PHILPOTT, M. P., PAUS R. 1998. Principles of hair follicle morphogenesis. In. *C. M. Chuong: Molecular Basis of Epithelial Appendage Morphogenesis,* Landes Bioscience Publ, Austin TX**,** 75-103.

PHILPOTT, M. P., SANDERS, D. A. & KEALEY, T. 1994. Effects of insulin and insulin-like growth factors on cultured human hair follicles: IGF-I at physiologic concentrations is an important regulator of hair follicle growth in vitro. *J Invest Dermatol,* 102**,** 857-61.

PIRROTTA, V. 1998. Polycombing the genome: PcG, trxG, and chromatin silencing. *Cell,* 93**,** 333-6.

POLJSAK, B. & DAHMANE, R. 2012. Free radicals and extrinsic skin aging. *Dermatol Res Pract,* 2012**,** 135206.

POSTLETHWAITE, A. E., KESKI-OJA, J., MOSES, H. L. & KANG, A. H. 1987. Stimulation of the chemotactic migration of human fibroblasts by transforming growth factor beta. *J Exp Med,* 165**,** 251-6.

QUELLE, D. E., ZINDY, F., ASHMUN, R. A. & SHERR, C. J. 1995. Alternative reading frames of the INK4a tumor suppressor gene encode two unrelated proteins capable of inducing cell cycle arrest. *Cell,* 83**,** 993-1000.

QUIGLEY, C. A., DE BELLIS, A., MARSCHKE, K. B., EL-AWADY, M. K., WILSON, E. M. & FRENCH, F. S. 1995. Androgen receptor defects: historical, clinical, and molecular perspectives. *Endocr Rev,* 16**,** 271-321.

RAGHOW, R., POSTLETHWAITE, A. E., KESKI-OJA, J., MOSES, H. L. & KANG, A. H. 1987. Transforming growth factor-beta increases steady state levels of type I procollagen and fibronectin messenger RNAs posttranscriptionally in cultured human dermal fibroblasts. *J Clin Invest,* 79**,** 1285-8.

RAMIREZ, P. T., GERSHENSON, D. M., TORTOLERO-LUNA, G., RAMONDETTA, L. M., FIGHTMASTER, D., WHARTON, J. T. & WOLF, J. K. 2001. Expression of cell-cycle mediators in ovarian cancer cells after transfection with p16(INK4a), p21(WAF1/Cip-1), and p53. *Gynecol Oncol,* 83**,** 543-8.

RANDALL, V. A. 2007. Hormonal regulation of hair follicles exhibits a biological paradox. *Semin Cell Dev Biol,* 18**,** 274-85.

RANDALL, V. A. 2008. Androgens and hair growth. *Dermatol Ther,* 21**,** 314-28.

RANDALL, V. A., HIBBERTS, N. A., THORNTON, M. J., MERRICK, A. E., HAMADA, K., KATO, S., JENNER, T. J., DE OLIVEIRA, I. & MESSENGER, A. G. 2001. Do androgens influence hair growth by altering the paracrine factors secreted by dermal papilla cells? *Eur J Dermatol,* 11**,** 315-20.

RANDALL, V. A., THORNTON, M. J., HAMADA, K. & MESSENGER, A. G. 1994. Androgen action in cultured dermal papilla cells from human hair follicles. *Skin Pharmacol,* 7**,** 20-6.

RANDALL, V. A., THORNTON, M. J., HAMADA, K., REDFERN, C. P., NUTBROWN, M., EBLING, F. J. & MESSENGER, A. G. 1991. Androgens and the hair follicle. Cultured human dermal papilla cells as a model system. *Ann N Y Acad Sci,* 642**,** 355-75.

RANDALL, V. A., THORNTON, M. J. & MESSENGER, A. G. 1992. Cultured dermal papilla cells from androgen-dependent human hair follicles (e.g. beard) contain more androgen receptors than those from non-balding areas of scalp. *J Endocrinol,* 133**,** 141-7.

RAY, P. D., HUANG, B. W. & TSUJI, Y. 2012. Reactive oxygen species (ROS) homeostasis and redox regulation in cellular signaling. *Cell Signal,* 24**,** 981-90.

REED, M. J., VERNON, R. B., ABRASS, I. B. & SAGE, E. H. 1994. TGF-beta 1 induces the expression of type I collagen and SPARC, and enhances contraction of collagen gels, by fibroblasts from young and aged donors. *J Cell Physiol,* 158**,** 169-79.

REYNOLDS, A. J. & JAHODA, C. A. 1992. Cultured dermal papilla cells induce follicle formation and hair growth by transdifferentiation of an adult epidermis. *Development,* 115**,** 587-93.

REYNOLDS, A. J., LAWRENCE, C., CSERHALMI-FRIEDMAN, P. B., CHRISTIANO, A. M. & JAHODA, C. A. 1999. Trans-gender induction of hair follicles. *Nature,* 402**,** 33-4.

RHEINWALD, J. G., HAHN, W. C., RAMSEY, M. R., WU, J. Y., GUO, Z., TSAO, H., DE LUCA, M., CATRICALA, C. & O'TOOLE, K. M. 2002. A two-stage, p16(INK4A)- and p53-dependent keratinocyte senescence mechanism that limits replicative potential independent of telomere status. *Mol Cell Biol,* 22**,** 5157-72.

RHYU, D. Y., YANG, Y., HA, H., LEE, G. T., SONG, J. S., UH, S. T. & LEE, H. B. 2005. Role of reactive oxygen species in TGF-beta1-induced mitogen-activated protein kinase activation and epithelial-mesenchymal transition in renal tubular epithelial cells. *J Am Soc Nephrol,* 16**,** 667-75.

ROBBINS, E., LEVINE, E. M. & EAGLE, H. 1970. Morphologic changes accompanying senescence of cultured human diploid cells. *J Exp Med,* 131**,** 1211-22.

ROBLES, S. J. & ADAMI, G. R. 1998. Agents that cause DNA double strand breaks lead to p16INK4a enrichment and the premature senescence of normal fibroblasts. *Oncogene,* 16**,** 1113-23.

RUAS, M. & PETERS, G. 1998. The p16INK4a/CDKN2A tumor suppressor and its relatives. *Biochim Biophys Acta,* 1378**,** F115-77.

RUDMAN, S. M., PHILPOTT, M. P., THOMAS, G. A. & KEALEY, T. 1997. The role of IGF-I in human skin and its appendages: morphogen as well as mitogen? *J Invest Dermatol,* 109**,** 770-7.

SAHARINEN, J., HYYTIAINEN, M., TAIPALE, J. & KESKI-OJA, J. 1999. Latent transforming growth factor-beta binding proteins (LTBPs)--structural extracellular matrix proteins for targeting TGF-beta action. *Cytokine Growth Factor Rev,* 10**,** 99-117.

SENTURK, S., MUMCUOGLU, M., GURSOY-YUZUGULLU, O., CINGOZ, B., AKCALI, K. C. & OZTURK, M. 2010. Transforming growth factor-beta induces senescence in hepatocellular carcinoma cells and inhibits tumor growth. *Hepatology,* 52**,** 966-74.

SERRANO, M. 1997. The tumor suppressor protein p16INK4a. *Exp Cell Res,* 237**,** 7-13.

SERRANO, M. & BLASCO, M. A. 2001. Putting the stress on senescence. *Curr Opin Cell Biol,* 13**,** 748-53.

SERRANO, M., HANNON, G. J. & BEACH, D. 1993. A new regulatory motif in cell-cycle control causing specific inhibition of cyclin D/CDK4. *Nature,* 366**,** 704-7.

SETTY, L. R. 1970. Hair patterns of scalp of white and Negro males. *Am J Phys Anthropol,* 33**,** 49-55.

SHERR, C. J. & MCCORMICK, F. 2002. The RB and p53 pathways in cancer. *Cancer Cell,* 2**,** 103-12.

SHIM, J. H., XIAO, C., PASCHAL, A. E., BAILEY, S. T., RAO, P., HAYDEN, M. S., LEE, K. Y., BUSSEY, C., STECKEL, M., TANAKA, N., YAMADA, G., AKIRA, S., MATSUMOTO, K. & GHOSH, S. 2005. TAK1, but not TAB1 or TAB2, plays an essential role in multiple signaling pathways in vivo. *Genes Dev,* 19**,** 2668-81.

SIITERI, P. K. & WILSON, J. D. 1970. Dihydrotestosterone in prostatic hypertrophy. I. The formation and content of dihydrotestosterone in the hypertrophic prostate of man. *J Clin Invest,* 49**,** 1737-45.

SILVER, R. I., WILEY, E. L., THIGPEN, A. E., GUILEYARDO, J. M., MCCONNELL, J. D. & RUSSELL, D. W. 1994. Cell type specific expression of steroid 5 alpha-reductase 2. *J Urol,* 152**,** 438-42.

STARKOV, A. A., FISKUM, G., CHINOPOULOS, C., LORENZO, B. J., BROWNE, S. E., PATEL, M. S. & BEAL, M. F. 2004. Mitochondrial alpha-ketoglutarate dehydrogenase complex generates reactive oxygen species. *J Neurosci,* 24**,** 7779-88.

STEIN, G. H., DRULLINGER, L. F., SOULARD, A. & DULIC, V. 1999. Differential roles for cyclin-dependent kinase inhibitors p21 and p16 in the mechanisms of senescence and differentiation in human fibroblasts. *Mol Cell Biol,* 19**,** 2109-17.

STENN, K. S. & PAUS, R. 2001. Controls of hair follicle cycling. *Physiol Rev,* 81**,** 449-494.

TAIPALE, J., KOLI, K. & KESKI-OJA, J. 1992. Release of transforming growth factor-beta 1 from the pericellular matrix of cultured fibroblasts and fibrosarcoma cells by plasmin and thrombin. *J Biol Chem,* 267**,** 25378-84.

TATTI, O., VEHVILAINEN, P., LEHTI, K. & KESKI-OJA, J. 2008. MT1-MMP releases latent TGF-beta1 from endothelial cell extracellular matrix via proteolytic processing of LTBP-1. *Exp Cell Res,* 314**,** 2501-14.

TAYLOR, P. J. 2009. Big head? Bald head! Skull expansion: alternative model for the primary mechanism of AGA. *Med Hypotheses,* 72**,** 23-8.

THANNICKAL, V. J. & FANBURG, B. L. 1995. Activation of an H2O2-generating NADH oxidase in human lung fibroblasts by transforming growth factor beta 1. *J Biol Chem,* 270**,** 30334-8.

THANNICKAL, V. J. & FANBURG, B. L. 2000. Reactive oxygen species in cell signaling. *Am J Physiol Lung Cell Mol Physiol,* 279**,** L1005-28.

THATIKUNTA, P., RAJ, G. V., KUNDU, M., KHALILI, K. & AMINI, S. 1997. The transcription factor E2F-1 modulates TGF-beta1 RNA expression in glial cells. *Oncogene,* 14**,** 2959-69.

THORNTON, M. J., HAMADA, K., MESSENGER, A. G. & RANDALL, V. A. 1998. Androgen-dependent beard dermal papilla cells secrete autocrine growth factor(s) in response to testosterone unlike scalp cells. *J Invest Dermatol,* 111**,** 727-32.

THORNTON, M. J., NELSON, L. D., TAYLOR, A. H., BIRCH, M. P., LAING, I. & MESSENGER, A. G. 2006. The modulation of aromatase and estrogen receptor alpha in cultured human dermal papilla cells by dexamethasone: a novel mechanism for selective action of estrogen via estrogen receptor beta? *J Invest Dermatol,* 126**,** 2010-8.

TIMIRAS, P. S. 1994. Disuse and aging: same problem, different outcomes. *J Gravit Physiol,* 1**,** P5-7.

TOBIN, D. J., GUNIN, A., MAGERL, M. & PAUS, R. 2003. Plasticity and cytokinetic dynamics of the hair follicle mesenchyme during the hair growth cycle: implications for growth control and hair follicle transformations. *J Investig Dermatol Symp Proc,* 8**,** 80-6.

TOUSSAINT, O., DUMONT, P., DIERICK, J. F., PASCAL, T., FRIPPIAT, C., CHAINIAUX, F., MAGALHAES, J. P., ELIAERS, F. & REMACLE, J. 2000. Stress-induced premature senescence as alternative toxicological method for testing the long-term effects of molecules under development in the industry. *Biogerontology,* 1**,** 179-83.

TRETTER, L. & ADAM-VIZI, V. 2004. Generation of reactive oxygen species in the reaction catalyzed by alpha-ketoglutarate dehydrogenase. *J Neurosci,* 24**,** 7771-8.

TRUEB, R. M. 2006. Pharmacologic interventions in aging hair. *Clin Interv Aging,* 1**,** 121-9.

TRUEB, R. M. 2009. Oxidative stress in ageing of hair. *Int J Trichology,* 1**,** 6-14.

TURRENS, J. F. 1997. Superoxide production by the mitochondrial respiratory chain. *Biosci Rep,* 17**,** 3-8.

UDVADIA, A. J., ROGERS, K. T., HIGGINS, P. D., MURATA, Y., MARTIN, K. H., HUMPHREY, P. A. & HOROWITZ, J. M. 1993. Sp-1 binds promoter elements regulated by the RB protein and Sp-1-mediated transcription is stimulated by RB coexpression. *Proc Natl Acad Sci U S A,* 90**,** 3265-9.

VAN DER LUGT, N. M., DOMEN, J., LINDERS, K., VAN ROON, M., ROBANUS-MAANDAG, E., TE RIELE, H., VAN DER VALK, M., DESCHAMPS, J., SOFRONIEW, M., VAN LOHUIZEN, M. & ET AL. 1994. Posterior transformation, neurological abnormalities, and severe hematopoietic defects in mice with a targeted deletion of the bmi-1 proto-oncogene. *Genes Dev,* 8**,** 757-69.

VAN LOHUIZEN, M., FRASCH, M., WIENTJENS, E. & BERNS, A. 1991. Sequence similarity between the mammalian bmi-1 proto-oncogene and the Drosophila regulatory genes Psc and Su(z)2. *Nature,* 353**,** 353-5.

VAN NESTE, D., LEROY, T. & CONIL, S. 2007. Exogen hair characterization in human scalp. *Skin Res Technol,* 13**,** 436-43.

VAN NESTE D, R. V. 1996. Ziller C. Pattern formation in neural crest derivatives. *In: Hair Research for the Next Millennium. Amsterdam: Elsevier Science***,** pp. 1-5.

VAN NESTE, D. & TOBIN, D. J. 2004. Hair cycle and hair pigmentation: dynamic interactions and changes associated with aging. *Micron,* 35**,** 193-200.

VAN OBBERGHEN-SCHILLING, E., ROCHE, N. S., FLANDERS, K. C., SPORN, M. B. & ROBERTS, A. B. 1988. Transforming growth factor beta 1 positively regulates its own expression in normal and transformed cells. *J Biol Chem,* 263**,** 7741-6.

VAN SCOTT, E. J. & EKEL, T. M. 1958. Geometric relationships between the matrix of the hair bulb and its dermal papilla in normal and alopecic scalp. *J Invest Dermatol,* 31**,** 281-7.

VAYALIL, P. K., ILES, K. E., CHOI, J., YI, A. K., POSTLETHWAIT, E. M. & LIU, R. M. 2007. Glutathione suppresses TGF-beta-induced PAI-1 expression by inhibiting p38 and JNK MAPK and the binding of AP-1, SP-1, and Smad to the PAI-1 promoter. *Am J Physiol Lung Cell Mol Physiol,* 293**,** L1281-92.

VAYALIL, P. K., OLMAN, M., MURPHY-ULLRICH, J. E., POSTLETHWAIT, E. M. & LIU, R. M. 2005. Glutathione restores collagen degradation in TGF-beta-treated fibroblasts by blocking plasminogen activator inhibitor-1 expression and activating plasminogen. *Am J Physiol Lung Cell Mol Physiol,* 289**,** L937-45.

VELARDE, M. C., FLYNN, J. M., DAY, N. U., MELOV, S. & CAMPISI, J. 2012. Mitochondrial oxidative stress caused by Sod2 deficiency promotes cellular senescence and aging phenotypes in the skin. *Aging (Albany NY),* 4**,** 3-12.

VON ZGLINICKI, T., SARETZKI, G., DOCKE, W. & LOTZE, C. 1995. Mild hyperoxia shortens telomeres and inhibits proliferation of fibroblasts: a model for senescence? *Exp Cell Res,* 220**,** 186-93.

WANG, E., ZHOU, S., ZHANG, J., LIU, Y., ZHANG, P., ZHANG, M. & LIU, G. 2005. Three-dimensional sutural expansion osteogenesis to expand zygomatic bone: an experimental study. *Br J Oral Maxillofac Surg,* 43**,** 68-71.

WANG, W. 2005. Oxygen partial pressure in outer layers of skin: simulation using three-dimensional multilayered models. *Microcirculation,* 12**,** 195-207.

WANG, W., WINLOVE, C. P. & MICHEL, C. C. 2003. Oxygen partial pressure in outer layers of skin of human finger nail folds. *J Physiol,* 549**,** 855-63.

WEI, Y. H., LU, C. Y., WEI, C. Y., MA, Y. S. & LEE, H. C. 2001. Oxidative stress in human aging and mitochondrial disease-consequences of defective mitochondrial respiration and impaired antioxidant enzyme system. *Chin J Physiol,* 44**,** 1-11.

WEINSTEIN, G. D., MOONEY, K.M 1980. Cell Proliferation kinetics in the human hair root. *J Invest Dermatol,* 74**,** 43-46.

WESTER, R. C., MAIBACH, H. I., GUY, R. H. & NOVAK, E. 1984. Minoxidil stimulates cutaneous blood flow in human balding scalps: pharmacodynamics measured by laser Doppler velocimetry and photopulse plethysmography. *J Invest Dermatol,* 82**,** 515-7.

WHITING, D. A. 1993. Diagnostic and predictive value of horizontal sections of scalp biopsy specimens in male pattern androgenetic alopecia. *J Am Acad Dermatol,* 28**,** 755-63.

WHITING, D. A. 2001. Possible mechanisms of miniaturization during androgenetic alopecia or pattern hair loss. *J Am Acad Dermatol,* 45**,** S81-6.

WILSON, C. L., DEAN, D. & WOJNAROWSKA, F. 1991. Pemphigus and the terminal hair follicle. *J Cutan Pathol,* 18**,** 428-31.

WILSON, J. D. 1975. Dihydrotestosterone formation in cultured human fibroblasts. Comparison of cells from normal subjects and patients with familial incomplete male pseudohermaphroditism, Type 2. *J Biol Chem,* 250**,** 3498-504.

WOOD, J. M., DECKER, H., HARTMANN, H., CHAVAN, B., ROKOS, H., SPENCER, J. D., HASSE, S., THORNTON, M. J., SHALBAF, M., PAUS, R. & SCHALLREUTER, K. U. 2009. Senile hair graying: H2O2-mediated oxidative stress affects human hair color by blunting methionine sulfoxide repair. *FASEB J,* 23**,** 2065-75.

WRANA, J. L., ATTISANO, L., WIESER, R., VENTURA, F. & MASSAGUE, J. 1994. Mechanism of activation of the TGF-beta receptor. *Nature,* 370**,** 341-7.

WRANA, J. L., CARCAMO, J., ATTISANO, L., CHEIFETZ, S., ZENTELLA, A., LOPEZ-CASILLAS, F. & MASSAGUE, J. 1992. The type II TGF-beta receptor signals diverse responses in cooperation with the type I receptor. *Cold Spring Harb Symp Quant Biol,* 57**,** 81-6.

YAMAMOTO, K., VOLKL, A., HASHIMOTO, T. & FAHIMI, H. D. 1988. Catalase in guinea pig hepatocytes is localized in cytoplasm, nuclear matrix and peroxisomes. *Eur J Cell Biol,* 46**,** 129-35.

YAMANISHI, K. 1998. Gene-knockout mice with abnormal epidermal and hair follicular development. *J Dermatol Sci,* 18**,** 75-89.

YAMASHITA, M., FATYOL, K., JIN, C., WANG, X., LIU, Z. & ZHANG, Y. E. 2008. TRAF6 mediates Smad-independent activation of JNK and p38 by TGF-beta. *Mol Cell,* 31**,** 918-24.

YEH, Y. H., KUO, C. T., CHAN, T. H., CHANG, G. J., QI, X. Y., TSAI, F., NATTEL, S. & CHEN, W. J. 2011. Transforming growth factor-beta and oxidative stress mediate tachycardia-induced cellular remodelling in cultured atrial-derived myocytes. *Cardiovasc Res,* 91**,** 62-70.

YU, B. P. & YANG, R. 1996. Critical evaluation of the free radical theory of aging. A proposal for the oxidative stress hypothesis. *Ann N Y Acad Sci,* 786**,** 1-11.

ZHU, J., WOODS, D., MCMAHON, M. & BISHOP, J. M. 1998. Senescence of human fibroblasts induced by oncogenic Raf. *Genes Dev,* 12**,** 2997-3007.